JURA

Journal of Undergraduate Research in Alberta

Volume 4 (2014)

UNIVERSITY OF CALGARY

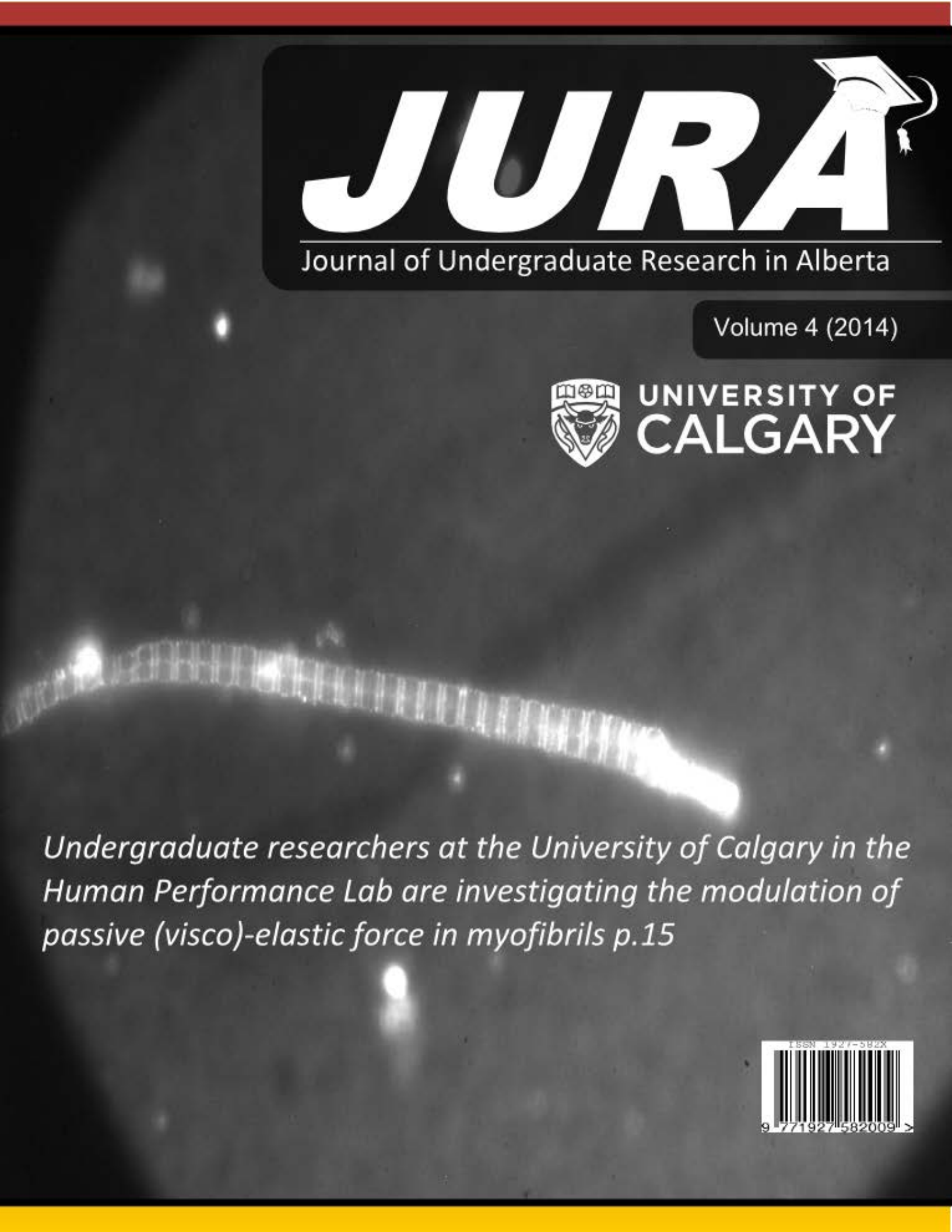

Undergraduate researchers at the University of Calgary in the Human Performance Lab are investigating the modulation of passive (visco)-elastic force in myofibrils p.15

ISSN 1927-582X

Contents

Volume 4, 2014

JURA
Journal of Undergraduate Research in Alberta

A Letter from the Editors

We are pleased to present the Fourth Edition of the Journal of Undergraduate Research in Alberta. JURA showcases some of the exceptional undergraduate research going on at the University of Calgary. This edition features a diverse array of research topics from Faculties across the University of Calgary campus. In this issue of JURA, you will find one review article, three extended abstracts and five full scientific articles, making it our largest edition to date. This edition showcases various topics, many of which directly relate to the Albertan environment and/or the health and wellness of the residents of Alberta.

We would like to start by thanking the previous editors of JURA, Swathi Damaraju and Emily Bishop, for their commitment to and continued support of JURA. We would also like to thank section editors, the JURA editorial board members and past and present reviewers for generously volunteering their time. We would like to thank the authors of this edition of JURA, whose efforts ensure that JURA remains a presence on the University of Calgary campus. Lastly, we would like to acknowledge Dr. Walter Herzog who has continued to provide mentorship and financial support to the Journal of Undergraduate Research of Alberta.

JURA is always accepting new submissions and we hope that our readers will spread the word of JURA to potential authors, reviewers and anyone who may be interested in joining the JURA team! We hope that you thoroughly enjoy the diversity and breadth of topics included in this edition of JURA.

Sincerely,

Krysta Powers & Kelsey Collins
Editors for the Journal of Undergraduate Research in Alberta

JURA

Journal of Undergraduate Research in Alberta • Volume 4 • 2014

Medical Education in Global Health: Ethical Considerations

T. Campbell, and A. Hull
University of Calgary

An increasing number of students are opting to participate in global health electives during their medical training. Such international rotations have been demonstrated to positively affect student behaviour by evoking a deeper understanding of the impact of poverty, developing cultural awareness, and inspiring students to pursue careers caring for the underserved. While opportunities to receive this experience are becoming more abundant, important ethical issues have arisen surrounding these international placements. Such ethical issues include: potential conflicts of interest, participation above the trainees clinical level, power imbalance, and burden on the host institution. We therefore review the aforementioned ethical considerations and include practical approaches to address these issues. Moreover, we highlight the concept of the creation of ongoing partnerships between sending and host institutions to establish mutually beneficial relationships, further strengthening the partnership and promoting the exchange of ideas.

Keywords: medical electives (educational and training placement undertaken as part of a medical degree), medical education (education related to training future physicians), global health (health of populations in a global context), ethics (branch of knowledge that deals with moral principles).

Introduction

Due to increased globalization and awareness of health determinants worldwide, a growing number of medical students are opting to participate in global health electives [1]. Research has demonstrated that such international rotations positively affect student behaviour by eliciting a deeper understanding of the impact of poverty, fostering cultural awareness, and inspiring students to pursue careers caring for underserved populations [2–4]. While opportunities to pursue this important experience are becoming more diverse and abundant, medical institutions and students are recognizing the emergence of numerous associated ethical considerations and are striving to mitigate these issues. Many of these ethical issues are now being incorporated into mandatory medical student pre-departure training, however, a standardized ethical framework to guide student actions and behaviour has yet to be solidified [1–5].

In light of the above circumstances, we explored ethical issues surrounding global health medical placements and included practical approaches to address these issues. First, since medical electives have an educational mandate alongside service, students can be faced with conflicting priorities while on an international placement. Second, students may step outside of their level of training to perform tasks beyond their current abilities. Misunderstanding of the health professional students responsibilities by the host institution may exacerbate this situation. Third, the major influence of socioeconomic status may create a power imbalance rendering local patients

vulnerable to potential exploitation. Fourth, despite their best intentions, students may tax local resources in an already impoverished society by requiring an interpreter or by monopolizing the time or resources of a local preceptor. Finally, the concept of the creation of ongoing partnerships between sending and host institutions is discussed. Establishing these mutually beneficial relationships may provide a platform to openly discuss ethical or logistical issues arising over time, further strengthening the partnership and promoting the exchange of ideas.

Ethical Consideration: Potential Conflicts of Interest

When participating in a global health elective, students must be cognizant of balancing their learning needs with the patients right to appropriate care. This potential conflict of interest can be a serious issue due to overburdened staff, limited local human resources, and a power imbalance resulting in vulnerable patients, a lack of supervision, and a low likelihood of negative ramifications for students who abuse their positions [5].

Moreover, it has been suggested that the demand for global health electives is increasing for as many career-driven reasons as altruistic ones [6]. For example, specific residency programs require applicants to have acquired international health care experience. Therefore, medical students may choose to participate in global health electives to build a strong curriculum vitae to gain entry into highly competitive residency programs that will likely result in urban-centric practice [6]. These goals are in stark contrast to the original altruistic motive of embarking on a global health elective.

Additionally, students may experience tensions between their service and training obligations and being in an exotic location that provides unique tourism opportunities [7]. This has also been referred to as voluntourism [8,9]. Although exploring the host country can be personally rewarding, it can be costly in local terms and may take the trainees away from their expected responsibilities. This can also cause local staff to have reservations about the students commitments to learning and the appropriate use of local funds [7].

Since these conflicts of interest can result in a decrease in the level of confidence and trust in the trainee by host healthcare providers, students need to be prepared to recognize when such conflicts arise and address them ethically. One method trainees can employ is participation in self-reflection and anti-discriminatory analysis [10]. This can assist the students in understanding the basis for their privilege, identifying multiple forms of oppression, and creating a worldview that considers issues such as imperialism, colonialism, and systemic social inequity [5–10].

Ethical Consideration: Participation Above the Trainees Clinical Level

Due to a strong desire to help and learn, medical students in resource-challenged settings may find themselves in a position to perform assessments, treatments, or procedures exceeding their present level of training. Though the intention may be noble, this can lead to ethical conflicts and leave both trainees and patients vulnerable to negative consequences [11]. When trainees step beyond their knowledge level, this can lead to poor patient outcomes, increased workload for local staff, negative repercussions on the local health care system, and associated student guilt [12].

Adding to the complexity of this ethical dilemma, research has shown that international patients may prefer to be treated by a western trainee and may be willing to undergo riskier procedures than they would otherwise permit a local physician to perform, even though local workers may be able to do a superior job using available resources [13,14]. Furthermore, Radstone [15] discovered that host country staff perceived that trainee doctors should be able to diagnose (94.9%), prescribe (84.6%), and treat patients (89.7%) without supervision, but were not aware that this was prohibited in the trainees home country. Language and cultural barriers can compound these circumstances.

This situation of practising beyond ones clinical skill level underscores a common misperception that people who live in poverty will benefit from any type of medical service, irrespective of the experience or lack thereof of the provider. In light of this, Shah and Wu suggest that medical students have an obligation to disclose their current level of training and to avoid acting beyond these capabilities in order to maintain a level of trust with the locals and host country [11].

JURA
Journal of Undergraduate Research in Alberta • Volume 4 • 2014

Ethical Consideration: Power Imbalance

In resource-poor settings, patients are exposed to dissymmetries in power in medicine [16]. These power imbalances can affect patients, local staff, and host institutions. Regarding those requiring medical attention, such power imbalances may render local patients vulnerable to possible exploitation. As mentioned previously, local patients are likely unaware of a medical students clinical skill level or restricted level of acceptable unsupervised duties [15]. Moreover, patients in host countries may be unable to demand superior care due to socioeconomic or cultural vulnerability [11].

This power imbalance may also muzzle the host institution with regards to reporting issues with visiting trainee conduct or hidden expenses because of fear of disrupting the relationship that may be providing another form of benefit to the institution, such as developing training opportunities for local staff or the provision of necessary equipment [7]. Host institutions may also lack the ability to monitor and record the benefits and costs that a medical student brings to their institution [7].

It is therefore critical that the sending institution prevent exacerbation of pre-existing inequities by avoiding misguided application of financial, human, or material resources for the sake of the medical student [17,18]. It is also important that the sending institution be aware of the true burden of the medical elective on the host institution, as discussed in the next section.

Ethical Consideration: Burden on the Host

Though the benefits of global health electives for medical students and sending institutions have been well-documented, little research has been performed regarding the benefit for host institutions. Recent reflections and analyses have suggested that these short-term international experiences may impose a significant burden on areas that are already resource-limited [7,9,11,12].

Local staff may be distracted from other important duties while helping orient trainees to the unfamiliar environment. The need for formal or informal translation services may also strain resources in the local community. Additionally, the supplementary supervision required by medical students may monopolize the time of local physicians and staff, thus interfering with regular health care service [7].

Hidden costs associated with accommodating trainees may also place a strain on the host institution. These expenses may include paying for visas, food, and incidental costs not covered by the sending institutions or medical students. Furthermore, as previously mentioned, host institutions may lack the capacity to monitor and document these hidden costs, resulting in an absence of appropriate reimbursement [7].

Crump and Sugarman therefore maintain that sending institutions have a moral obligation to ensure that the patients and host institutions in which these programs take place are at minimum not left worse off as a result of this collaboration [7]. They go on to suggest that the sending institutions arguably also have a moral obligation to help improve care and service delivery. One way to accomplish this is to establish long-term reciprocal relationships between institutions. This is explored in the subsequent section.

Next Steps: Building International Partnerships

One of the principal challenges for global health initiatives is bridging the gaps of geography, language, culture and resources between the foreign hosting sites and the sending institutions. Numerous approaches have been undertaken with mixed results, but a common critical component seems to be an ongoing partnership between both parties that is based upon a shared mission of service and education, and maintained through honest and open communication [9]. These long-term sustainable relationships promote accountability, exchange of ideas, and collaborative agreement among all involved parties, thus promoting consistency of practice and achievement of local community goals [19].

The development of these partnerships requires long-term planning, careful management, and rigorous regulation. An example of a successful partnership specifically pertaining to health elective training exists between the Indian Institute of Cerebral Palsy (IICP) in Kolkata, India and the Faculty of Health Sciences at the University of

Sydney, Australia. This relationship has resulted in the development of an ongoing program in which speech therapists and occupational therapists from the University of Sydney attend placements at the IICP with careful consideration to ensuring a positive impact at the IICP [20]. Another example of a successful medical training partnership is the Making The Links service-learning project through the University of Saskatchewan [21]. The purpose of this project is to teach medical students the social aspects of medicine through community service and long-term partnerships with underserved communities. This project consists of five distinct phases: (1) orientation to health issues of underserved populations, (2) northern community experience, (3) volunteer experience in a student-run clinic in an underserved urban area, (4) international experience in Mozambique, and (5) reflection and evaluation. According to Meili et al., this project has shown promising results, including an increase in student awareness of social accountability [21].

Finally, when creating global health partnerships, it is essential to establish a method to assess the effectiveness of the relationship for both parties. Systematic data collection within existing short-term global health experience programs is needed to inform host and sending institutions about the true cost of these programs so that unknown disparities can be addressed. Additionally, efforts should be directed at developing a means of assessing the potential benefits and harms to both medical trainees and to patients or other intended beneficiaries in the host country. Moreover, formal ethical guidelines, such as those developed in the context of the research setting, should be established and universally applied [7,22]. The Working Group on Ethics Guidelines for Global Health Training (WEIGHT) recently proposed a set of such guidelines for institutions, trainees, and sponsors of field-based global health training. The incorporation of ethical consideration into both pre-departure and post-departure training was suggested, as well as steps to achieve mutual and reciprocal benefit [22].

Conclusion

Many medical educational institutions provide students with an opportunity to participate in global health electives. The benefits of such short-term training are acknowledged for the trainees, but there are important ethical considerations inherent to sending individuals from resource-abundant settings for service experiences in resource-constrained locations [7]. Such considerations include: potential conflicts of interest, participation above the trainees clinical level, power imbalance, burden on the host, and building international partnerships. Awareness of and careful attention to these ethical issues by both the sending organization and the medical students themselves can significantly improve the experience for all stakeholders. Moreover, the featured approaches may be useful to incorporate into the medical student pre-departure training that routinely occurs before embarking on an international placement, as is suggested by the global health training guidelines proposed by WEIGHT [22]. Finally, a long-term partnership can provide an opportunity for communication that can lead to potential solutions to these and other intrinsic challenges. Projects such as Making The Links provide a platform for the development of these partnerships and a method to teach social accountability during medical training [21].

References

1. Shaywitz, D.A., Ausiello, D.A. (2002). Global health: A chance for western physicians to give - and receive. Am J Med. 113, 354-357.

2. McKinley, D.W., Williams, S.R., Norcini, J.J., Anderson, M.B.(2008). International Exchange Programs and U.S. Medical Schools. Acad Med. 83, 53-57.

3. Ramsey, A.H., Haq, C., Gjerde, C.L., Rothenberg, D. (2004). Career influence of an international health experience during medical school. Fam Med. 36, 412-416.

4. Elansary, M. et. al. (2011). Ethical Dilemmas in Global Clinical Electives. JGH. 1, 24-27.

5. Pinto, A.D., Upshur, R.E. (2009). Global health ethics for students. Dev World Bioeth. 9, 1-10.

6. Huish, R. (2012). The Ethical Conundrum of International Health Electives in Medical Education. JGCEE. 2, 1-19.

7. Crump, J.A., Sugarman, J. (2008). Ethical considerations for short-term experiences by trainees in global health. JAMA. 300,1456-1458.

8. Snyder, J., Dharamsi, S., Crooks, V.A. (2011). Fly-By Medical Care: Conceptualizing the Global and Local Social Responsibilities of Medical Tourists and Physician Voluntourists. Global Health. 7, 6.

9. Stoltenberg, M., Rumas, N., Parsi, K. (2012). Global health and service learning: lessons learned at US medical schools. Med Educ Online. 17, 18848.

10. Razack, N. (1999). Anti-discriminatory practice: Pedagogical struggles and challenges. Brit J Soc Work. 29, 231-250.

11. Shah, S., Wu, T. (2008) The medical student global health experience: professionalism and ethical implications. J Med Ethics. 34, 375-378.

12. Sinha, R. (2011). Ethical Considerations in International Health Electives Fam Med 43(8): 592, 2011.

13. Dupuis, C. (2004). Humanitarian missions in the third world: a polite dissent. Plast Reconstr Surg. 113, 433-435.

14. Ramsey, K.M. (2008). International surgical electives: reflections in ethics. Arch Surg-Chicago. 143, 10-11.

15. Radstone, S.J. (2005). Practising on the poor? Healthcare workers beliefs about the role of medical students during their elective. J Med Ethics. 31, 109-110.

16. Farmer, P., Campos, N.G. (2004). Rethinking medical ethics: a view from below. Dev World Bioeth. 4, 17-41.

17. Loh, L.C., Rhee, D.S., Heckman, J.E., Chae, S-R. (2012). Not just more global healthsmarter global health. Can Fam Physician. 58, 376-378.

18. Benatar, S.R., Singer, P.A. (2000). A new look at international research ethics. BMJ. 321, 824-826.

19. Gilbert, B.J., Miller, C., Corrick, F., Watson, R.A. (2013). Should trainee doctors use the developing world to gain clinical experience? The annual Varsity Medical Debate London, Friday 20th January, 2012. Phil Eth Hum Med. 8, 1.

20. Balandin, S., Lincoln, M., Sen, R., Wilkins, D.P., Trembath, D. (2007). Twelve tips for effective international clinical placements. Med Teach. 29, 872-877.

21. Meili, R., Fuller, D., Lydiate, J. (2011). Teaching social accountability by making the links: qualitative evaluation of student experiences in a service-learning project. Med Teach. 33, 659-666.

22. Crump, J.A., Sugarman, J., Working Group on Ethics Guidelines for Global Health Training (WEIGHT). (2010). Ethics and Best Practice Guidelines for Training Experiences in Global Health. Am J Trop Med Hyg. 83, 1178-1182.

JURA

Journal of Undergraduate Research in Alberta • Volume 4 • 2014

Did Rules and Regulations Aimed at Reducing Head Contact in Ice Hockey Change the Risk of Concussion and Injury in Youth Hockey Players in Alberta?

M. Krolikowski, A. Black, J. Kang, C. Emery
University of Calgary

Introduction

Ice hockey is a popular winter sport in Canada, with over 600,000 youth players registered in Hockey Canada [1]. Among high participation and high injury rates, concussion has become a significant public concern, accounting for the greatest proportion (>25%) of all injuries in youth ice hockey [2,3]. In an effort to make the game safer to play, a recent policy change implemented by Hockey Canada introduced a new zero-tolerance head contact rule (Rule 6.5) at the beginning of the 2011-2012 hockey season aimed to reduce the number of head contact injuries (i.e. concussion) that occur with the sport in youth ice hockey [4].

A thorough assessment is needed to examine the effects and desired outcomes of policy changes in sport [5]. The objective of this study is to determine if the risk of concussion and other injury significantly differ for Pee Wee (ages 11-12) and Bantam (ages 13-14) players following the 2011 rule enforcement policy change "zero tolerance for head contact or head checks" compared to players in similar divisions prior to the rule enforcement change.

Methods

This is an historical cohort study. Player recruitment included 588 Pee Wee (Divisions 1-7, ages 11-12) and 244 Bantam (Divisions AAA, AA, ages 13-14) ice hockey players in Alberta in the 2011/12 season. Data from historical cohorts included 891 Pee Wee players (Divisions 1-7) in the 2007/08 season and 378 Bantam players (Divisions AAA, AA) in the 2008/09 season. Previously validated prospective injury surveillance methodology was used across all study years [2]. Injury definition included any game related injury resulting in the inability to complete a session, miss a subsequent session, and/or required medical attention. All players with a suspected concussion were referred to the study sport medicine physician for evaluation and confirmation of diagnosis. Incidence Rate Ratios (IRRs) were estimated based on multivariate Poisson Regression analysis controlling for clustering by team and other important covariates (e.g. year of play, level of play, player position, and previous injury/concussion) and offset by game exposure hours.

JURA
Journal of Undergraduate Research in Alberta • Volume 4 • 2014

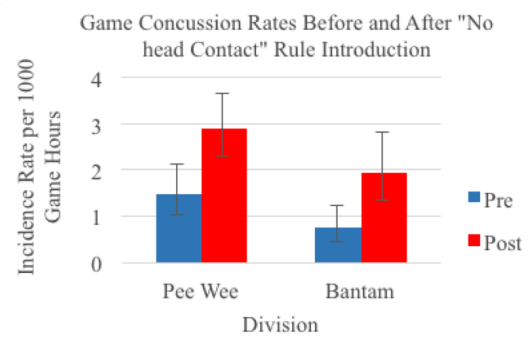

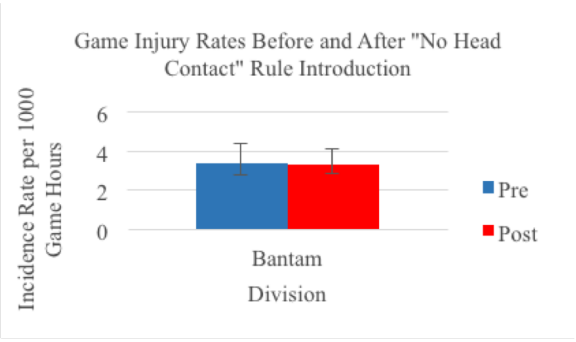

Results

The risk of game concussion increased in both age cohorts in the season following the 2011 rule enforcement policy change "zero tolerance for head contact or head checks" compared to players in similar divisions prior to the rule enforcement change (Pee Wee concussion IRR = 1.89 [95% CI; 1.20-2.97] and Bantam concussion IRR = 2.29 [95% CI; 1.05-5.01]). The risk of other injury (excluding concussion) did not change in the Bantam level (Bantam other injury IRR = 1.03 [95% CI; 0.64-2.87]).

Discussion and Conclusions

The zero tolerance for head contact or head checks rule did not reduce the risk of game related concussion in Pee Wee or Bantam ice hockey players. It is possible however that concussion referral bias related to a greater awareness of concussions in youth ice hockey affected this result despite consistent injury surveillance methodology. Other injury rates were unaffected by the new rule. Further investigation examining referee enforcement of head contact rule change is warranted.

References

1. Hockey Canada. Hockey Canada Minor Hockey web site. Available at: http://www.hockeycanada.ca/en-ca/Corporate/About/Basics.aspx Accessed May 6th, 2013
2. Emery, C. and Meeuwisse, W. AJSM, (34)1960-1969. 2006
3. Helly KD, Lissel HL, Rowe BH, et al. CJSM, (11)77-81. 2001
4. Hockey Canada. Hockey Canada Minor Hockey web site. Available at: http://www.hockeycanada.ca/en-ca/news/2011-GN-018-en. Accessed May 6th, 2013
5. Benson BW, McIntosh AS, Maddocks D, Herring SA, Raftery M & Dvorak J. BJSM, (47) 321-326. 2013

JURA
Journal of Undergraduate Research in Alberta • Volume 4 • 2014

Determining Expression Levels Of The Inflammatory Marker IL-8 In Human Alveolar Basal Epithelial A549 Cells Following Exposure To Amorphous Silicon Dioxide Micro- And Nanoparticles In The Presence Of IL-1β

F. Mahdi & M.Hlasny
University of Calgary

Introduction

Exposure to nano- and microparticles can have adverse health effects, particularly for the increasing population with pre-existing inflammatory lung conditions (COPD, asthma, etc.). This is of concern as there is an increased usage of small particles in the workplace and in consumer products (1). Large particles are cleared from the lung via the mucociliary escalator (the cilia of the airways, pushing the particles up and out of the lung). Nanoparticles in particular reach the peripheral lung, where the mucociliary escalator is not present (1). We studied how particle exposure affected inflammation in cell cultures of A549 cells, including cells pre-exposed to inflammation. A549s are immortalized human alveolar basal epithelial cells that closely resemble Type II lung epithelial cells (2). Interleukin(IL)-1β was used to induce an inflammatory response and assessed by measuring IL-8 (3). IL-8 is an important pro-inflammatory cytokine expressed in respiratory cells of the human lung, induced upon environmental insults by particles and is associated with neutrophil recruitment (4). The particles used were amorphous silicon dioxide (silica) nano- and microparticles. Earlier we determined that the nanoparticles form agglomerates similar in size to individual silica microparticles. The nanoparticle agglomerates are vigorously up-taken, but by a different pathway (5).

Methods

Microparticle and Nanoparticle Exposure

Procedure 1: A549 cells were cultured on 96-well plates in F12 media supplemented with 10% fetal bovine serum (FBS). Particles were serially diluted three times with IL-1β (1ηg/ml) media containing 10% FBS for a total of four concentrations per particle type. Particle solutions and standards with or without IL-1β were added to the plates for an exposure length of 2 hours. Note: 2 and 6 hours were most commonly used standard procedure time for ELISA analysis.

JURA
Journal of Undergraduate Research in Alberta • Volume 4 • 2014

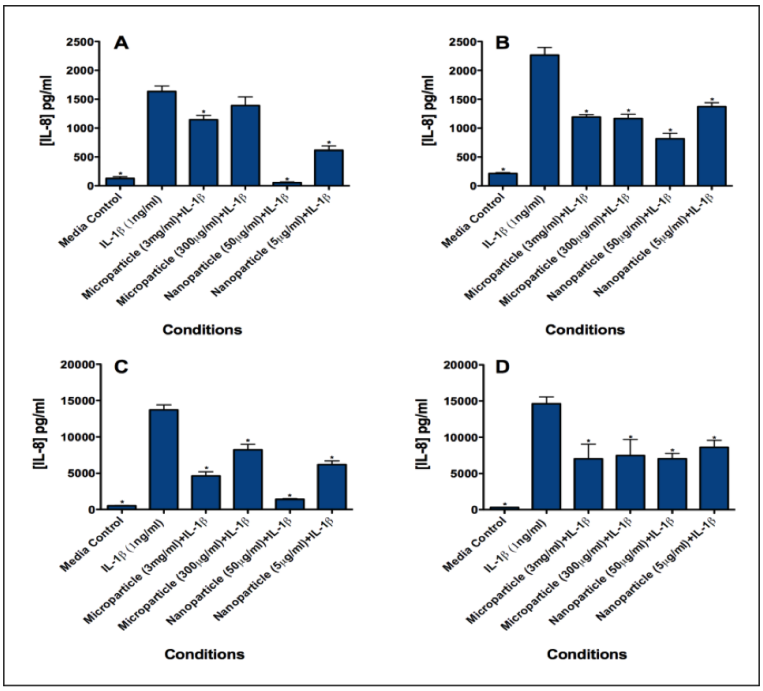

Figure 1:

Effect of long and brief exposure of nanoparticles and microparticles on IL-8 expression of cells, stimulated by IL-1β. A549 cells in (A) and (C) were exposed to particles and IL-1β (1ηg/mL) for 2 and 6 hour incubations, respectively. (B) and (D), cells were pre-incubated for 30 minutes with IL-1β, washed, exposed to particles for 5 minutes and incubated for 2 and 6 hours respectively with IL-1β. N=12. Even a short exposure to particles strongly dampens A549s inflammatory response. SEM were measured using Prism Software. Represents conditions significantly different than IL-1β using a one-way ANOVA. Statistics were also carried out to compare against the negative media control. All sets were significantly different than media except nanoparticles (50μg/mL) in both A and C.

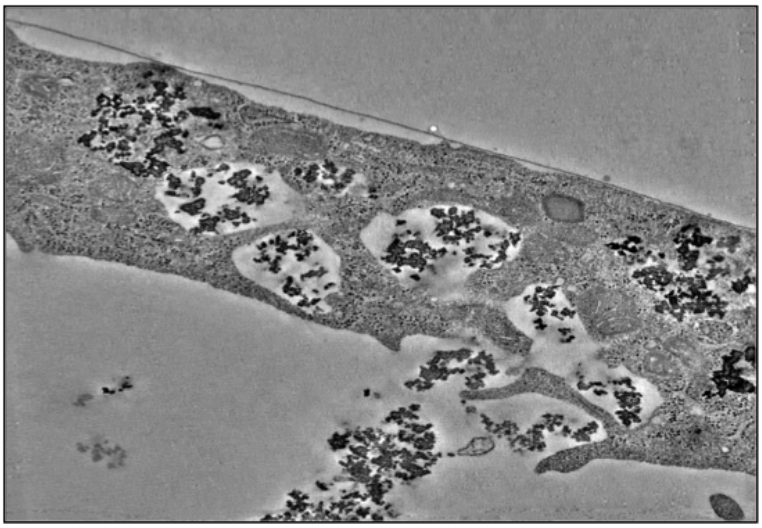

Figure 2:

A549 cell exposed to silica nanoparticles. The picture above shows the formation of nanoparticle agglomerates. The agglomerates are taken up by the cells and encapsulated in endosomes.

Procedure 2: Two concentrations of silica nanoparticles (5μg/mL and 50μg/mL) or microparticles (300μg/mL and 3mg/mL) were diluted in media containing 10% serum for treatment of A549 cells by 2 separate treatment methods:

1. Cells were exposed to particles for 5 minutes and then washed 3 times with media. Fresh media containing 10% serum with or without IL-1β was added for 2-hours.

2. Cells were treated with IL-1β for 30 minutes. Then, cells were washed once prior to particle exposure for 5 minutes followed by three additional washes. Fresh media with or without IL-1β was added to the cells for an exposure length of either 2 or 6 hours.

All supernatants were harvested for analysis by IL-8 ELISA assay. Transmission electron microscopy techniques were used to characterize the uptake of particles.

Detection of IL-8 Levels

Silica microparticle and nanoparticle exposure was performed on A549 cells, and cell supernatants were removed and stored at -20°. An ELISA kit from R&D Systems was used following the manufacturers method. Absorbance levels at a wavelength of 450nm were measured using a FluroStar plate reader to determine IL-8 concentrations. SEM were calculated using Prism software and one-way ANOVA was performed to determine statistical significance.

Cell Viability

A549 cells were exposed to silica microparticles and nanoparticles for 2 hours and 6 hours. The A549 cells were then trypsinized and stained with either Erythrocin B stain or Trypan Blue solution. Cells were counted using a hemocytometer.

Results

Results are shown in Figures 1 and 2.

Discussion and Conclusions

Silicon dioxide nano- and microparticles alone did not elicit the release of IL-8, which leads to inflammation, in A549 cells. Surprisingly, the particles were anti-inflammatory. After 6 hours, particles strongly dampened the release of IL-8 in IL-1β-triggered cells. This was not related to cell death, which was overall quite low (less than 20%) in all treatments. Even brief exposure (5 minutes) of cells to particles strongly dampened the inflammatory response triggered by IL-1β, for both the 2 and 6 hour time points (Figure 1). Nanoparticles appeared to dampen inflammation slightly more than microparticles. Electron microscopy showed that particles were strongly taken up and transcytosed by A549 cells. To explain our results, we speculate that uptake and transcytosis are an efficient clearance mechanism for particles that reach the peripheral lung, where the mucocilliary elevator is absent. Transcytosis is not associated with inflammation and is even anti-inflammatory, thus preventing unnecessary damage to the lung in the process

Future Directions

It would be interesting to examine the activation of transcription factors such as nuclear factors, NF kappa beta and activator protein-1, that control pro-inflammatory genes. Also, it is a valuable experiment to perform treatment with selected inhibitors to gain an understanding of the relation between particle uptake in the presence of inflammation and cellular response to inflammation. Finally, the next step would be to perform Fluorescence Microscopy to investigate the kinetics of real time particle uptake in primary cell cultures.

References

1. Hussain M et al. The Health. 2(2):51-59, 2011.
2. Lieber, M et al. Int. J. Cancer, 17(1), 62-70.1978.
3. Hetland RB et al. J Toxicol Environ Health, 60(1), 47-65. 2012
4. Bhatia M & Moochhala S. J Pathol. 202: 145-156. 2004.
5. Tehranian S. Adhesion and uptake mechanisms of amorphous silica micro and nanoparticles in an in vitro model of human alveolar epithelial cells. PhD Thesis. 2011.

JURA
Journal of Undergraduate Research in Alberta • Volume 4 • 2014

Monophyly of Eusocial Wasps (Hymenoptera: Vespidae): Molecules and Morphology Tell Opposing Histories

P. Piekarski, R. Longair, S. Rogers
University of Calgary

Introduction

The evolution of insect societies, as seen in eusocial ants, bees and wasps, is one of the most exceptional biological phenomena to ever occur. Eusociality involves a phenotypic decoupling of workers and queens (i.e. the incipience of castes) where some individuals forfeit direct reproductive success and instead cooperatively rear the brood of another (i.e. altruism). Social insects comprise just 2% of all insect species, but over half the total biomass of insects [1]. Although eusociality is related to ecological dominance, presumably the emergence of social life is contingent upon evolutionarily 'expensive' precursor traits. Although not for bees, subsociality is generally recognized as a salient precursor for eusociality in vespid wasps [2]. Subsociality involves progressive provisioning (offspring fed in daily increments, not in mass), which prolongs offspring dependency. Vespidae is comprised of over 5000 wasp species, of which approximately 1100 are eusocial [3]. In primitively eusocial wasps worker status may be temporary; all females are potential queens (e.g. independent-founding Polistinae; Stenogastrinae). Highly eusocial wasps possess a permanent worker caste (e.g. swarm-founding Polistinae; Vespinae).

Phylogenies provide insight into the ancestral states and environmental contexts that subserve worker/queen decoupling, and thus are the framework for understanding origins of eusociality. We present a thorough phylogenetic analysis of the Vespidae, utilizing phenotypic and molecular data of previous studies [3,4] in conjunction with newly acquired data, in an effort to explain how solitary ancestors may have crossed the threshold of eusociality. Previous studies show conflicting phylogenies for Vespidae and differ in their conclusions regarding whether eusociality has evolved once or twice in these wasps [3,4]. Here we explore the primary drivers of phylogenetic incongruence complicating reconstruction of the Vespidae phylogeny.

Methods

Simultaneous analysis of phenotypic characters (269 morphological and 66 behavioral) and molecular data (COI, 28S, 16S, 12S) for 74 taxa was performed to clarify the subfamily relationships of the Vespidae. Sequence alignments were implemented within Codon-code aligner v.3.7.1.2 using the ClustalW option and subsequently vetted by-eye. All COI sites were included in the final alignment because an underlying protein code guides the vetting process. However, many sites of rDNA were excluded. Encryption of indel events is unfeasible for regions of rDNA sequences that are hyper-variable

(i.e. functionally unconstrained). The number of possible multiple sequence alignments corresponding to these indel-rich regions are legion a mere ten sequences with a length of 5 base pairs each yields 1.35 x 1038 possible alignments [5] making the search for an exclusive alignment of minimum cost problematic. Thus, these regions were ignored and only the most confidently aligned nucleotide sites are included as input for phylogenetic analyses. The final concatenated alignment was comprised of 4051 base pairs, of which 1056 were parsimony informative, and 335 phenotypic characters. The phenotypic characters are adopted from previous work [3]. Gaps were consistently treated as missing data and the ingroup was forcefully constrained.

In addition to simultaneous analysis of all data, we performed analyses based solely on molecular data, and on all data except behavioral. To account for incongruence brought on by different analytical methods, we employed Maximum Likelihood, Bayesian Inference and Maximum Parsimony for all data-inclusion schemes. Model testing was implemented in jModelTest 2 [6] to determine the best-fit model for each partition of molecular data. A separate unlinked model was applied to each COI codon because this partitioning scheme returned the lowest Akaike Information Criterion score. The third codon position was included despite potential homoplasy because no major differences were observed between the COI gene trees retrieved from utilization of only the first two codon positions and all codon positions (not shown).

To find the most parsimonious trees, a new technology search strategy of 1000 random additions, each with 40 rounds of parsimony ratchet, 20 rounds of tree drifting and 30 rounds of fusing was implemented within TNT [7]. Phenotypic characters were treated as non-additive in our analyses. ML analyses were performed in GARLI [8]. The models implemented were: GTR+I+G for the first codon of COI, TVM+I+G for the second codon of COI, TPM1uf+I+G for the third codon of COI, GTR+I+G for 28S, GTR+I+G for 16S and HKY+I+G for 12S. An Mkv unordered model was specified to the phenotypic characters. Bayesian analyses were performed with MrBayes 3.2 [9]. Priors were left flat. All DNA partitions were assigned the GTR+I+G model, except 12S was assigned the simpler HKY+I+G model. Phenotypic data was assigned an Mkv model with gamma rate heterogeneity. In both ML and Bayesian analyses, models were unlinked and allowed to evolve with independent rates of evolution. A relative burn-in of 25% was set and 2 runs with 4 chains each were performed. All analyses were allocated 3 million generations and reached a standard deviation of split frequencies below 0.01.

Results

Simultaneous analysis of all evidence supports a (Stenogastrinae + (Polistinae + Vespinae)) clade and thus a single origin of eusociality (Fig. 1A, D, G). Phylogenies derived strictly from molecular evidence consistently support a dual origin of eusociality (Fig. 1C, F, I). Our results more-or-less support the novel tribal relations of Polistinae recently proposed [3] as (Ropalidiini + (Mischocyttarini + (Polistini + Epiponini))), but the strength of support for a Polistini + Epiponini clade diminishes with the addition of phenotypic data (Fig. 1). Both the nuclear and mitochondrial DNA trees did not support monophyly of the eusocial wasps (not shown).

Discussion and Conclusions

Our reanalysis shows that previous studies recovering diphyly (two distant clades) of eusocial wasps [4] may withstand the effects of low taxon sampling, suboptimal alignments and a two-step approach causing phylogenetic error; we achieved similar topologies using three-fold more terminal ingroups and a different suite of loci. Additionally, our two-step regime retrieved a similar maximum parsimony topology (Fig.1G) as a study that employed one-step direct optimization [3]. Our findings elicit an original perspective concerning Vespidae systematics: There are biological processes causing phylogenetic conflict, which are presumably driving conflict more prominently than methodological drivers.

Our results qualitatively show that a portion of phylogenetic incongruence is attributable to method choice, but that the primary driver of incongruence is data type inclusion that is, the topology produced changes when phenotypic data is included (Fig.1). We conclude that vespid subfamily relationships are muddled by the fact

that phenotypic and molecular evidence are at odds. One or several of the following processes may be responsible for phylogenetic incongruence: phenotypic and/or molecular saturation; phenotypic and/or molecular adaptive convergence; paralogy; introgression; and incomplete lineage sorting. Addressing the significance of biological processes driving phylogenetic conflict in vespids will require analyses of vast genomic data.

We advocate topologies retrieved from simultaneous analysis of all available evidence. It can be inferred that facultative nest sharing, cooperative rearing and a rudimentary worker phenotype evolved concurrently under a context of simultaneous progressive provisioning (SPP) before divergence of Stenogastrinae and Polistinae + Vespinae. We posit that the emergence of SPP is pivotal to the incipience of a temporary worker caste. The energetic costs of brood care inhibit ovarian development [10]. If the queen transfers the burden of larval care onto emerging daughters, then the latter will be coerced into becoming temporary workers. Furthermore, the sting venom of progressively provisioning wasps is free to exapt a novel function and in eusocial wasps has specialized as an anti-vertebrate defense due to its dissociation from prey handling. Anti-vertebrate venom likely evolved after eusocial habits and is thus important in the maintenance, rather than origin, of eusociality. The capacity for allomaternal care (adopting orphaned larvae) has evolved independently in multiple lineages of vespids [2], indicating that vespid wasps have a propensity for it. SPP may have provided a novel social context that exploited and altered pre-existing behavioral flexibility, resulting in exaptation of allomaternal care into cooperative allomaternal care and the emergence of a rudimentary worker phenotype via transference of strenuous larval care onto emerging daughters. Also, the phylogeny infers at least four independent origins of swarm-founding behavior [10] (Provespa (Vespinae); Epiponini; and twice within Ropalidiini), implying that a permanent worker caste has evolved multiple times.

References

1. Wilson, E.O & Hlldobler, B. PNAS. 102:13367-13371, 2005
2. Cowan, D.P. In: The social biology of wasps, Ross, K.G & Matthews, R.W, Eds. Cornell Univ. Press, London 33-73, 1991
3. Pickett, K.M & Carpenter, J.M. Arthropod Syst. Phylogeny. 68:3-33, 2010
4. Hines, H. et al. PNAS. 104:3295-3299, 2007
5. Slowinski, J.B. Mol. Phylogenet. Evol. 10:264-266, 1998
6. Darriba, D. et al. Nat. Methods. 9:772, 2012
7. Goloboff, P.A et al. Cladistics. 24:774-786, 2008
8. Zwickl, D.J. Ph.D. dissertation, The University of Texas, 2006
9. Ronquist, F. Syst. Biol. 61:539-542, 2012
10. Hunt, J.H. J. Evol. Biol. 25:1-19, 2011.

JURA
Journal of Undergraduate Research in Alberta • Volume 4 • 2014

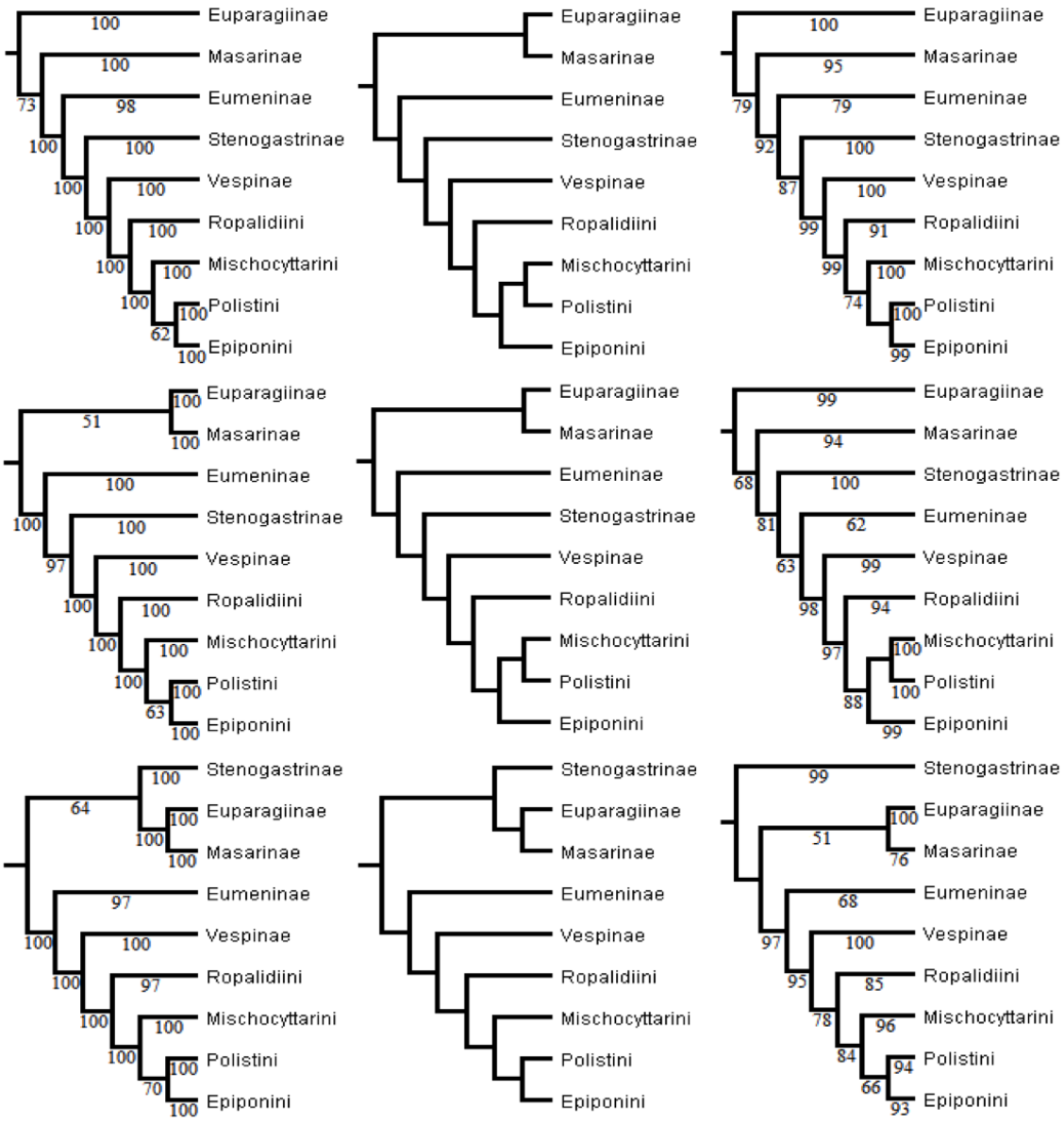

Figure 1:

Condensed phylogenies of the Vespidae obtained in the current study via Bayesian Inference (BI), Maximum Likelihood (ML), and Maximum Parsimony (MP). **A, B, C**: Bayesian consensus tree resulting from analysis of: **(C)** all molecular characters; **(B)** all molecular and morphological characters; **(A)** all molecular, morphological and behavioral characters. **D, E, F**: ML tree resulting from analysis of: **(F)** all molecular characters; **(E)** all molecular and morphological characters; **(D)** all molecular, morphological and behavioral characters. **G, H, I**: Strict consensus MP tree, from analysis under equal weights of: **(I)** all molecular characters; **(H)** all molecular and morphological characters; **(G)** all molecular, morphological and behavioral characters. Bootstrap support values deduced from 500 replicates and Bayesian posterior probabilities indicated under branches if ≥ 50.

JURA
Journal of Undergraduate Research in Alberta • Volume 4 • 2014

Modulation of Passive (Visco-) Elasticity in Cyclic Stretch-Shortening Experiments of Skeletal Muscle Myofibrils

J. Herzog, T. Leonard, A. Jinha, W. Herzog
University of Calgary

Titin is the third most abundant protein in sarcomeres and fulfills a number of mechanical and signaling functions. Specifically, titin is responsible for most of the passive forces in sarcomeres and the passive visco-elastic behaviour of myofibrils and muscles. It has been suggested, based on mechanical testing of isolated titin molecules, that titin is an essentially elastic spring if Ig domain un/refolding is prevented either by working at short titin lengths, prior to any unfolding of Ig domains, or at long sarcomere (and titin) lengths when Ig domain un/refolding is effectively prevented. However, these properties of titin, and by extension of muscles, have not been tested with titin in its natural structural environment within a sarcomere. The purpose of this study was to gain insight into the Ig domain un/refolding kinetics and test the idea that titin could behave essentially elastically at any sarcomere length by preventing Ig domain un/refolding during passive stretch-shortening cycles. Although not completely successful, we demonstrate here that titin?s visco-elastic properties appear to depend on the Ig domain un/refolding kinetics and that indeed, titin (and thus myofibrils) can become virtually elastic when Ig domain un/refolding is prevented. **Keywords:** skeletal muscle, titin, actin, myosin, stretch-shortening cycles, passive properties, stiffness, elastic, visco-elastic, energy loss, hysteresis, muscle properties, cross-bridge theory, sliding filament theory, sarcomere, sarcomere mechanics.

Introduction

When a muscle is stretched to a certain threshold length (which differs between muscles), it starts to exhibit passive forces that increase non-linearly with increasing muscle lengths [1–3]. These passive forces are caused primarily by collagen fibrils embedded into the muscles connective tissues and by the structural protein titin, the third most abundant protein in sarcomeres [4–6]. While the connective tissues and associated collagen fibrils are (visco-) elastic structures with predictable properties, titins properties are not nearly as predictable. Titin contributes to force regulation in actively stretched muscle by changing its stiffness through binding of calcium at specific sites [7–9] and is thought to change its free spring length by binding or interacting with actin [10–14]. During passive stretching, the various domains of titin are successively engaged [15] and give rise to the changing passive properties observed in myofibrils [16].

JURA
Journal of Undergraduate Research in Alberta • Volume 4 • 2014

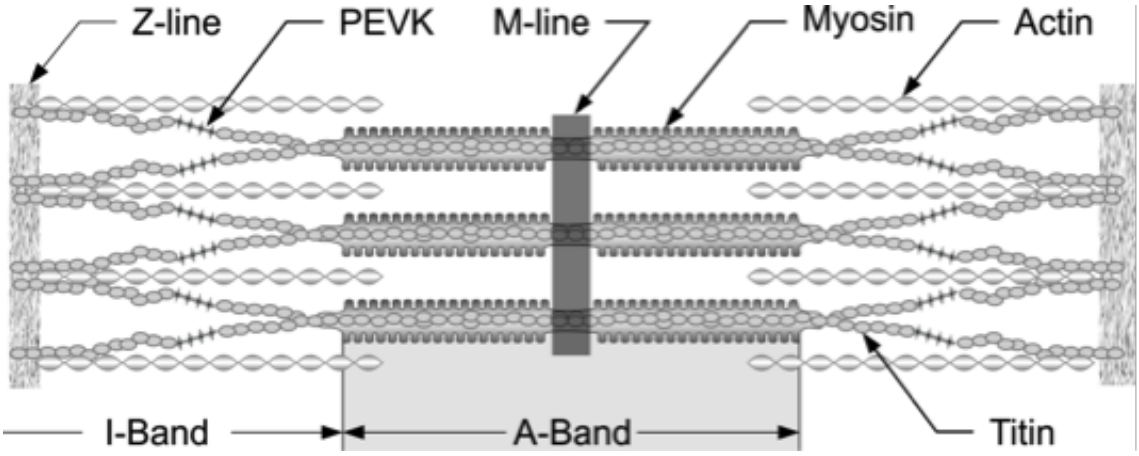

Figure 1:
Schematic drawing of a sarcomere with the contractile proteins actin and myosin, and the structural protein titin. Titin spans the half-sarcomere from the M-line in the middle of the sarcomere to the Z-line at the ends of the sarcomere. It is fixed to myosin and is inextensible in the A-Band region, but acts as a molecular spring in the I-Band region. Its primary spring elements are the proximal and distal Ig domains (schematically indicated by the blue circles close to the Z-line and the A-Band, respectively and the PEVK region separating the two Ig domains adapted from [17], with permission).

Titin (also called connectin) is a sarcomeric protein that spans the half sarcomere from the M-line to the Z-line [5−6,18] (Figure 1). It produces most of the passive force within the contractile unit, the sarcomere [19−20], provides stability to the thick (myosin) filament in the centre of the sarcomere [21−22], contributes to the residual force enhancement observed in muscles following active stretching [8,23−24], is responsible for force regulation in actively stretched muscles [25−26], and provides stability for serially arranged sarcomeres on the descending limb of the force-length relationship [27−28]. Titin acts like a spring in its extensible I-Band region. At short sarcomere lengths and small passive forces, the immunoglobulin (Ig) domains of titin are thought to align. With increasing sarcomere lengths, the so-called PEVK region, named so for its abundance in proline (P), glutamate (E), valine (V), and lysine (K) residues, is thought to become stretched, while at very long lengths, the Ig domains start to unfold [15].

Exploring the passive mechanical properties of titin has been difficult, as isolation of this giant protein has proven tricky, and the individual domains of titin have vastly differing properties [30−31]. However, Kellermayer et al. [29,32] were able to isolate single titin molecules and test their mechanical properties using a laser trap approach. By attaching a bead to one end of titin that could then be trapped using a laser, and by fixing the other end of titin rigidly, they performed stretch-shortening experiments of different magnitudes, thereby exploring the properties of titin when different regions became recruited during stretch. Kellermayer et al. [29,32] observed that single titin molecules behaved essentially elastic below a stretch force of approximately 25pN but highly viscoelastic above 25pN (Figure 2). However, if the stretch-shortening cycles were repeated, the hysteresis of the force-elongation/shortening curves became smaller, and if stretch-shortening cycles were restricted to long lengths (and high passive forces) where Ig domain unfolding and refolding was essentially abolished, titin was shown to exhibit virtually elastic properties with little or no hysteresis [3]2. They argued that if titin was completely unfolded, and refolding of Ig domains was prevented during cyclic stretch shortening cycles, titin would act as an elastic spring, while it would behave viscoelastic if un/refolding of Ig domains was allowed. Since large hystereses in stretch-shortening cycles are associated with great losses of energy, it would be of distinct advantage if such losses were minimized in working muscles.

Kellermayer et al.[29] found that titin forces need to be very small (<2.5pN) for effective Ig domain refolding, and we demonstrated that even in the

JURA
Journal of Undergraduate Research in Alberta • Volume 4 • 2014

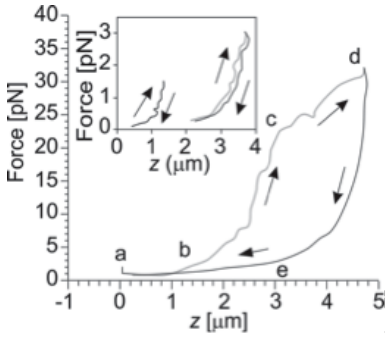

Figure 2:
Force-elongation curves for isolated titin molecules stretched using a laser tweezer approach [29]. Titin shows an inflection point (c) at the point where Ig domain unfolding is supposed to occur, and shows a great hysteresis when stretched and shortened beyond point (c). Below length (c), titin behaves essentially elastic (inset short length). Similarly, titin also behaves virtually elastic at long length (inset long length), but only if stretch-shortening occurs without appreciable unfolding and refolding of Ig domains (adapted from Kellermayer et al. 1997, with permission).

absence of measurable force, titin refolding remained incomplete even after as long as ten minutes in single myofibrils of rabbits when held at average sarcomere lengths of 2.6 μm [16]. These results suggest that stretching of titin easily unfolds Ig domains, while shortening does not readily allow for refolding [33], thus, in repeat stretch-shortening cycles titin becomes increasingly more elastic and loss of energy is minimized. Therefore, we hypothesized that titin is a (visco-) elastic spring that can change its domain of virtually elastic behaviour to any sarcomere lengths of repeated use if Ig domain un/refolding is prevented.

The purpose of this study was to test if titin behaves essentially elastic at long lengths where effective un/refolding of Ig domains is prevented, thereby testing Kellermayers ideas for the first time with actin in its proper structural environment. Furthermore we wanted to test if the rate of refolding of Ig domains, in the absence of force, is sarcomere length dependent. All experiments were performed using isolated myofibrils from rabbit psoas muscle, which allows for accurate determination of the mechanical properties of titin in its native structural arrangement [16,33]

Methods

Preparation: Myofibrils were prepared for mechanical testing as outlined previously by our group [8,16,25,34]. Briefly, myofibrils were obtained from psoas muscles of New Zealand White rabbits, and were chemically and mechanically isolated to form single fibrils with serially arranged sarcomeres. Isolated myofibrils were then immersed into a bath on top of an inverted microscope in a rigor solution (see solutions below). After ten minutes of stabilization, the rigor solution was replaced with a low calcium relaxation solution (see solutions below) that prevented any active actin-myosin based-cross bridge forces [8]. Myofibrils in suspension were then washed away, leaving those attached to the bottom cover glass. Myofibrils of appropriate length (typically 6-12 sarcomeres in series) that showed distinct striation patterns were then selected for mechanical testing by attaching them at one end to a silicon nitride lever for force measurements (stiffness of 68pN/nm, force resolution of 0.5nN, and spatial resolution of 7nm) and at the other end to a rigid glass needle attached to a motor for controlled, sub-nanometre step size, length changes (Fig. 3). Three distinct experiments were performed as outlined below.

The image of the attached myofibrils was projected onto a high density photo diode array (Schafter/Kirschoff, Hamburg, Germany, resolution of 7nm) for identification of the A- and I-bands, z-lines, and the calculation of sarcomere lengths from z-line to z-line or between the centroids of adjacent A-bands if z-lines were not clearly visible.

Solutions: The rigor solution (pH 7.4) was composed of (in mM): 50 Tris, 100 NaCl, 2 KCl, 2 MgCl2, and 10 EGTA. Protease inhibitors were added to the final solution, in the following concentrations (in pM): 10 leupeptin, 5 pepstatin A, 0.2 PMSF, 0.5

JURA
Journal of Undergraduate Research in Alberta • Volume 4 • 2014

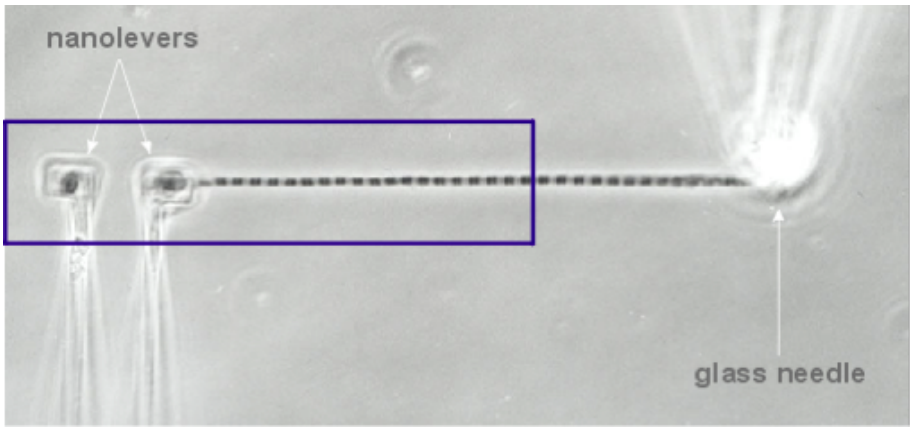

Figure 3:
Myofibril set up for mechanical testing. A myofibril with approximately 30 sarcomeres is attached at its right end to a rigid glass needle, which in turn is attached to a motor with less than nm step resolution for imposing computer controlled stretch-shortening cycles. The left end of the myofibril is attached to one of a pair of nano-levers for force measurements. Upon force production the myofibril will pull the attached lever away from its reference lever, and knowing the stiffness of the lever (68pN/nm in this case), instantaneous forces can be determined with a resolution of less than 0.5nN. For reference, myofibrils are approximately 0.7-1.0μm in diameter and sarcomeres shown here have an average length of approximately 2.2μm.

N, and 0.5 DlT. The relaxing solution (pH = 7.0; pCa2 = 8) was composed of (in mM): 10 MOPS, 64.4 K+ proprionate, 5.23 M proprionate, 9.45 Na2SO4, 10 EGTA, 7 ATP, 10 creatine phosphate. Note specifically that the low calcium concentration of the relaxing solution did not permit any actin-myosin based active force production during the experiments [8,25,35].

Protocol: Experiment 1: Myofibrils (n=8) were passively stretched [8] from a nominal initial average sarcomere length of about 2.6μm by nominal amounts of 2.0, 2.5, and 3.0 μm/sarcomere at a speed of 0.1μm/s/sarcomere [16] and then released at the same speed to the starting length. Three consecutive stretch-shortening cycles were performed without rest, followed by one or two subsequent sets of three stretch-shortening cycles separated by a ten minute rest at an average sarcomere length of 2.6μm.

Experiment 2: Using separate myofibrils (n=8), the testing protocol described in the previous paragraph was repeated with the exception that myofibrils were rested for ten minutes between sets at an average sarcomere length of 1.8 μm (instead of 2.6μm used in the first protocol). Note that neither resting length was associated with a measurable passive force.

Experiment 3: Finally, another set of myofibrils (n=5) was stretched passively from an average sarcomere length of 2.6μm by a nominal amount of 2.0μm/sarcomere at a speed of 0.1μms/sarcomere. When the final stretch length was reached, myofibrils were subjected to ten stretch-shortening cycles of nominal magnitude 0.5, 1.0, or 1.5μm per sarcomere, and then, following the last of these cycles, released to the starting length. In contrast to the first two experiments where at least partial re-folding of Ig domains was expected during myofibril shortening, in these last set of experiments, Ig domain re-folding was not expected to occur because of the length of titin during the repeat stretch-shortening cycles and the significant amount of force [29,32–33].

Analysis: The primary outcome measures in this study were the peak forces obtained in the stretch shortening cycles, the loading energies of all stretch cycles, the hysteresis for the three repeat stretch-shortening cycles of experiments 1 and 2, and the peak forces, loading energies, and hysteresis for the ten stretch-shortening cycles of 0.5μm amplitude in experiment 3. Loading energies were calculated as the integral of the force-elongation curves during the loading phase. Unloading energies were calculated as the integral of the force-elongation curves during the unloading phase. Hystereses were calculated as the loading minus the corresponding unloading energy in a stretch-shortening cycle.

The primary statistical analyses that were performed included comparisons of the anticipated

JURA
Journal of Undergraduate Research in Alberta • Volume 4 • 2014

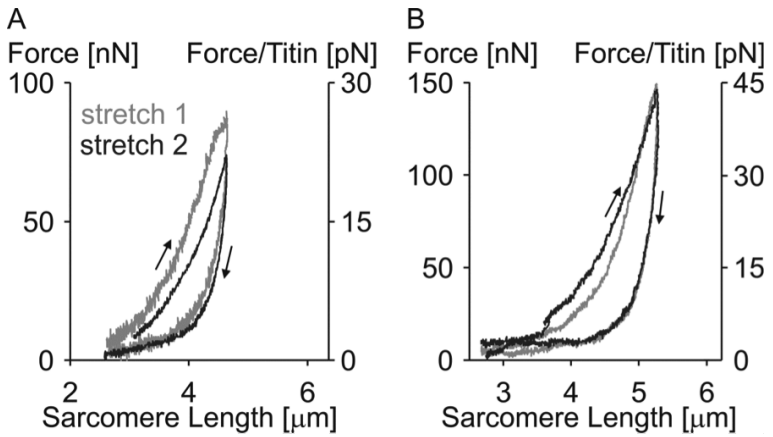

Figure 4:

Exemplar stretch-shortening cycles of a single myofibril stretched from an initial average sarcomere length of about 2.6μm. (A) Stretch 1 is the first stretch-shortening cycle of set 1, while stretch 2 is the first stretch-shortening cycle of set 2 which occurred after a ten minute rest period with the myofibril relaxed at an average sarcomere length of 2.6μm. Note that the peak force and loading energy is substantially decreased in stretch 2 compared to stretch 1, indicating incomplete recovery, and thus incomplete refolding of Ig domains in the ten minute rest period. (B) Stretch 1 is the third stretch-shortening cycle of set 1, while stretch 2 is the first stretch-shortening cycle of set 2 which occurred after a ten minute break with the myofibril relaxed at an average sarcomere length of 2.6μm. Note the similarity in loading energy and peak force between the first stretch of set 2 and the last stretch of set 1, suggesting that there was little (if any) recovery of passive force in the ten minute rest period at a sarcomere length of 2.6μm. indicating little or no refolding of Ig domains in the break. Forces on the left axes are the measured myofibril forces (nN) while forces on the right axes represent an estimate of the forces in a single titin molecule (pN) assuming 2700 titin molecules per μm2.

decrease in peak forces, loading energies, and hysteresis for the three repeat stretch-shortening cycles, the recovery of peak force and hysteresis after the ten minute rest at average sarcomere lengths of 2.6μm (experiment 1) and 1.8μm (experiment 2), and the decrease in peak force, loading energies, and hysteresis in the ten repeat shortening-stretch cycles of 0.5μm amplitude at the long sarcomere lengths of experiment 3. All values are given as means ±1SE, and changes in outcome measures between repeat stretch-shortening cycles (either with or without break) were assessed using non-parametric Friedmans repeated measures testing [36] with a=0.05.

Results

Experiment 1: Peak forces during the stretch shortening cycles were reduced significantly ($p<0.05$) by 16% and 11% for cycles 1, 2, and insignificantly for cycle 3 (3%), respectively of set 2 compared to the corresponding cycles in set 1 (Fig. 4A). Furthermore, the peak forces of the 1st cycle of the second set were similar (109±26nN) to the peak forces of the 3rd cycle of the first set (112±26nN), indicating that there was no significant force recovery in the 10 minute rest period between sets, when myofibrils were rested at an average sarcomere length of 2.6μm (Fig. 4B). Similarly to the peak forces, the loading energies were reduced significantly ($p<0.05$) by 30% and 13% for cycles 1, 2, but not for cycle 3 (0%), respectively of set 2 compared to the corresponding cycles in set 1 (Fig. 4A). Also, the loading energies of the 1st cycle in the 2nd set were similar (86±25nNμm) to the 3rd cycle in the first set (78±18nNμm), indicating that there was no substantial recovery of loading energy in the 10 minute rest period between sets, when myofibrils were rested at an average sarcomere length of 2.6μm (Fig. 4B). The energy loss (hysteresis) expressed relative to the corresponding loading energies were the same for the first and second sets and averaged 60, 53, and 48% for cycles 1, 2, and 3, respectively.

Experiment 2: In contrast to experiment 1, the peak forces during the stretch-shortening cycles were not reduced between the first and second set of stretch-shortening cycles in experiment 2 (Fig. 5A). In fact, peak forces in the second set tended to be slightly (but not significantly) higher by 8%, 7%,

JURA
Journal of Undergraduate Research in Alberta • Volume 4 • 2014

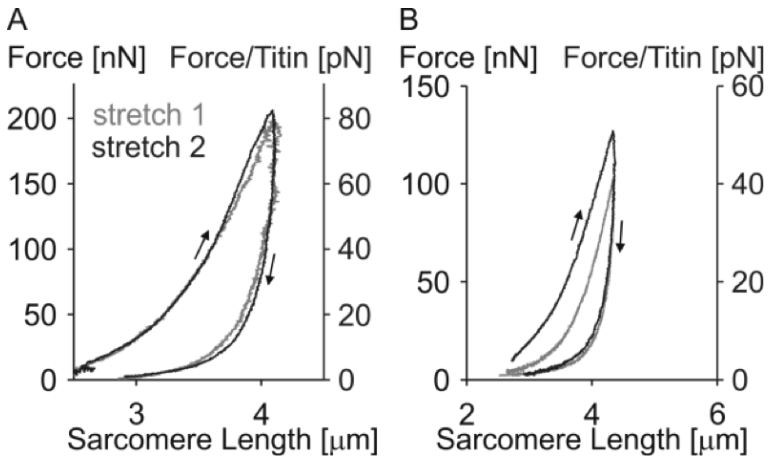

Figure 5:
Exemplar stretch-shortening cycles of a single myofibril stretched from an initial average sarcomere length of about 2.6μm. (A) Stretch 1 is the first stretch-shortening cycle of set 1, while stretch 2 is the first stretch-shortening cycle of set 2 which occurred after a ten minute rest period with the myofibril relaxed at an average sarcomere length of 1.8μm. Note that the peak force and loading energy are essentially the same, indicating complete recovery, and thus complete refolding of Ig domains in the ten minute rest period. (B) Stretch 1 is the third stretch-shortening cycle of set 1, while stretch 2 is the first stretch-shortening cycle of set 2 which occurred after a ten minute break with the myofibril relaxed at an average sarcomere length of 1.8μm. Note the substantial increase in loading energy and peak force in the first stretch of set 2 (purple) compared to the last stretch of set 1 (yellow), suggesting a big recovery of passive force in the ten minute rest period at a sarcomere length of 1.8μm, indicating substantial refolding of Ig domains in the rest period. Forces on the left axes are the measured myofibril forces (nN) while forces on the right axes represent an estimate of the forces in a single titin molecule (pN) assuming 2700 titin molecules per um^2.

and 7% respectively for cycles 1, 2, and 3 compared to the corresponding peak forces in the first set. Consistent with these results, the peak forces in the 1st cycle of the second set were significantly higher ($p<0.05$) (107±11nN) than the peak forces in the 3rd cycle of the first set (92±11nN), indicating a susbstantial recovery of force when myofibrils were rested for ten minutes at an average sarcomere length of 1.8μm (Fig. 5B). Although the loading energies were slightly reduced in the second set by 11%, 4%, and 4% for cycles 1, 2, and 3, respectively, only the values for the first cycle were statistically different (Fig. 5A). In agreement with the peak forces, the loading energy of the 1st cycle in the second set was significantly ($p<0.05$) higher (79±8nNμm) than the loading energies of the 3rd cycle in the first set (51±6nNμm), thereby indicating a great recovery of loading energy in the ten minute rest period when myofibrils were held at an average sarcomere length of 1.8μm (Fig. 5B). Energy losses (hysteresis) relative to the loading energies were the same for the corresponding stretch-shortening cycles in the first and second set and averaged 68, 49, and 45% for cycles 1, 2, and 3, respectively, values similar to those obtained in experiment 1.

Experiment 3: The loss in peak force across the ten repeat stretch-shortening cycles at long sarcomere lengths was 11

Most importantly, however, the hystereses observed in experiments 3 were much smaller than in experiments 1 and 2 and ranged from 5nNμm (for cycle 1) to 1nNμm (for cycle 10) with an average value of 3nNμm, compared to 72 nNμm (cycle 1, experiment 1) to 37nNμm (cycle 3, experiment 1), and 61 nNμm to 23nNμm, for cycle 1 and 3, respectively of experiment 2. However, the absolute hysteresis might not be good for comparison, since the stretch-shortening amplitude affects these values. However, by expressing the hysteresis (energy loss) in terms of the loading energy provides an indication of the energy loss in the different experiments.

The energy loss (hysteresis) relative to the loading energies averaged 14%, 14% and 27% for stretch-shortening amplitudes of 0.5, 1.0 and 1.5μm, respectively, with the highest value of 34% (1st cycle for 1.5μm amplitude) and the smallest value of 8%

(cycles 7-10 for 0.5μmm amplitude). These values are all much smaller than the corresponding values given above for experiments 1 (48-60%) and 2 (45-68%), indicating a much more elastic (less energy loss) response. The smallest energy loss values of 8% are similar to those obtained for tendinous materials [37].

Discussion

Titins I-band regions act as a molecular spring [15], providing most of the passive force in isolated sarcomeres [8,23] and myofibrils [8,23,33,35]. Titin consists of several spring regions with different properties arranged in series [15,29–32]: the proximal Ig domain, the N2A and PEVK domains, and the distal Ig domain. While studying isolated titin molecules using a laser tweezer approach, Kellermayer and colleagues [29] discovered that titin acted virtually elastically for stretch-shortening cycles corresponding to short sarcomere lengths and forces below approximately 25pN (Fig. 2), and at lengths corresponding to long sarcomeres where Ig domains were assumed to remain permanently unfolded [29,32]. However, when titin was pulled to lengths beyond Ig domain unfolding, it showed a large hysteresis with a corresponding great loss of energy in the stretch-shortening cycle. These results by Kellermayer et al. [29,32]suggest that titin can act as a virtually elastic spring, if Ig domain unfolding and refolding is prevented. Such situations could occur at very short sarcomere lengths, prior to any Ig domain unfolding [33], and at long sarcomere lengths if Ig domain un/refolding is prevented. Since it appears impossible to have all Ig domains unfolded within physiologically relevant sarcomere lengths [16,29,33], the elastic region of titin can potentially be shifted to different sarcomere lengths, by pre-unfolding titin Ig segments permanently in cyclic movements over a given range of sarcomere lengths.

However, these theoretical considerations, and experimental findings on isolated titin molecules have never been tested systematically for titin in their native and structurally correct environment of a sarcomere, although detailed analysis of titins properties at sarcomere lengths below which Ig domain unfolding occurs (3.0-3.5μm) in rabbit psoas muscles - [16,29] have been made [33]. Therefore, the purpose of this study was to test under what conditions Ig domain refolding occurs in sarcomeres, and if there is indeed a virtually elastic region of passive sarcomere stretch-shortening cycles when Ig domain refolding is prevented at long sarcomere lengths. Experiments were performed using isolated myofibrils from rabbit psoas muscles which have been shown to have passive forces that originate almost exclusively from titin, and represent titin properties well [16,33].

We would like to emphasize two major results obtained in this study. The first is that after ten minutes of recovery, peak forces and loading energies did not recover substantially when myofibrils were rested at an average sarcomere length of 2.6μm (Figs 4A and B), but peak forces and loading energies recovered almost completely when myofibrils were rested at an average sarcomere length of 1.8μm (Figs. 5A and B). These findings suggest that in the ten minute recovery between stretch-shortening sets, unfolded Ig domains were able to refold at sarcomere lengths of 1.8μm but not at sarcomere lengths of 2.6μm. There is no passive force in psoas myofibrils at sarcomere lengths of 2.6μm or less, thus forces in titin would be zero too. This result suggests, that in contrast to isolated experiments in titin [29], and previous work in rabbit psoas myofibrils [33] spontaneous refolding of Ig domains does not necessarily occur when forces in titin become low (less than about 2-3pN [29,32]), but requires sarcomere lengths, and thus titin lengths, to be short as well for effective refolding. The threshold length for Ig domain refolding to occur effectively lies somewhere between 2.6 and 1.8μm (for rabbit psoas), but cannot be narrowed down at present as only observations from these two resting lengths are available.

When no rest was given between stretch-shortening cycles, peak forces, loading energies, and hysteresis decreased from cycles 1-3 in experiments 1 and 2, indicating that Ig domains remained permanently unfolded after the first cycle, thereby providing a more elastic response with increasing cycle number. This property has been observed in a previous study on isolated myofibrils [16,33] and is consistent with observations on isolated titin molecules [29,32].

The second result to be emphasized is the virtually elastic behaviour of myofibrils in the last few stretch-shortening cycles of experiment 3, in which effective Ig domain un/refolding was prevented by the experimental protocol design (Fig. 6). Experiment 3 was designed to minimize Ig domain refolding for

JURA
Journal of Undergraduate Research in Alberta • Volume 4 • 2014

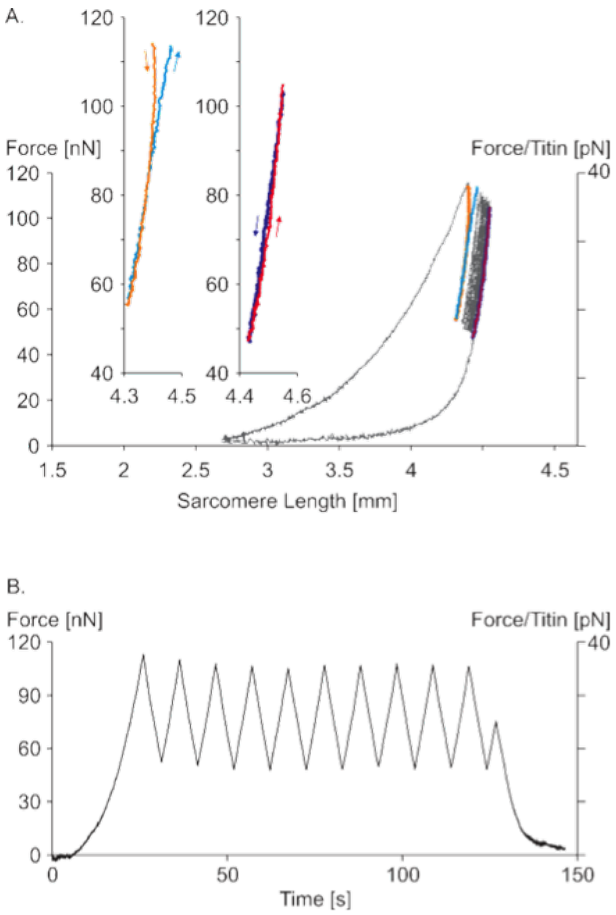

Figure 6:

Force-sarcomere length (A) and force-time relationships (B) for an exemplar myofibril in experiment 3. The myofibril was stretched from an initial length of approximately 2.7μm/sarcomere to a final length of about 4.2μm/sarcomere followed by ten repeat shortening-stretch cycles of small magnitude (note the last cycle is only half the magnitude of the previous cycles). There is a small loss of peak force in the ten repeat stretch-shortening cycles indicating visco-elastic creep. Note the virtually elastic behaviour for the ten repeat stretch-shortening cycles at long sarcomere lengths where (some) Ig domains are unfolded. The left inset shows the first of the ten stretch-shortening cycles, the right inset the tenth one. In the left inset, the shortening (yellow) is matched by the subsequent stretch (blue) curve for the low force values (50-90nN) but then the stretch curve (blue) falls off to longer length. This behaviour suggests that there was no effective refolding of Ig domains, but that towards the end of the stretch, additional Ig domains became unfolded, causing the slight decrease in peak force and increased length. In the right inset (tenth full cycle), the red (shortening) and blue (stretching) curves essentially overlap, thereby displaying an essentially elastic response, suggesting that effective unfolding and refolding of Ig domains was prevented. This is in stark contrast to the big hysteresis (and energy loss), when the myofibril is returned to its original (2.7μm) length. Forces on the left axes are the measured myofibril forces (nN) while forces on the right axes represent an estimate of the forces in a single titin molecule (pN) assuming 2700 titin molecules per μm2.

stretch-shortening cycles at long sarcomere lengths where Ig domains were known to have unfolded in the first stretch cycle. Experiments for all three magnitudes of stretch-shortening cycles (0.5, 1.0 and 1.5μm) at these long sarcomere lengths showed substantially less energy loss (hysteresis) relative to the loading energies, than stretch-shortening cycles in experiments 1 and 2. This finding suggests that titin can act almost elastically at long lengths, if Ig domain refolding is prevented, thereby minimizing energy loss for repeat passive motion. The sarcomere lengths where this virtually elastic behaviour can be

elicited can vary, as it merely requires that the Ig domains within the range of the stretch-shortening cycle remain permanently unfolded. This range of sarcomere lengths can vary, as the number of permanently unfolded Ig domains determines at what lengths elastic behaviour is observed.

The reason why the stretch-shortening cycles of experiment 3, even after ten repeat cycles were not perfectly elastic (there remained a tiny hysteresis of about 8%), is likely associated with the time-dependent unfolding of Ig domains [7,38,39]. Ig domain unfolding does not only depend on the force acting on titin and its Ig domains, but is also a stochastic process, in which the energy barrier for Ig domain unfolding can be exceeded even in the absence of high external forces. Since our stretch-shortening cycles were performed at a slow speed (0.1μm/s per sarcomere) a stretch-shortening cycle of 0.5μm/s per sarcomere takes 10s to complete, which is ample time for Ig domains to unfold. We predict however, that if our experiments had been done at a greater speed (lets say 1μm/s per sarcomere), the hysteresis observed in experiment 3 would have been essentially abolished giving a virtually elastic passive behaviour of the myofibrils. Another way to test the idea of stochastic unfolding of Ig domains in the stretch-shortening experiments of experiment 3 would be to stretch myofibrils to the initial long lengths, but then allow the myofibrils to stress relax to allow for time-dependent unfolding of Ig domains to occur. Starting the ten repeat stretch-shortening cycles after such stress relaxation should give an essentially elastic behaviour of passive myofibrils as all Ig domains would be unfolded (in the ideal experiment) and no refolding could occur as force and sarcomere length are too high for refolding to occur. This last experiment would essentially mimic the approach by Kellermayer and colleagues [32] where they stretched isolated titin molecules to such long lengths that all Ig domains were unfolded. Shortening from such long lengths then revealed an essentially elastic behaviour of titin. Unfortunately, such an experiment cannot be performed with titin in situ, as the stretch required for all Ig domains of titin to unfold, would go beyond the failure lengths of intact sarcomeres [40]. However, increasing the stretch-shortening speed, and achieving (near) complete Ig domain unfolding with a stress relaxation test at long sarcomere lengths, should allow for testing the changing mechanical properties of titin.

A secondary result of potential importance is the fact that stiffness of titin changes as a function of the history of loading. For example, in Fig. 6, stiffness of titin for the first stretch cycle from 2.7-4.2μm is substantially smaller than the stiffness observed in the ten repeat stretch shortening cycles, as can be seen by the slope of the force-sarcomere length curves. Therefore, it appears that not only titins visco-elastic properties but also its stiffness at a given (sarcomere-) length can change substantially and affect the instantaneous passive properties of muscle. In summary, our results suggest that titin is a molecular spring with high visco-elasticity and associated energy loss during passive stretch-shortening cycles when Ig domain unfolding and refolding is allowed to occur. However, at lengths prior to Ig domain unfolding (average sarcomere lengths of about 3.0-3.5μm for rabbit psoas) [16,29], or at lengths after Ig domain unfolding has occurred (3.5μm) but Ig domain refolding is prevented, titin can act as an essentially elastic spring, thereby minimizing energy losses in passive stretch-shortening cycles. Since not all Ig domains will ever be unfolded within feasible sarcomere lengths, it appears that the region of near-elastic behaviour can be adapted to any lengths for repeat stretch-shortening cycles if Ig domain refolding is prevented either by the speed of the stretch-shortening cycles or by the length of the sarcomeres.

Titins properties are known to vary with activation because of calcium binding, phosphorylation and titin-actin interaction in active muscle [13,14,27,41−45]. It will be important to elucidate the detailed behaviour and properties of titin in stretch-shortening cycles while activated. However such experiments are infinitely more difficult to perform than the passive experiments presented here, as one must distinguish between the time dependent cross-bridge forces and titin forces contributing to the total force in activated preparations.

In conclusion, we suggest that titin is a molecular spring whose (visco-) elastic properties and stiffness are governed by the unfolding/refolding kinetics of the Ig domains, and that the elastic behaviour of titin can shift to the required working range for repeat stretch-shortening cycles.

References

1. Wilkie, D. R. Studies in Biology, No. 11, Muscle. 1968. London, Edward Arnold Publishers Ltd.
2. Herzog, W., in Biomechanics of the Musculoskeletal System, Nigg, B. M. and Herzog, W., Eds. John Wiley and Sons Ltd. ed. 2nd , 1999, p.p. 148-188.
3. Woledge, R. C., Curtin, N. A., and Homsher, E. Energetic aspects of muscle contraction. 245. 1985. London, Academic Press.
4. Wang, K., Mcclure, J., and Tu, A., Proc Natl.Acad.Sci U.S.A 76 (8), 1979.
5. Maruyama, K., J Biochem. 80 (2), 1976.
6. Maruyama, K., FASEB J. 11 , 1997.
7. Duvall, M. M., Gifford, J. L., Amrein, M., and Herzog, W., Eur.Biophys.J. 42 , 2012.
8. Joumaa, V., Rassier, D. E., Leonard, T. R., and Herzog, W., Am J Physiol Cell Physiol 294 (1), 2008.
9. Labeit, D., Watanabe, K., Witt, C., Fujita, H., Wu, Y., Lahmers, S., Funck, T., Labeit, S., and Granzier, H. L. M., Proc Natl Acad Sci U S A 100 , 2003.
10. Astier, C., Raynaud, F., Lebart, M. C., Roustan, C., and Benyamin, Y., FEBS Lett. 429 (1), 1998
11. Kulke, M., Fujita-Becker, S., Rostkova, E., Neagoe, C., Labeit, D., Manstein, D. J., Gautel, M., and Linke, W. A., Circ.Res. 89 (10), 2001.
12. Linke, W. A., Kulke, M., Li, H., Fujita-Becker, S., Neagoe, C., Manstein, D. J., Gautel, M., and Fernandez, J. M., Journal of Structural Biology 137 , 2002.
13. Nagy, A., Cacciafesta, P., Grama, L., Kengyel, A., Malnasi-Csizmadia, A., and Kellermayer, M. S. Z., J Cell Sci 117 (Pt 24), 2004.
14. Herzog, W., Duvall, M., and Leonard, T. R., Exerc.Sport Sci.Rev. 40 (1), 2012.
15. Granzier, H. L. M. and Labeit, S., Muscle Nerve 36 (6), 2007.
16. Herzog, J. A., Leonard, T. R., Jinha, A., and Herzog, W., J.Biomech. 45 (11), 2012.
17. Granzier, H. L. M. and Labeit, S., Exerc Sport Sci Rev 34 (2), 2006.
18. Maruyama, K., Kimura, S, Kuroda, M, and Handa, S, J.Biochem 82 , 1977.
19. Granzier, H. L. M., Kellermayer, M. S. Z., Helmes, M., and Trombits, K., Biophys J 73 , 1997.
20. Linke, W. A., Popov, V. I., and Pollack, G. H., Biophys J 67 (2), 1994.
21. Horowits, R. and Podolsky, R. J., J Cell Biol 105 , 1987.
22. Horowits, R., Kempner, E. S., Bisher, M. E., and Podolsky, R., Nature 323 , 1986.
23. Joumaa, V., Rassier, D. E., Leonard, T. R., and Herzog, W., Pflgers Arch - Eur J Physiol 455 , 2007.
24. Herzog, W. and Leonard, T. R., J Exp Biol 205 , 2002.
25. Leonard, T. R. and Herzog, W., Am.J Physiol Cell Physiol 299 , 2010.
26. Leonard, T. R., Duvall, M., and Herzog, W., Am J Physiol Cell Physiol 299(6) , 2010.
27. Herzog, W., Leonard, T., Joumaa, V., Duvall, M., and Panchangam, A., Mol.Cell Biomech. 9 (3), 2012.
28. Rassier, D. E., Herzog, W., and Pollack, G. H., Proc.R.Soc.Lond.B 270 , 2003.
29. Kellermayer, M. S. Z., Smith, S. B., Granzier, H. L. M., and Bustamante, C., Science 276 (5315), 1997.
30. Rief, M., Gautel, M., Oesterhelt, F., Fernandez, J. M., and Gaub, H. E., Science 276 (5315), 1997.
31. Tskhovrebova, L., Trinick, J., Sleep, J. A., and Simmons, R. A., Nature 387 , 1997.
32. Kellermayer, M. S., Smith, S. B., Bustamante, C., and Granzier, H. L., J.Struct.Biol. 122 (1-2), 1998.
33. Minajeva, A., Neagoe, C., Kulke, M., and Linke, W. A., J Physiol (Lond) 540.1 , 2002.
34. Joumaa, V., Leonard, T. R., and Herzog, W., Proc R Soc B 275 , 2008.
35. Bartoo, M. L., Linke, W. A., and Pollack, G. H., Am J Physiol 273 , 1997.
36. Hinkle, D. F., Wiersma, W., and Jurs, S. G., in Applied Statistics for the Behavioural Sciences Rand McNally College Publishing Co , 1979, p.p. 332-367.
37. Alexander, R. M. and Bennet-Clark, H. C., Nature 265 , 1977.
38. Best, R. B., Fowler, S. B., Herrera, J. L., Steward, A., Paci, E., and Clarke, J., J Mol Biol 330 (4), 2003.
39. Best, R. B., Brockwell, D. J., Toca-Herrera, J. L., Blake, A. W., Smith, D. A., Radford, S. E., and Clarke, J., Anal.Chim.Acta 479 , 2003.
40. Leonard, T. R., Joumaa, V., and Herzog, W., J.Biomech. 43 (15), 2010.
41. Coulis, G., Becila, S., Herrera-Mendez, C. H., Sentandreu, M. A., Raynaud, F., Richard, I., Benyamin, Y., and Ouali, A., Biochemistry (Mosc). 47 (35), 2008.

42. Funatsu, T., Higuchi, H., and Ishiwata, S., J Cell Biol 110 (1), 1990.

43. Tatsumi, R., Maeda, K., Hattori, A., and Takahashi, K., J Muscle Res Cell Motil 22(2) , 2001.

44. Anderson, B. R., Bogomolovas, J., Labeit, S., and Granzier, H. L. M., J.Struct.Biol. 170 , 2010.

45. Yamasaki, R., Wu, Y., McNabb, M., Greaser, M., Labeit, S., and Granzier, H. L. M., Circ.Res. 90 (11), 2002.

JURA
Journal of Undergraduate Research in Alberta • Volume 4 • 2014

No Evidence for S Isotope Fractionation During SO_2 Oxidation at a Continental Location

J. Kolodziej, A.L. Norman, O. Rempillo
University of Calgary

Sulfur isotope fractionation during SO_2 oxidation has been shown to occur in laboratory experiments [1] but this has not been observed in whole air samples [2]. Here we replicate the laboratory experiments in a systematic manner using ambient air. Particulate matter and SO_2 in ambient air were collected at Calgary in the Fall of 2012 using high volume samplers and impingers. Atmospheric SO_2 and SO_4 concentrations and isotope characteristics were determined. Variations in the concentration of SO_2 and SO_4 in the atmosphere did not reflect changes in $\delta^{34}S$ values, suggesting the independence of $\delta^{34}S$ from concentration. Average $\delta^{34}S_{SO2}$ (± std. dev.) from the high volume samplers was + 13.2‰ ± 0.2‰. SO_2 from the impinger method over the same sampling period yielded a $\delta^{34}S_{SO2}$ value of +14.0‰ ± 0.2‰. Standard deviation for the impinger samples could not be calculated and hence this ± 0.2‰ is the precision due to the spectrometer. $\delta^{34}S_{SO4}$ values (± std. dev.) ranged from + 9.9‰ ± 0.5‰ to +15.3‰ ± 0.2‰. $\delta^{34}S_{SO2}$ values from the high volume and impinger samples were similar (+13.2‰ versus +14.0‰, respectively) which shows these collection methods are equivalent. Differences between the impinger and high volume sampler $\delta^{34}S$ values for SO_2 and submicron aerosol SO_4 were used to gauge sulfur isotope fractionation. Standard deviations for differences were greater than averages ($\Delta\delta^{34}S_{SO2}$ avg.= -0.80‰, s=1.76‰; fine $\Delta\delta^{34}S_{SO4}$ avg.=+0.28 ‰, s=5.15‰), indicating little to no fractionation. Additionally, $\delta^{34}S_{SO2}$ and $\delta^{34}S_{SO4}$ values were compared to the maximum percent SO_2 that may have reacted to form SO_4. No pattern was evident so the conclusion is that sulfur isotope fractionation in ambient air is negligible under the conditions sampled.

Literature: 1.Harris, E., Sinha, B., Hoppe, P., Foley, S., Borrmann, S. (2012). Fractionation of sulfur isotopes during heterogeneous oxidation of SO 2 on sea salt aerosol: a new tool to investigate non-sea salt sulfate production in the marine boundary layer. Atmos. Chem. Phys. 12. 2. Norman, A.L., Krouse, H.R., MacLeod, J. (2004). Air Pollution Modeling and Its Application XVI.

Keywords: Isotopes – atoms of an element with the same number of protons but a different number of neutrons in the nucleus, Fractionation – a change in the ratio of heavy to light isotopes due to some biological, chemical, or physical process, Sulfur, Sulfate, Sulfur dioxide, Oxidation, Atmosphere.

JURA
Journal of Undergraduate Research in Alberta • Volume 4 • 2014

$$\delta^{34}S(‰) = \left(\frac{\left\{\frac{^{34}S}{^{32}S}\right\}_{sample}}{\left\{\frac{^{34}S}{^{32}S}\right\}_{standard}} - 1 \right) \times 1000$$

Figure 1:
Chemical equations for the oxidation of SO_2 to SO_4 with photochemistry. M refers to light energy. H_2SO_4 is a diprotic acid and is ionized to H+ and SO_4^{2-}

Introduction

Variations of natural sulfur isotope abundances in atmospheric sulfur compounds have been used to track the contributions of isotopically distinct sources of SO_2 (sulfur dioxide), and their oxidation to SO_4 (sulfate) in marine and continental airsheds [1]. For example, SO_2 isotope analysis of well-mixed air on Saturna Island, Canada, indicated SO_2 contributions to the atmosphere originating from a U.S. oil refinery and tidal flats [2]. A key assumption in these apportionment studies is that isotope fractionation during SO_2 oxidation is small so that they accurately reflect their source. This assumption can be tested by studying if fractionation either occurs or not during oxidation, which is detectable by comparing isotope values of SO_2 and SO_4. Isotope fractionation is the separation of isotopes of an element as a result of the difference in mass between their nuclei. Processes resulting in large sulfur isotope fractionation include bacterial conversion of sulfur compounds, such as in bacterial sulfate reduction wherein the heavy sulfur isotope (^{34}S) is favored in the product, H_2S (hydrogen sulfide), which is consequently lost from the reactant pool. However, very little isotope fractionation has been observed in association with many other sulfur conversion processes, such as mineral salt formation, condensation of sulfate precipitates, or dissolution of sulfides [3].

Atmospheric sulfur can be both naturally occurring and anthropogenic. Sources of naturally occurring sulfur include volcanic exhalations, sea spray, and hydrogen sulfide from anoxic ocean waters and sea marshes. Anthropogenic sources include aeolian transport of pulverized sulfide ores or sulfur emissions from ore smelting activities, vehicular emissions, as well as the combustion of coal, and petroleum products. Especially in Alberta, emissions from processing and extracting sour gas (any gas containing large amounts of hydrogen sulfide) could be contributing significantly to local levels of atmospheric sulfur [4]. Of the naturally occurring isotopes of sulfur, the four most stable are ^{32}S, ^{33}S, ^{34}S and ^{36}S [3].

SO_2 in the atmosphere is oxidized in gas phase, in aqueous phase in raindrops, and on the surfaces of particles [5]. The rates of oxidation processes within the atmosphere are influenced by temperature and reactions with light (photochemistry). A common pathway for the oxidation of SO_2 to SO_4 (sulfate) with the effects of photochemistry is given in Figure 2 [5,6]. Finlayson-Pitts and Pitts [5] also found that SO_2 oxidation is greater during the day and in the summer months than at night and in the winter months. This may have changed the findings of the study if it was performed during summer instead of the winter (though collection occurred during both day and night). It is during the above process and similar processes that sulfur isotope fractionation may occur.

In a study performed by Harris et al. (2012), isotopic fractionation of sulfur was demonstrated during heterogeneous oxidation of SO_2 on sea salt aerosol [7]. It was also found that as pH increased isotopic fractionation was larger. Harris et al. also studied isotope fractionation for SO_2 oxidation reactions with O_3 (ozone) and salts. The fractionation factor ($\alpha 34 = R_{product}/R_{reactant}$ where $R = {}^{34}S/{}^{32}S$) Harris et al. measured showed that fractionation by ozone in water droplets and sea salt aerosol favoured the heavier sulfur isotope, ^{34}S, in the product sulfate (αseasalt = 1.0124 ± 0.0017). Conversely, oxidation in NaOCl (sodium hypochlorite) droplets favoured ^{32}S, in sulfate (αOCl = 0.9882 ± 0.0036). As such, the products were enriched in ^{34}S and ^{32}S respectively. Samples for Harris et al.s [7] study were collected using an impinger (liquid filled vial into which air or a gas is bubbled), which is one method used in this study to find $\delta^{34}S$ values of SO_2.

Whether or not sulfur isotope fractionation occurs during SO_2 oxidation in ambient samples in the atmosphere has been the focus of a number of studies. For example, Norman et al. (2004 and 2009) showed no evidence for sulfur isotope fractionation during SO_2 oxidation in the city of Calgary, Alberta and on

JURA
Journal of Undergraduate Research in Alberta • Volume 4 • 2014

the west coast of Canada [2,8]. High volume samplers, rather than impingers were used to collect particulate matter on a series of filters, followed by a filter treated with a K_2CO_3 (potassium carbonate) or triethanolamine and glycerol mixture, to trap SO_2. The discrepancy between the findings of Harris et al. and Norman could in fact be due to the different collection methods (impinger vs high volume). In the current study the high volume method from Norman [9] was used to obtain $\delta^{34}S$ values for both SO_2 and submicron aerosol SO_4, which was then compared directly to the impinger SO_2 values to resolve the discrepancy in methods.

The experiment described here replicates the methods of Harris et al.s [7] study to determine whether sulfur fractionation is indeed occurring during SO_2 oxidation in the atmosphere. If the null hypothesis is rejected then sulfur isotope fractionation does occur during SO_2 oxidation in ambient air in a non-marine environment. This will be evidenced by little to no difference between the $\delta^{34}S_{SO2}$ and $\delta^{34}S_{SO4}$ values. Marine and non-marine environments may differ in regards to fractionation as sea salt aerosols could influence the process [7]. If the high volume and impinger samplers yield the same isotope values then the question of collection method interfering with fractionation will also be resolved.

Methods

2.1 Nomenclature and Notation: The isotopic composition of a sample is expressed with the δ (delta) notation, which is defined as the ratio of a heavy isotope to the most abundant isotope in the sample compared to a standard (Fig. 1). The most abundant isotope in this case is ^{32}S. Since isotope effects are commonly quite small, it is useful to refer to the differences in parts per thousand (‰). The accepted standard that is used is $^{32}S/^{34}S = 22.22$ from troilite in the Canyon Diablo meteorite [3].

2.2 Impingers: The impinger method was used to obtain only SO_4 samples. Air was bubbled into a series of impingers in a manner similar to the setup used in the study performed by Harris [7]. Two of the three impingers were filled with a solution of 5% H_2O_2 (30% H_2O_2 and de-ionized water in a 1:5 ratio). Each impinger was filled with ∼70 mL of this solution and an additional amount was sometimes added to samples during collection if the solution was running low. An empty third impinger was used for overflow; in the event some solution entered the tubes it would be deposited here instead of in the diaphragm pump (Fig. 3A). The impingers were placed inside a rooftop laboratory at the University of Calgary. Tubing with a 0.45 micron glass filter to remove dust was brought through a window and was connected to the impinger. A diaphragm pump was attached to the downstream side of the impinger and drew in air at a rate of 1.0 L/min ± 0.1 L/min (± precision). Six samples were collected for an average of three days each from Oct. 18, 2012 through to Dec. 6, 2012.

Sample solutions from the impingers were poured into a graduated cylinder and rinsed with de-ionized water to quantitatively transfer all the SO_4. The total volume was recorded and two 10mL vials were filled for ion chromatography from which a concentration was obtained. $BaCl_2$ (5ml) was added to the remaining sample to precipitate $BaSO_4$ and sufficient HCl (hydrochloric acid) was added to ensure no $BaCO_3$ was present (pH <3). The solutions were then evaporated on a hot plate and reduced to less than 50 mL. The samples were then filtered using a 0.4μm nucleopore filter paper, similar to the process in Seguin et al. [10]. The precipitate mass, normalized for the volume of air sampled, was used to obtain sulfate concentrations gravimetrically. Samples were run through the mass spectrometer in the Applied Isotope Geochemistry lab in the University of Calgary. The analytic precision for the isotopic analyses was ± 0.2‰ and the values were also corrected for blank sulfur.

2.3 High Volume Samplers: The high volume sampler method yielded both SO_2 and SO_4 samples. Air was drawn through a series of slotted filter papers using high volume samplers so that particulate matter in the air was filtered out. Two high volume samplers were run in unison in this study, one to obtain $\delta^{34}S_{SO2}$ values and the other to obtain $\delta^{34}S_{SO4}$ values . On one sampler a total particulate filter overlaying an SO_2 filter was deployed so that any particulates such as dust particles would be filtered out and only the SO_2 would be collected. The second sampler was fitted with five slotted size-segregated filters, housed in a cascade impactor, so only fine aerosols (<0.49 microns in diameter) were collected on the underlying particulate fibre filter (Fig. 3B). Flow rates were 800 L/min ± 1 L/min and 1000 L/min ± 1 L/min for the two samplers respectively. A malfunction occurred

JURA
Journal of Undergraduate Research in Alberta • Volume 4 • 2014

$$SO_2 + OH\ (+M) \xrightarrow{yields} HSO_3$$
$$HSO_3 + O_2 \xrightarrow{yields} SO_3 + HO_2$$
$$SO_3 + H_2O \xrightarrow{yields} H_2SO_4$$

Figure 2:
Formula for delta notation. Delta notation is the standard way to represent the isotopic composition of a sample.

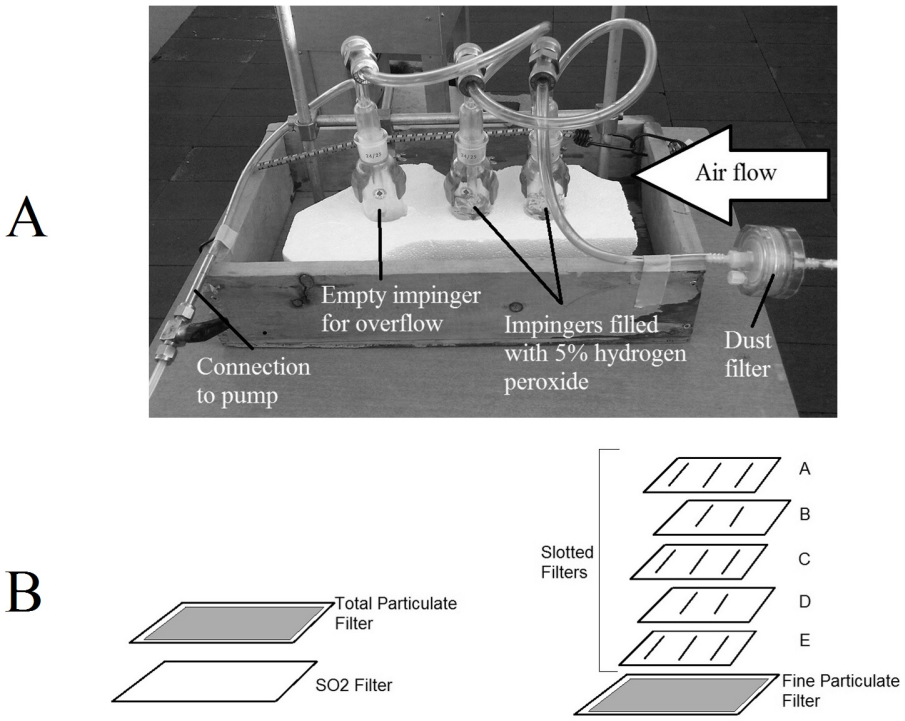

Figure 3:
Set-up of the impinger (A) and high volume (B) apparatus that were used to collect the samples from which δS values were then obtained. The high volume setup on the left collected for SO_2 while the setup on the right collected fine particulates for SO_4.

during the collection period of sample 2 resulting in unreliable concentrations for the fine particulate matter sample. A new high volume sampler (1020 L/min ± 1 L/min) was then installed and for samples 3 through 6, the new sampler operated with the cascade impactor while the total particulate filter and SO_2 filter were on the second sampler (740 L/min ± 1 L/min). Six samples were collected outdoors on the roof of Science B (approx. 100m above ground) at the University of Calgary from Oct. 18, 2012 through to Dec. 6, 2012: each sampling period was approximately three days and corresponded to impinger sampling times. The flow rates and total times that each sample was collected for were then used to calculate the total volume of air that passed through the filters and hence the concentrations of SO_4 and SO_2 could then be calculated. Precipitation conditions were noted as particulates could adhere to snow or rain, and hence would not be collected by the high volume samplers (Table 1).

Filter papers collected at the end of each sampling period were prepared according to the methods detailed in Seguin et al. [10].

2.4 Measurement Uncertainties: A variety of equipment was used during sample collection, each with its associated uncertainties. Sampling time

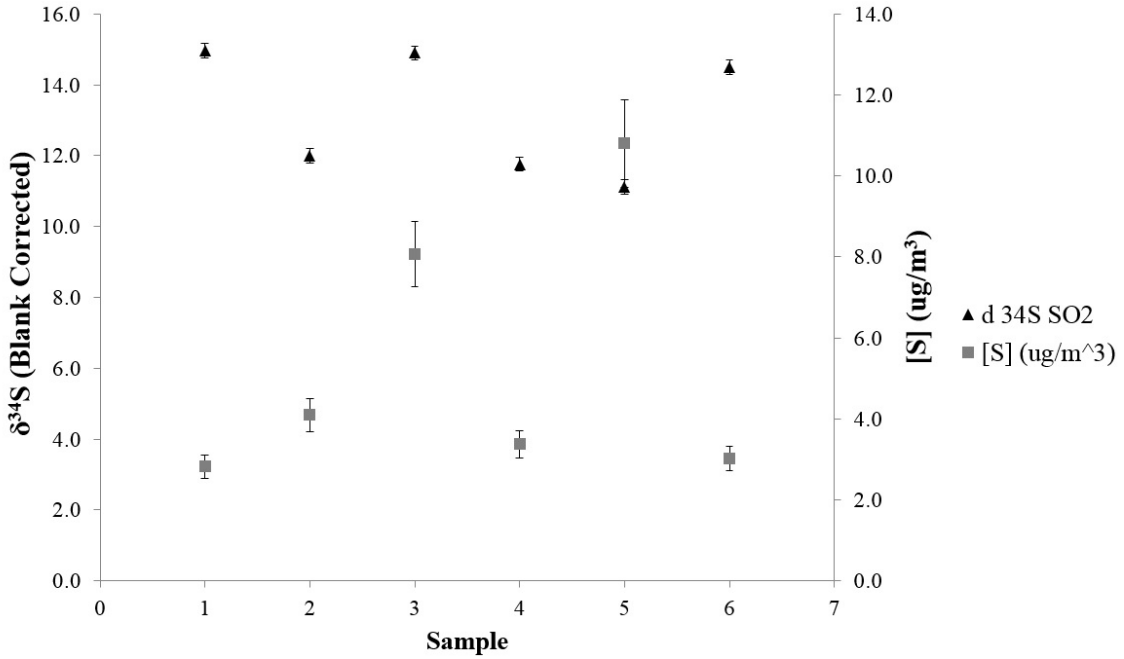

Figure 4:
$\delta^{34}S_{SO2}$ values and concentrations of SO_2 in the atmosphere from six different samples collected using SO_2 filters in a high volume sampler. Bars represent the total uncertainty introduced in analysis and in the measurements made. No apparent correlation between $\delta^{34}S_{SO2}$ and SO_2 concentration can be noted.

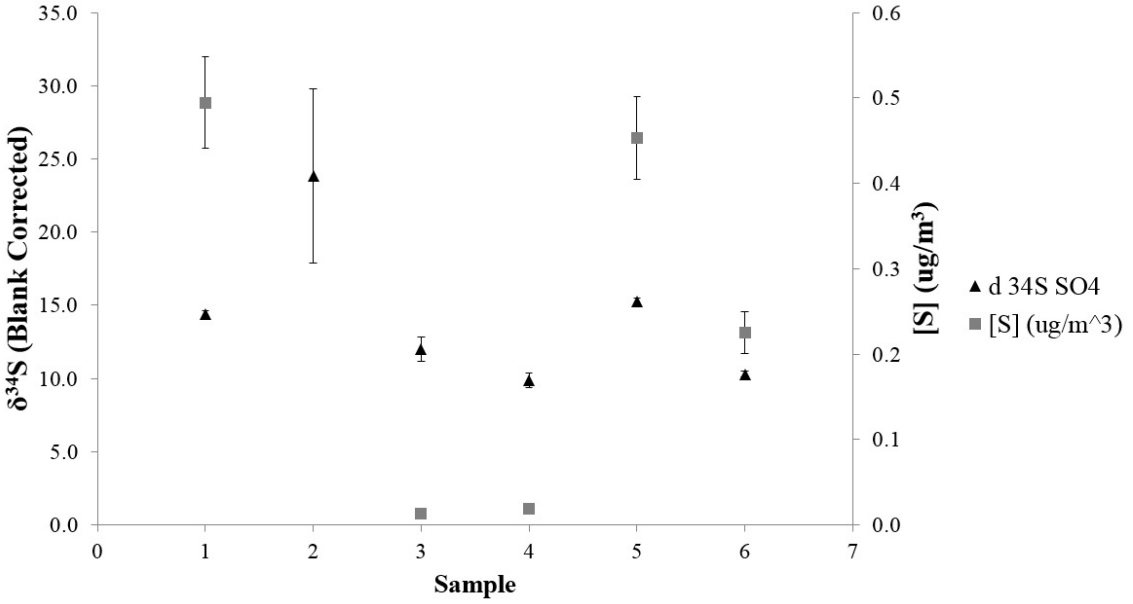

Figure 5:
$\delta^{34}S_{SO4}$ values and concentrations of SO_4 in the atmosphere from six different samples collected using fine particulate filters in a high volume sampler. Bars represent the total uncertainty introduced in analysis and in the measurements made. For sample 2 the high volume sampler malfunctioned and an accurate time period was not known, so [S] was not calculated. No apparent correlation between $\delta^{34}S_{SO4}$ and SO_4 concentration can be noted.

was monitored on an iPhone®clock to the nearest minute. A graduated cylinder to measure volume had an uncertainty of 1mL. A Kurz Instruments Inc. High-Volume Sampler Calibrator was used to measure the air flow rate into the samplers with an uncertainty of 14.2 L/min. The impinger flow rate, measured with a rotameter, had an uncertainty of 0.20 L/min.

Quantities which were then calculated based on these measurements used the standard error propagation formula proposed by NIST (National Institute of Standards and Technology) to find the associated uncertainties [11].

Results

3.1 Impingers: Impinger sample 2 froze during collection and was disregarded. Samples 1, 3, 4, and 5 had minimal precipitate and were combined into one sample to obtain a $\delta^{34}S_{SO2}$ value of +14.0‰ ± 0.2‰. As such, standard deviation could not be calculated and hence the ±0.2‰ is precision due to the spectrometer. A weighted average (the sum of each samples SO_2 concentration multiplied by its collection time, divided by collection time of all samples) of these four samples was calculated and this was used to obtain an SO_2 concentration in the air of 6.4μg/m^3 ± 1.3μg/m^3 (± std. dev.). Impinger sample 6 was not detected by the mass spectrometer.

3.2 High Volume Samplers: The $\delta^{34}S_{SO2}$ values obtained from the SO_2 from the high volume samplers was, on average (± std. dev.) +13.2‰ ± 0.2‰ (Fig. 4). $\delta^{34}S_{SO2}$ values ranged from +11.1‰ ± 0.2‰ to +15.0‰ ± 0.2‰, similar to what has been observed for Calgary in previous occasions by Norman et al. [2]. No pattern in $\delta^{34}S$ values for SO_2 was observed over time or with concentrations (Fig. 4).

$\delta^{34}S_{SO4}$ values for submicron aerosols were similar for samples 1, 3, 4, 5, and 6 while sample 2 had the most positive $\delta^{34}S$ value measured in this study (+23.8‰ ± 5.9‰) (Fig. 5, Table 1). Note that the sampling period for sample 2 was shorter than for the other samples. $\delta^{34}S_{SO4}$ values for submicron aerosols ranged from +9.9‰ ± 0.5‰ to +15.3‰ ± 0.2‰. Concentrations for SO_4 in the six samples were significantly smaller (t=3.80, df=5.06, p <0.05) than the corresponding SO_2 concentrations by an order of magnitude and varied from 0.0μg/m^3 to 0.5μg/m^3 ± 0.1μg/m^3. Samples 3 and 4 had much smaller concentrations than samples 1, 5, and 6; essentially at 0μg/m^3. Such small concentrations are indicative of very clean air, which is common after precipitation events, and which likely affected sample 4 but not 3 (Table 1). However, this did not appear to have an effect on their$\delta^{34}S_{SO4}$ values: the sulfur isotope composition of samples 3 and 4 were similar to the other samples collected.

$\delta^{34}S$ values and concentrations from the SO_2 and fine particulate filters did not follow patterns as would be expected if a particular oxidation pathway and isotope fractionation process were favoured [7]. Snow events were logged during the collection of samples 1, 2, 4, and 5 (Table 1) but this appears to have had no effect on the data obtained as the SO_2 and SO_4 $\delta^{34}S$ values remained within a narrow range and, in some cases, were similar to the samples collected when no snow events occurred.

Discussion

This study is the first to directly compare two methods of assessing fractionation of sulfur. The two methods compared were those of impingers and high volume samplers. A mean $\delta^{34}S_{SO2}$ value of +13.2‰ ± 0.2‰ was found for SO_2 from the high volume sampler and variations in SO_2 concentrations ranged from 2.8 ± 0.3μg/m^3 to 10.8 ± 1.1μg/m^3. $\delta^{34}S_{SO2}$ values were independent of SO2 concentration. Similarly, $\delta^{34}S_{SO4}$ values for fine particulate matter ranged between +9.9‰ ± 0.5‰ to +15.3‰ ± 0.2‰ while the SO_4 concentrations were highly variable. Again this suggests that the $\delta^{34}S_{SO4}$ values were not dependent upon the SO_4 concentration in the air. Samples 3 and 4 had minimal SO_4 concentrations, indicating the air on the days these samples were collected was exceptionally clean. These two samples should be particularly representative of whether or not fractionation occurred as the smallest fraction of SO_2 reaction can be reasonably assumed. This low SO_4 concentration is particularly common after precipitation events and a snow event was recorded during the collection of sample 4.

The $\delta^{34}S_{SO2}$ values from the SO_2 filters were plotted against the $\delta^{34}S_{SO4}$ values from the fine particulate filters in Fig. 6 to determine whether isotope fractionation could be detected. If fractionation were to occur, a consistent difference in the $\delta^{34}S_{SO2}$ and $\delta^{34}S_{SO4}$ values should be observed.

JURA
Journal of Undergraduate Research in Alberta • Volume 4 • 2014

High Volume Filter Results								
Sample	Dates of Collection (mm/dd)	Total Time Collected (minutes)	Snow Event (Yes/No)	$\delta^{34}S_{SO2}$ (‰)	$[SO_2]$ ($\mu g/m^3$)	$\delta^{34}S_{SO4}$ (‰)	$[SO_4]$ ($\mu g/m^3$)	Max S Reacted (%)
1	18/10 to 23/10	2954 ± 0.5	Y	15.0 ± 0.2	2.8 ± 0.3	14.4 ± 0.2	0.5 ± 0.1	17.5
2	6/11 to 9/11	4135 ± 0.5	Y	12.0 ± 0.2	4.1 ± 0.4	23.8 ± 5.9	-	-
3	21/11 to 27/11	4277 ± 0.5	N	14.9 ± 0.2	8.1 ± 0.8	12.0 ± 0.8	0.0 ± 0.0	0.2
4	27/11 to 30/11	3952 ± 0.5	Y	11.8 ± 0.2	3.4 ± 0.3	9.9 ± 0.5	0.0 ± 0.0	0.6
5	30/11 to 3/12	4077 ± 0.5	Y	11.1 ± 0.2	10.8 ± 1.1	15.3 ± 0.2	0.5 ± 0.0	4.2
6	3/12 to 6/12	4091 ± 0.5	N	14.5 ± 0.2	3.0 ± 0.3	10.3 ± 0.2	0.2 ± 0.0	7.5
Impinger Results								
1-5	18/10 to 3/12	15289 ± 0.5	-	+14.0 ± 0.2	6.4 ± 1.3			
6	3/12 to 6/12	4100 ± 0.5	-	-	-			

Table 1:
Dates and times the six samples were collected for, precipitation events, and results. No concentration for high volume sample 2 was calculated as the time of collection was unknown. Impinger samples 1-5 were combined to get a single reading (except for sample 2 which froze). Impinger sample 6 was below the detection limit of the mass spectrometer.

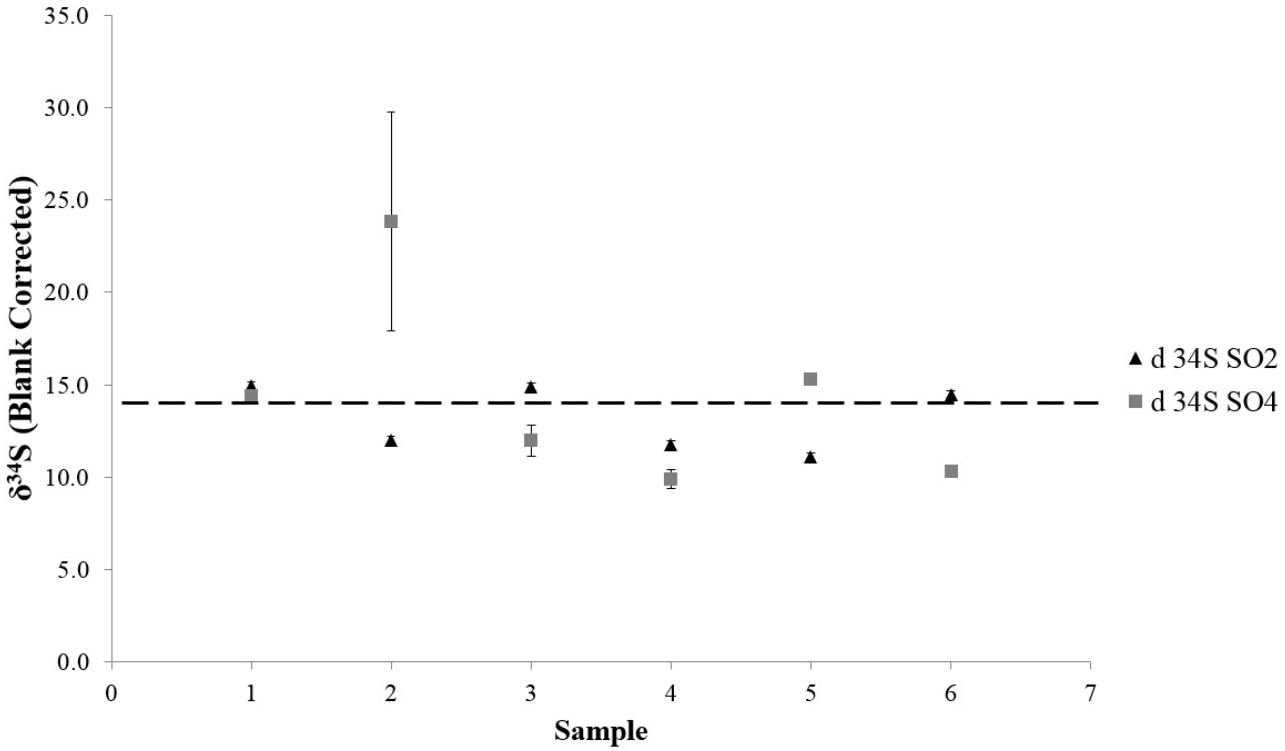

Figure 6:
Comparison of $\delta^{34}S_{SO2}$ and $\delta^{34}S_{SO4}$. Bars represent the total uncertainty introduced in analysis and in the measurements made. The line at 14.01‰ represents the $\delta^{34}S_{SO2}$ value obtained by impinger samples 1 through 5. Note that sample number is not a variable of interest but rather was included to help organize the data. The similarity between the $\delta^{34}S_{SO2}$ and $\delta^{34}S_{SO4}$ values but lack of a consistent difference indicates no sulfur isotope fractionation occurred. The similarity between the $\delta^{34}S_{SO2}$ values and the impinger value (dotted line) indicates that the high volume and impinger method yield similar isotopic results.

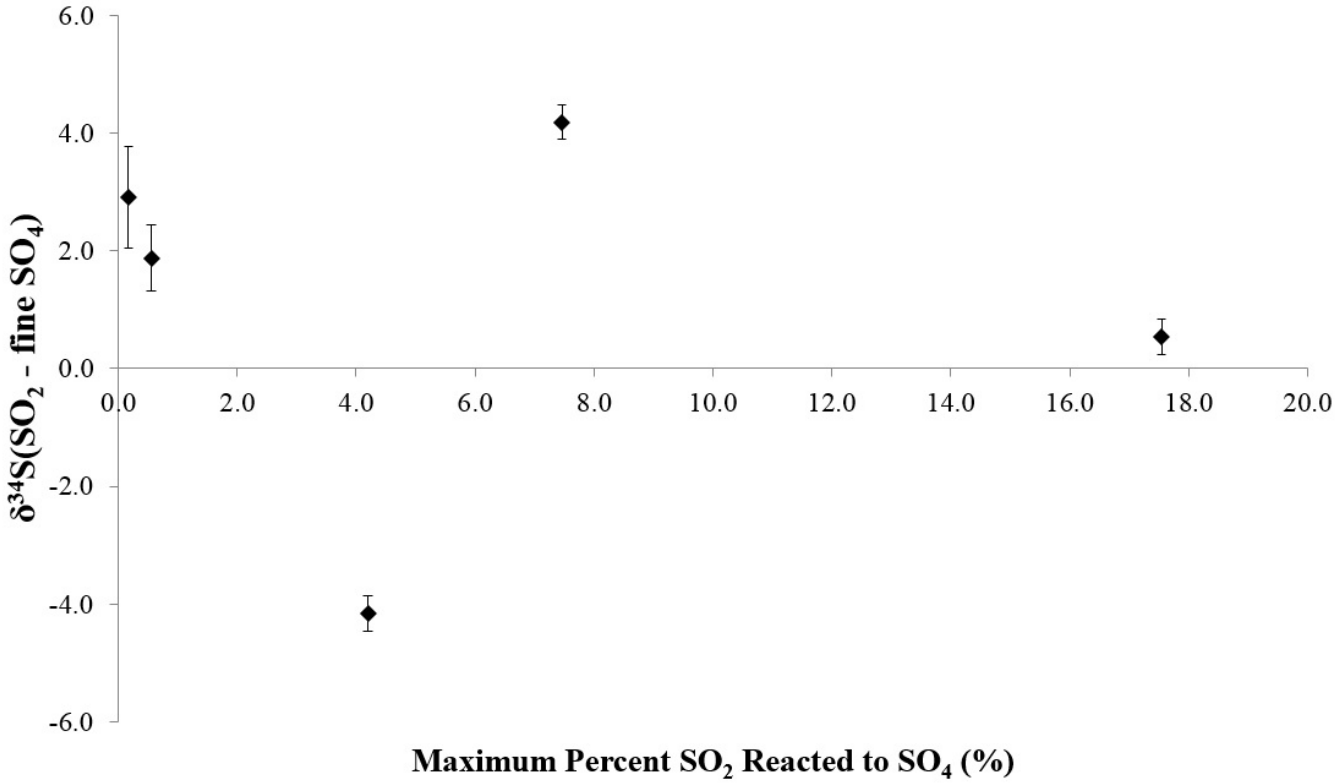

Figure 7:
Comparison of the $\Delta\delta^{34}S_{SO2-SO4(fine)}$ to the maximum percent of SO_2 that reacted to form SO_4. No trend between fraction of reaction (percent SO_2 reacted) and difference in delta values was noticeable and so no sulfur isotope fraction was occurring.

Sample	Δδ34S(SO2-impinger)	Δδ34S(fine SO4-impinger)
1	0.96	0.42
2	-2.01	9.83
3	0.89	-2.02
4	-2.25	-4.12
5	-2.89	1.27
6	0.48	-3.70
Average	-0.80	0.28
Standard Deviation	1.76	5.15

Table 2:
Quantification of Figure 6. Differences between the impinger values and the $\delta^{34}S_{SO2}$ and $\delta^{34}S_{SO4}$ with the associated averages and standard deviations. The standard deviations were larger than the averages, indicating a lack of consistent differences and hence no sulfur isotope fractionation.

JURA
Journal of Undergraduate Research in Alberta • Volume 4 • 2014

Aside from sample 2 (which is associated with a high volume sampler malfunction), the $\delta^{34}S_{SO2}$ and $\delta^{34}S_{SO4}$ values of the remaining samples were very close to one another and, on average, were near +14‰, the value obtained for SO_2 by the impingers. The similarity in the $\delta^{34}S_{SO2}$ and $\delta^{34}S_{SO4}$ values (but lack of a consistent difference) in the samples indicates that no sulfur isotope fractionation occurred. Figure 6 is also quantified in Table 2 , where the averages and standard deviations of the differences between $\delta^{34}S_{SO2}$ and $\delta^{34}S_{SO4}$ from the high volume samplers compared to the $\delta^{34}S_{SO2}$ from the impinger were calculated. It was found that the standard deviations were larger than the averages, indicating lack of a consistent difference (Table 2). Further verification that no fractionation occurred is seen in Figure 7. The $\delta^{34}S_{SO2}$ and $\delta^{34}S_{SO4}$ values were compared by subtracting the $\delta^{34}S_{SO4}$ from the $\delta^{34}S_{SO2}$ then calculating the maximum percent of SO_2 that reacted to form SO_4. The difference in δ values was plotted versus the maximum percent of SO_2 that reacted (Fig. 7), and if isotope fractionation were occurring then a trend (such as an increase in the difference between $\delta^{34}S_{SO2}$ and $\delta^{34}S_{SO4}$ with an increase in maximum percent SO_2 reacted) in the data as the fraction of reaction proceeded [3] should be evident. The lack of a trend with fraction of reaction demonstrates that no fractionation occurred.

Though this study was replicated over time, there was not a spatial component. Based on sampling location, the occurrence and amount of fractionation could vary due to large differences in atmospheric SO_2 concentrations, environmental conditions, or other such factors (such as sea salt aerosols in a marine setting). Confidence is added to this study though given that no relation was found between sulfur concentration and $\delta^{34}S$ value (Fig.4 and Fig. 5). Furthermore, a range of high volume samplers could also be implemented to account for possible bias from a specific sampler. This may have been adjusted for when one of the high volume samplers malfunctioned and a new one was implemented, but this possibility could also be incorporated into future studies (along with a spatial component).

As a result of the findings, the study failed to reject the null hypothesis but is in contrast to what Harris [7] found by sampling sea salt aerosols with impingers. It does however correspond to the findings of Norman [8] who also showed no evidence of fractionation occurring. As such, apportionment studies of sulfur isotopes can assume that isotope fractionation during SO_2 oxidation is small and hence accurately reflect their source. It is important to note that the $\delta^{34}S_{SO2}$ value of $+14.0‰ \pm 0.2|permil$ obtained by the impingers was nearly identical to the $\delta^{34}S_{SO2}$ values obtained by the SO_2 filter papers $+13.2‰ \pm 0.2‰$ (Fig. 6). The impingers and the SO_2 filters also yielded close results for the same concentration of SO_2 in the atmosphere for the same sampling period. The similarity in the results of both methods means that neither is detecting a unique artifact that is not being picked up by the other method, hence either method could be used with confidence that similar results would be obtained.

Conclusion

Impingers and high volume samplers with total particulate, fine particulate, and SO_2 filters were used to collect samples from which$\delta^{34}S_{SO2}$, $\delta^{34}S_{SO4}$, $[SO_4]$, and $[SO_2]$ values were calculated. It was found that the impinger method and the SO_2 filters yielded similar $\delta^{34}S_{SO2}$ values of around +14.0‰. The important finding of this study is that no fractionation was found to occur during SO_2 oxidation in ambient air in a non-marine environment.

Acknowledgements

Thanks to Dr. Michelle Seguin for assistance in the methodologies, analysis, and equipment setup, Farzin Malekani for running the ion chromatography, Nenita Lozano for the packing of samples for sulfur analysis, Stephen Taylor for performing the mass spectrometry, and Jesusa Overend-Pontoy for assistance in the laboratory.

References

1. Krouse, H.R. (1980). Handbook of Environmental Isotope Geochemistry Vol 2: The Terrestrial Environment, Elsevier Pub. Co., New York, NY, p.p. 435-471.

2. Norman, A.L., Belzer, W., Barrie, L. (2004). Insights into the biogenic contribution to total sulphate in aerosol and precipitation in the Fraser Valley afforded by isotopes of sulphur and oxygen. J. Geophys. Res.-Atmos. 109.

3. Krouse, H.R., Grinenko, V.A. (1991). Scope 43: Stable Isotopes, John Wiley & Sons, Ontario, Toronto, p.p.1-21.

4. Macdonald, W.S., Bietz, B.F. (1996).Acidifying Emissions Symposium, Red Deer, AB.

5. Finlayson-Pitts, B.J., Pitts Jr., J.N. (1986). Atmospheric Chemistry: Fundamentals and Experimental Techniques, Wiley, New York, NY, p.p. 1098.

6. Calvert, J.G., Stockwell, W.R. (1984). SO2, NO, and NOx Oxidation Mechanisms: Atmospheric Considerations, Butterworth Publishers, Ontario, Toronto, p.p. 1-62.

7. Harris, E., Sinha, B., Hoppe, P., Foley, S., Borrmann, S. (2012). Fractionation of sulfur isotopes during heterogeneous oxidation of SO 2 on sea salt aerosol: a new tool to investigate non-sea salt sulfate production in the marine boundary layer. Atmos. Chem. Phys. 12.

8. Norman, A.L. (2009). Atmos. Chem. Phys. Discuss. 9.

9. Norman, A.L., Krouse, H.R., MacLeod, J. (2004). Air Pollution Modeling and Its Application XVI.

10. Seguin, A.M., Norman, A.L., Eaton, S.J., Wadleigh, M.A., Sharma, S. (2010). Elevated biogenic sulphur dioxide concentrations over the North Atlantic. Atmospheric Environment 44(9).

11. Ku, H.H. (1966). J. Res. Nat. Bur. Stand C. Engineering and Instrumentation 70(C).

JURA
Journal of Undergraduate Research in Alberta • Volume 4 • 2014

Effect of Obesity on Gait Symmetry Following Anterior Cruciate Ligament Transection

C. Meeuwisse, K. Collins, W. Herzog
University of Calgary

Obesity is considered a risk factor for both the onset and progression of osteoarthritis (OA). Obesity, OA and mechanical instability have all been identified individually to increase gait asymmetry. The purpose of this study was to assess the effect of obesity on the progression of gait asymmetry as a component of a diet induced obesity (DIO) OA model in the presence of mechanical instability. Methods: 17 Sprague Dawley Rats were assigned to a high fat, high sucrose diet or a low fat diet group (LFD). Twelve weeks post diet assignment, groups receive an anterior cruciate ligament transection (ACL-X), or SHAM surgery. Pre-surgery, 1-week, 8-week, and 16-weeks post-surgery, kinetic data were collected by 3-D force plate analysis. Peak vertical ground reaction force (pVGRF), vertical impulse, and stance times were quantified then compared between limbs to quantify an asymmetry index (AI). Results: There were no differences in normalized pVGRF AI between hind limbs in the DIO or LFD group animals. Stance times decreased for both hind limbs in both DIO group animals. DIO ACL-X group animals had a greater AI for vertical impulse compared to LFD group animals at 1-week post-surgery, and both DIO group animals had greater AI at 8 and 16 weeks post-surgery, compared to LFD group animals. Conclusion: DIO group animals exhibited gait patterns with increased asymmetries compared to LFD group animals, regardless of presence or absence of ACL-X.

Introduction

Osteoarthritis (OA) is defined as a progressive disease characterized by degradation of cartilage and bone leading to joint pain and disability [1]. There are several identified risk factors for the onset and progression of OA, including joint trauma, age, gender and obesity [2]. Investigation into the relationship between obesity and OA is essential because unlike other risk factors, obesity can be modified through diet and exercise [3]. Obesity has been suggested to increase the progression and severity of OA due to the increase in body mass and associated increase in force through load bearing joints [4]. However evidence is emerging that obesity influences OA through mechanisms beyond mechanical joint loading, as obese individuals are found to have 5-8 times more OA in non-load-bearing joints of the hand [5].

Diet induced obesity (DIO) is associated with chronic inflammation, which is thought to exacerbate OA [6]. In a study by Mooney et al. [7], DIO accelerated the progression of OA with no correlation to weight gain, which suggests that intrinsic factors

due to diet are more important factors than the mechanical loading. Brunner et al. [8] and Louer et al. [9], found that DIO increases the progression and severity of OA. Griffin et al. [3] fed mice a high fat diet and found that these mice had elevated OA compared to controls [3]. These findings suggest that diet induced obesity accelerates the progression of OA.

Experimental models of OA have been developed and used in animals such as dogs, rabbits, cats, and rats [10,11,12,13]. In these models, joint instability following an injury or surgical intervention was shown to decrease the time from injury to disease onset, and contribute to the progression of OA. One such surgical intervention is the transection of the anterior cruciate ligament (ACL-X), which results in knee joint instability [10]. The ACL-X is a validated model of OA onset and progression [11,13]. These surgical models of mechanical intervention are helpful because the time from intervention to disease onset and progression is controlled [9].

Gait analysis, or movement analysis, is a method used to examine the functional deficits associated with OA in human patients and pre-clinical animal models of OA [10]. Commonly, gait data is used to understand the effects of OA on joint loading and unloading, and possible compensation when painful joints are favoured relative to healthy joints. Previous work by Herzog et al [13] and Suter et al [14] in ACL-deficient cats showed differences in vertical ground reaction forces between the experimental and contralateral limb for up to 12 weeks post-surgery. These differences in ground reaction forces demonstrate an asymmetric gait. After this time point, ground reaction forces had become about equally shared between hind limbs suggesting a trend towards a recovery of gait symmetry. Contrary to these results, it was previously found that dogs and rats did not recover gait symmetry over time; following induced mechanical instability [10,15]. These studies suggest that different species exhibit different gait compensation strategies following an induced mechanical instability procedure.

To our knowledge, Brady et al. [16] were the first to study the effects of diet on gait variables. They found that obese dogs exhibited a greater range of motion for the shoulder, elbow, hip and tarsal joints during the stance phase than lean control group dogs [16]. Furthermore, obese animals had greater vertical ground reaction forces than the lean control animals. However, this latter result is to be expected as vertical ground reaction forces are strongly correlated with body mass [16], and values were not normalised in this study. Brady et al. determined gait differences in lean and obese animals, but the study did not address how diet affects gait following a mechanical instability intervention.

Male Sprague-Dawley (SD) rats respond well to diet induced obesity [17] by gaining mass shortly after diet initiation. They tend to gain fat mass viscerally and abdominally, similar to humans [10], validating their use as an obesity model that may be representative of human obesity. Osteoarthritis is usually diagnosed late in the disease process, often resulting in delayed treatment [18]. To our knowledge, the combined effects of obesity and knee instability produced by anterior cruciate ligament transection (ACL-X) have yet to be evaluated to understand functional gait adaptions in the presence of these two primary risk factors for osteoarthritis. The purpose of this study was to determine the effects of obesity on gait with and without ACL-X in rats. It has been shown that OA is exacerbated by ACL-X and by obesity in isolation [13,14,15,16,19], so we are interested in the combined effect. With gait analysis as a means to assess the functional deficits of OA, we speculate that greater gait asymmetry is associated with more severe OA. We hypothesized that (1) DIO animals will have greater gait asymmetries than LFD animals, and that (2) gait asymmetry will increase and be sustained over time for the DIO animals, regardless of surgical intervention.

Methods

Twenty-eight male Sprague-Dawley rats (8-12 weeks old) were randomly assigned to either a high fat diet (DIO) or a low fat diet (LFD) group. The DIO group (n=18) received high fat sucrose food (40% fat, Diet 102412, Dyets, Inc) and the LFD group (n=10) received lean chow (13.5% fat, LabDiet 5001). Twelve weeks post obesity induction, ground reaction forces were measured during locomotion using a 1-meter custom runway with two embedded side-by-side 7.5 x 30 cm 3-dimensional force plates (Bertec, Columbus, OH). The force plates had a sampling rate of 500Hz. Sagittal plane kinematics were recorded using a

JURA

Journal of Undergraduate Research in Alberta • Volume 4 • 2014

high-speed camera filming at 200Hz. Animals were acclimatized to the runway prior to measurements, and a dark hiding area was positioned at the end of the runway to entice the rats to walk towards the hiding area across the force platforms. A trial was deemed successful if the animal walked over the force plates at a uniform speed, with no stopping or pausing, with only one hind limb landing on each plate. Speed was determined in video analysis by comparing the time it took the rat to cross a known distance. A minimum of two successful trials was needed for a rat to be included in the final analysis. Following baseline testing, all animals were assigned to receive a unilateral ACL-X (DIO n=12, LFD n=5) or a unilateral SHAM surgery (DIO n=6, LFD n=5). The surgical limb (ACL-X or SHAM) was randomly assigned. The same individual conducted all surgeries. ACL-X surgery was initiated by creating an incision on the lateral aspect of the knee. The joint capsule was then opened, the anterior cruciate ligament cut, and the incision closed. The SHAM surgery consisted of opening the capsule, spraying the knee joint with saline, then sealing the incision. Kinetics and kinematics were measured 1-week post-surgery, 8-weeks post-surgery, and 16-weeks post-surgery.

The primary kinetic outcome measures were the peak vertical ground reaction force (pVGRF) and the vertical impulse. Stance times for hind limbs were determined from the high-speed video. Similar to the study by Brady et al., a linear relationship was found between mass and ground reaction forces and impulses, so values were normalized to body weight. Hind limb asymmetry was determined using an Asymmetry Index (AI) based on the normalized vertical impulses of the experimental and contralateral limbs:

$$AI = \frac{Impulse_{CL} - Impulse_{EX}}{Impulse_{CL}} * 100\% \quad (1)$$

Larger AI values indicate a greater difference in the vertical impulse between limbs. Data will be normalized to the individual animal body mass. A non-parametric Kruskal-Wallis statistical test was used to compare the main factors diet (DIO and LFD), intervention (ACL-X and SHAM), and time (Pre-surgery, 1 week, 8 weeks and 16 weeks post-intervention). A Kruskal-Wallis test was also done to compare the mass and stance time variables. The level of significance was set a priori at =0.05.

Measure	DIO	LFD	p-value
Δ Stance EXP	-68.8 (±12.8)	3.04 (±15.2)	0.001
Δ Stance CON	-66.4 (±12)	16 (±15.2)	0.002

Table 1: *The stance change in stance times comparing the stance times at baseline and 16 weeks for both the DIO and LFD groups. The p-value is for the change in stance times for the DIO.*

Ethics was obtained from the Life and Environmental Sciences Animal Care Committee at the University of Calgary.

Results

After exclusion of rats because of an insufficient number of acceptable trials, 8 DIO ACL-X, 4 DIO SHAM, 5 LFD ACL-X, and 0 LFD SHAM (total n=17) group animals were analyzed. At 16 weeks post intervention, the mean body mass of DIO ACL-X, DIO SHAM, and LFD ACL-X group animals was 828 ± 51.93g, 762 ± 69.53g, and 611 ± 39.93g respectively. Both DIO group animals were significantly heavier than the LFD group animals ($p<0.05$). All animals were relatively the same weight prior to diet intervention, ranging between 400-500g. There was no statistical difference in mass between the DIO ACL-X and the DIO SHAM group animals, although the DIO ACL-X animals had a higher average mass.

The body mass normalized pVGRFs were similar for all three groups and at all time points. Walking speeds remained consistent within all groups at all time points. Stance times ranged from 188 ms to 470 ms. Stance times in DIO group animals decreased from baseline to 16 weeks post intervention by 69 ± 13 ms and 66 ± 12 ms for the experimental and contralateral limb respectively despite consistent walking speeds. Stance times for the LFD group animals did not change over the 16-week experimental period for either hind limb as shown in Table 1.

The mean AI for the normalized vertical impulses from DIO ACL-X animals at baseline, 1-week, 8-week, and 16-week post surgery was 17 ± 13%, 37 ± 5% ($p<0.05$), 44 ± 10% ($p<0.05$), and 45 ± 14% ($p<0.05$) respectively (Fig. 1). The DIO SHAM group had AIs of 16 ± 17%, 34 ± 7%, 44 ± 13% ($p<0.05$), and 45 ± 9% ($p<0.05$) respectively. The LFD ACL-X group had AIs of 12 ± 15%, 20 ± 7%, 17 ± 6%, and 25 ±

13% respectively. Significant difference between DIO and LFD groups indicated by ($p<0.05$). AIs increased in all groups at 1-week post-surgery, with the DIO ACL-X group animals having a significantly higher AI than the LFD ACL-X group animals ($p<0.05$). Both DIO group animals demonstrated a greater normalized AI vertical impulse when compared with the LFD ACL-X group animals at 8-weeks and 16 weeks post-surgery ($p<0.05$). No differences exist between the AIs of the DIO ACL-X group animals and the DIO SHAM group animals. There was a main effect of diet, with the DIO animals exhibiting greater asymmetries than the LFD group. There was no observable effect of diet between the DIO ACL-X and the DIO SHAM group animals. There was a main effect of time for the DIO group animals, with both groups experiencing an increased AI at 16-weeks compared to baseline values.

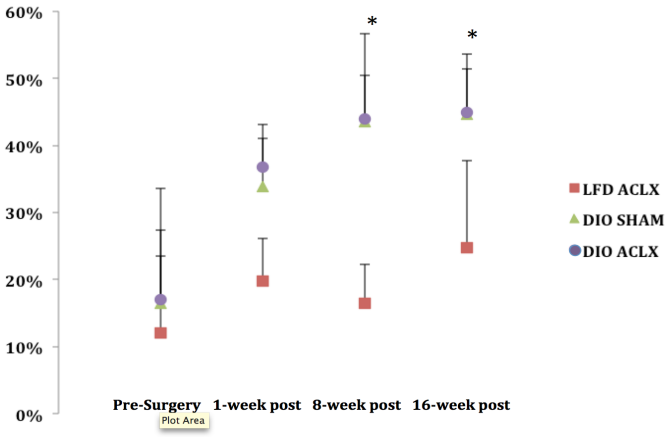

Figure 1:
Normalized AI vertical impulse demonstrated over time for four time points: pre-surgery, 1-week post surgery, 8-week post-surgery, and 16-weeks post surgery. Bars demonstrate SE, * Indicates differences between LFD and DIO, $p<0.05$.

Discussion

Kinetic data from this cohort of DIO rats was highly variable between subjects with large standard errors. Large gait variability could be attributed to the DIO, because similar variability has been seen in obese human populations [20,21]. This variability may explain why no differences were found in the normalized pVGRF between groups. However, when evaluating vertical impulses, which is a measure of cumulative load over the stance time, we found differences between groups of animals. The vertical impulse represents a measure of force over the entire stance time, rather than just an isolated value in time, and thus may be a better indicator of gait than pVGRF alone. The literature suggests that analysis of pVGRF and vertical impulse typically show similar trends, but the vertical impulse appears to be less variable, and thus may be the more meaningful and valid measure of ground reaction force than pVGRF [10].

Stance time on contralateral and experimental limbs was decreased in the DIO animals from baseline to 16-weeks. This decrease in stance times occurred while the average walking speed remained the same, thus we speculate that stride length decreased, but stride frequency increased at 16 weeks following intervention compared to baseline. Our data support the finding by Brady et al. (2013) who found that stride length decreased in obese dogs compared to lean controls. Further investigation into stride length and stride frequency would be valuable in future studies. There was no change in stance times for the LFD group animals in the present study, and no difference in stance times between the experimental and contralateral hind limbs. This result where the stance times are similar between limbs, is contrary to those found by Allen et al (2012) where lean Lewis rats were found to have shorter stance times on the experimental compared to the contralateral limb 9, 16 and 23 days post-surgery. These results suggest that rats do not show the limping gait following ACL transection that other animals often exhibit and that obesity in rats is associated with a distinct change in stance time patterns during walking.

Rats received limited training on the walkway prior to baseline testing. A surprising result is the progression of asymmetry in the LFD ACL-X group. Previous data indicates lean animals are asymmetric immediately following ACL-X, but then tend to recover after several weeks [11,13,14,15]. The results in the present study suggest an agreement with this data however the trend between baseline and 16-week AI values for the LFD ACL-X group animals is not statistically significant. Our results demonstrated exacerbated AI for the DIO ACL-X 1-week post surgery compared to the LFD ACL-X group, as well

as both DIO groups compared to the lean controls at 8 and 16 weeks post surgery. Importantly, it is worth noting the similarities between the DIO ACL-X and the DIO SHAM group, demonstrating that increased asymmetry occurs regardless of surgical intervention in this cohort. Opening the joint capsule, as was done in the SHAM surgery, has been shown to alter synovial inflammation in the joint that may cause animals to offload [22]. This could explain why asymmetries were seen in the same direction for both DIO ACL-X group and DIO SHAM.

Obesity has been shown to be associated with muscle weakness [23]. Consequently, we speculate this muscle weakness, in conjunction with a heavier body mass, results in more joint instability. Future work will include evaluating intramuscular fat content in lean and DIO animals to determine if differences exist. Recovery of gait symmetry in LFD groups in the literature suggests that animals develop gait compensations to deal with the progression of OA in the affected limbs [11,13,14,15]. However the results of this study suggest that obesity has a larger affect on AI impulse, and a recovery of gait symmetry was not observed. Due to the elevated asymmetry in these DIO animals, it can be speculate that the intrinsic factors of DIO have a greater affect on gait than the mechanical driver of surgery alone. Obesity may affect the joint through factors such as inflammation and muscle weakness, resulting in asymmetries similar to ones observed in DIO ACL-X subjects.

The LFD SHAM group was not included in the analysis because the animals did not meet the minimum inclusion criteria, for each of the time points. The exclusion of the LFD SHAM group was unexpected because this group was expected to have the least deviation from normal values, whereas the DIO animals were expected to have the greatest. Due to a large expected variation in the DIO animals, it was speculated that more animals would be excluded from this group and so more subjects were included in this group to begin the study (n=18). Having no LFD SHAM group is a limitation of the study. Future work should consider including larger numbers to more comprehensively study gait in this group. It has been previously shown that, control rats had more symmetrical loading on the hind limbs, indicating a more symmetrical walk, than ACL-X experimental group animals [10]. Therefore, we speculate that the AI for the LFD SHAM group would have been similar or lower than that of the LFD ACL-X.

Rats inherently walk with a non-uniform motion, and tend to pause frequently while walking [24]. Video analysis was used to eliminate unsuccessful trials. Only vertical forces were obtained, so it was not possible to determine movements in the medial and lateral direction by video analysis, or force plate analysis. 3D analysis could be used to better characterize gait characteristics. Future work will include evaluating medial/lateral and anterior/posterior force vectors to provide insight into gait properties. Future gait studies will also employ real time speed feedback using timing gates.

Conclusion

Diet-Induced Obesity increases gait asymmetries in the presence and absence of an ACL-X. Obesity may have biological drivers as well as mechanical drivers that increase gait asymmetries. With the ACL-X as a valid model for OA onset and progression [11,13], and gait analysis as a means to assess functional deficits in OA subjects [10], it can be speculated that due to the observed increased asymmetries in the DIO groups, obesity may accelerate the onset and progression of OA. Further work is needed to determine the individual effects of obesity from high fat/high sucrose diet versus ACL-X alone, on gait characteristics. A larger cohort of non-surgical diet-induced obesity animals is currently under experimentation to examine the effect of diet on gait symmetry without a surgical intervention. Future work is needed to support the preliminary findings of this study and further investigation is needed to better understand the interaction between intrinsic factors of obesity and function, specifically in the medial/lateral and anterior/posterior directions.

Acknowledgements

We would like to thank NSERC CREATE for funding the work on this project. We would also like to thank Tim Leonard, Ph.D, and Azim Jinha, M.Sc, for their assistance in this project.

References

1. A.P. Hills, E.M. Hennig, N.M. Byrne, J.R. Steele, Obes. Rev. 3(1), 2002.

2. L. R. Shelton, Nurs. Pract. 38(7), 2013.
3. T.M. Griffin, J.L. Huebner, V.B. Kraus, Z. Yan, F. Guilak, Arthritis. Rheum. 64(2), 2012.
4. S.A. Oliveria, D.T. Felson, P.A. Cirillo, J.I. Reed, A.M. Walter, Epidemiology. 10(2), 1999.
5. M.F. Gregor, G.S. Hotamisligil, Annu. Rev. Immunol. 29. DOI: 10.1146/annurev-immunol-031210-101322, 2011.
6. R.A. Mooney, E.R. Sampson, J. Lerea, R.N. Rosier, M.J. Zuscik, Arthritis Res. Ther. 13(6), 2011.
7. A.M. Brunner, C.M. Henn, E.I. Drewniak, A. Lesieur-Brooks, J. Machan, et al. Osteoarthr. Cartilage. 20(6), 2012.
8. C.R. Louer, B.D. Furman, J.L. Huebner, V.B Kraus, S.A. Olson, F. Guilak, Arthritis Rheum. 64(10), 2012.
9. K.D. Allen, B.A. Mata, M.A. Gabr, J.L. Huebner, S.B. Adams, et. al, Arthritis Res. Ther. 14(2), 2012.
10. K.A Clarke, S.A. Heitmeyer, A.G. Smith, Y.O. Taiwo, Physiol. Behav. 62(5), 1997.
11. A.M Bendele, C. Degen, JMNI, 1(4), 2001.
12. W. Herzog, M.E. Adams, J.R. Matyas, J.G. Brooks, Osteoarthr. Cartilage. 1(4), 1993.
13. E. Suter, W. Herzog, T.R. Leonard, H. Nguyen, J. Biomech. 31(6), 1998.
14. B.L. OConnor, D.M. Visco, D.A. Heck, S.L. Myers, K.D. Brandt, Arthritis Rheum, 32(9), 1989.
15. R.B. Brady, A.N. Sidiropoulos, H.J. Bennett, P.M. Rider, D.J. Marcellin-little, et. al, Am. J. Vet. Res. 74(5), 2013.
16. D.T. Felson, C.E. Chaisson, Bailliere. Clin. Rheum. 11(4), 1997.
17. J.W. Bijlsma, F. Berenbaum, F.P. Lafeber, Lancet. 377(9783), 2011.
18. M.Z.C. Ruan, R.M. Patel, B.C. Dawson, M.M. Jiang, B.H.L. Lee, Osteoarthr. Cartilage. 21(9), 2013.
19. J.S. Dufek, R.L. Currie, P. Gouws, L. Candela, A.P. Gutierrez, et. al, Movement Sci. 31(4), 2012.
20. A.P. Hills, A.W. Parker, Child Care Hlth. Dev. 18(1), 1992.
21. B.J. Heard, Y. Achari, M. Chung, N.G. Shrive, C.B. Frank, J. Orthopaed. Res. 29(8), 2011.
22. R.M. Palmieri-Smith, A.C. Thomas, C. Karvonen-Gutierrez, M.F. Sowers, Am. J. Phys. Med. Rehabil. 89(7), 2010.
23. G.D. Muir, I.Q. Whishaw, Behav. Brain Res. 103(1), 1999.

JURA
Journal of Undergraduate Research in Alberta • Volume 4 • 2014

Valuing life in our soils: Effects of Microbial Activity in Vermicompost Tea on Sunflower Fitness

A. Pulwicki, J. Sekhon, L. Wonneck, M. Noriega
University of Calgary

Vermicompost tea (VCT) is a concentrated solution of microbes and nutrients that has been shown to increase plant growth. This study investigated the effects of microbes and nutrients in VCT on the growth (measured by plant biomass and rate of height increase) of sunflower (Helianthus annuus) under ideal-water and drought-simulated conditions. Three solutions (VCT, VCT without microbes, and water) were applied to groups of twenty greenhouse-grown sunflowers under ideal-water and drought-simulated conditions. Bacterial plates and carbon dioxide respiration tests measured soil microbial activity. We found that VCT increased plant heights and biomass under drought-simulated conditions and decreased plant heights and biomass under ideal-water conditions. VCT without microbes had the lowest level of growth throughout the study. Given that bacterial abundance was highest in soils with VCT added, the differing effects of VCT under ideal-water and drought-simulated conditions may have been due to the presence of different microbial communities. For example, certain microbes can increase drought-tolerance of plants by solubilizing limiting nutrients, while others can harm plants when water is in excess due to anaerobic processes. Plant-microbe symbiotic relationships, nutrient availability and hydrological factors need to be considered when evaluating the potential benefits of VCT application to agricultural crops.

Introduction

As the global population continues to increase at an accelerated rate, the demand and availability of food resources is becoming a greater cause for concern [1-2]. Although high crop yields are currently being maintained, soil in many areas is losing its ability to support agriculture without the addition of chemical fertilizers [3-4]. Healthy, productive soil requires not only water and nutrients, but also robust and diverse communities of micro- and macro-organisms [5]. Industrial agricultural practices tend to focus on maintaining sufficient water content and nutrient concentrations in the soil through irrigation and chemical fertilization, respectively, while largely disregarding the biological aspect. However, soil biology provides a number of agriculturally relevant ecosystem services such as the decomposition of organic matter, cycling of nutrients, soil rotation, and suppression of diseases and pests [5].

In the rhizosphere the zone of soil that surrounds plant roots microbe concentrations can be 10 to 1000 times greater than in surrounding soil due to relatively high amounts of available carbon

from root exudates [6-7]. Certain bacteria in this rich community, known as plant-growth promoting rhizobacteria (PGPR), are particularly important to plant growth. Some of these bacteria increase nutrient availability for plants [7-8], while others suppress pathogens such as other bacteria, fungi, and viruses [9]. Certain PGPR can directly improve plant growth by supplying them with hormones and enzymes that stimulate plant growth or increase plant resistance to abiotic stresses such as drought [10]. Stressful growing conditions, including drought, can increase the importance of PGPR in aiding plant growth. Low water conditions can immobilize nutrients and make plants more susceptible to disease [11].

The importance of the biological component of the soil has been increasingly recognized in recent years, which has resulted in the development of a variety of agricultural techniques that attempt to introduce and sustain rich soil microbial communities. One such technique is the application of vermicompost tea (VCT). VCT is a highly concentrated solution of soil microbes, including active bacteria and fungi, and nutrients derived by soaking vermicompost in aerating water. Vermicompost consists of digested organic matter in the form of earthworm excrement (e.g., Lumbricus rubellus, Eisenia foetida) [12]. VCT has been shown to increase plant yield and health [13], which has been attributed to the high amounts of mineralized nutrients and to the presence of microbes that increase nutrient availability, suppress pathogens, and supply the plant with hormones and enzymes as described above [12-13].

Most research on VCT has focused on its ability to reduce the incidence of plant disease [14-15]. Of the few studies that have measured the effects of VCT application on plant growth, none have managed to determine whether the observed changes are a result of the nutrients or the microbes [12-13]. There has also been no research that has investigated whether VCT has differing effects when used with different types of moisture regimes. We aimed to address these research gaps by determining the effects that VCT, with and without microbes, had on the growth (defined as a collective measure of height and biomass) of sunflowers (Helianthus annuus) under both ideal and drought-simulated growing conditions. We selected sunflowers because they are an important agricultural crop [16], and are well suited to study due to their drought sensitivity, tall stature and rapid growth rate [17]. For reasons described above, we predicted that VCT would have a positive effect on plant growth, and that this effect would be greater in drought-simulated growing conditions.

Methods

Experimental Design

We conducted the experiment in a greenhouse, with full spectrum overhead lights used to simulate 16 hours of daylight. Although a greenhouse is limited by the fact that the plants within it are not subject to many of the abiotic and biotic stresses that they would normally endure in an agricultural environment, growing the plants in this way gave us greater control over the variables that we wished to manipulate, and as well also minimized many confounding factors (e.g. pests, disease heterogeneous soils, etc.). The sunflowers were grown for 63 days between January 8th and March 11th, 2013. Four sunflower seeds were planted in each 15 cm diameter pot filled with commercial potting soil. After the plants reached cotyledon the two shortest plants in each pot were removed, leaving two plants per pot.

Three different treatment solutions, each with 20 replicate pots, were applied directly after the plants were thinned. The first solution was VCT, brewed as per supplier recommendations. The materials and ingredients for VCT were provided by Living Soil Solutions of Calgary, AB. VCT was brewed on site by placing vermicompost in a mesh bag and suspending it in a bucket of deionized water in a 1:40 ratio (weight of vermicompost to water). Additional ingredients were added in accordance with the instructions for 20 L of water: 21 mL of kelp, 16 mL of fish extract, 21 mL of Soluplks (humic acid) and 60 mL of molasses. The mixture was then aerated for 24 hours, after which it was considered VCT. 200mL of VCT were applied to each pot of the treatment group titled vermicompost tea with microbes (VM) within four hours of brewing.

The second solution was autoclaved VCT. It was made by autoclaving VCT at 120C for 20 minutes to kill the microbes in the mixture. After autoclaving, the solution was placed in an ice bath to cool it to room temperature. 200mL of autoclaved VCT were applied to each pot of the treatment group titled vermicompost tea with no microbes (VNM) at the

same time as the other solutions.

The third solution was deionized water. 200mL of deionized water were applied to each pot of the treatment group titled water only control (WOC) at the same time as the other solutions.

Regular watering was done using equal amounts of deionized water twice a week for half of each of the three treatment groups, to simulate ideal-water conditions. Watering was done once a week using the same amount for the other half of each treatment group to simulate drought conditions. In this way, the treatments under drought simulation received only half the water. The authors determined the watering regime arbitrarily.

Data Collection

The distance between the two plants in each pot was measured (hereafter termed distance) after the plants had first been thinned to account for differences in competition effects. Plant heights were measured weekly throughout the growth period.

We estimated bacterial abundances for the three treatment solutions pre-application using nutrient agar plates. We applied the three treatment solutions to nine nutrient agar plates (three for each solution), and had planned on counting bacteria colonies after a 40-hour period. Unfortunately, due to the high number of colonies it was impossible to determine the number of colonies at that time, and so instead the plates were visually analyzed to qualitatively determine whether there were morphological differences between them. The pH values of the treatment solutions were also measured.

We estimated soil bacterial abundances from 100 g soil samples 49 days after treatment application. Seven soil samples were taken from each of the six treatment group/water condition combinations. Soil samples were homogenized and 1 g of 2 mm sieved 99 mL of soil was suspended in distilled water using a VORTEX. This solution (100 L) was applied to nutrient agar plates and then left for one week before colonies were counted. We intended to estimate soil fungi abundances using a similar method unfortunately, the results had to be discarded due to experimental error.

We conducted carbon dioxide (CO2) respiration tests on one pot from each treatment group directly after application using a dynamic closed-chamber system. Each replicate was left inside the chamber for one hour; the methods were conducted as per Pumpanen et al. [18].

We measured wet and dry aboveground and root biomasses after the plants were harvested. We measured root biomass by removing the soil from roots manually and rinsing clean using tap water. The roots of the two different plants in each pot could not be separated therefore, we measured the root biomasses for the entire pot (reducing the number of replicates from 20 to 10). Finally, we measured dry biomasses for both aboveground and roots after the plants had been dried at 65C for 72 hours. It is important to note that the weights that were being measured (especially for the plants under drought-simulated conditions) were so small that the measured values approached the precision limit of the weight scale that was used.

Data Analysis

We analyzed data using the statistical program JMP, version 10.0.2, 2012. A repeated measures multiple regression was conducted to determine the effects of treatment solution, water condition, and distance on mean plant heights individual plant and pot were included as random variables within the regression, and the effects of the cofactors were nested within day of measurement. Two variables were used from this analysis to compare treatment groups growth rates (i.e. slope of the change in height at the mean day of the experiment), and least squared mean (LSM) heights over the course of the experiment. These two variables were used because they both have their advantages and disadvantages growth rates are more sensitive to differences between treatment groups than least squared mean heights, but also can be misleading when growth is not linear.

Further multiple regressions were conducted to determine the effects of treatment, water condition, and distance on dry aboveground, belowground, and total plant biomass. A two-way ANOVA was conducted to determine the effects of treatment and water condition on soil bacterial abundance, while a one-way ANOVA was conducted to determine the effect of treatment on the carbon dioxide respiration flux of soil microbes. An alpha value set as 0.05, and differences between treatment groups were determined by comparing 95% confidence intervals. Data were reported as mean 95% confidence intervals, unless otherwise noted.

JURA
Journal of Undergraduate Research in Alberta • Volume 4 • 2014

All data used for ANOVAs and ANCOVAs were analyzed to determine whether they met assumptions of homogeneity and normality of variances using Levennes and Shapiro-Wilks tests respectively. All data met the assumptions except for soil bacterial abundances, which met neither. Logarithmic and square root transformations were attempted but made no differences on whether either assumption was met. Non-parametric tests such as the Mann-Whitney U and Kruskal Wallis were considered but rejected because they assume homogeneous variances as well, and ANOVAs are relatively robust to violations of assumptions [19].

Results

Height

All of the plants steadily increased in height over the 55-day period of measurement, although rates appeared to slow for the plants under drought simulated conditions after approximately day 35 (Fig. 1). Mean heights differed among treatment and water condition, after adjusting for day, when the repeated measures of individual plants and pots and the effect of time were taken into account as random effects and the covariate day (i.e., slope for this factor is an estimate of growth rate) was nested within each level of treatment and water condition (overall model R^2=0.98, p<0.001). Distance had no effect on either model, and so was removed from the analysis . Inspection of Fig. 1 shows non-linear growth, but we used a linear term in the model because a quadratic term (day2) was a weaker predictor of plant height when combined in the same model (F=276 for day2 versus F=703 for day). At the mean day of the experiment, the growth rate (i.e. the slope of the change in height) of the plants in VM was higher than that of the plants in either WOC or VNM under drought-simulated conditions, while the growth rate of the plants in WOC was higher than that of the plants in either VC or VNM under ideal water conditions (Table 1).

There was also a significant interaction between treatment and water condition at explaining least squared mean heights (F(2,54.08)=3.30, p=0.04), meaning that the strength of the treatment effect differed between water conditions. The least squared mean (LSM) heights of the treatment groups followed a similar pattern to growth rates, except that differences were less pronounced VCT and WOC were statistically similar under both water conditions (Table 1).

Biomass

Treatment solution and water conditions had interactional effects on aboveground and total plant dry biomass, as well as the belowground:aboveground dry biomass ratio (Table 2). Under drought simulated conditions, mean aboveground, belowground, and total dry biomasses were the same for all treatments, while the belowground:aboveground ratio was higher for WOC (Fig. 2). Under ideal water conditions, WOC had higher aboveground and total mean dry biomasses than VM and VNM, while the belowground biomass and belowground:aboveground ratio were the same for all treatments. Distance was positively related to belowground and total plant dry biomass.

Soil microbial activity

VCT increased mean soil CO2 respiration flux immediately after it was applied to the pots (F(2,12591)=68319.10, p<0.001). Over the course of the hour of measurement, VM had a mean respiration flux of 191.18±0.19m/m, which was higher than that of WOC (93.97±0.19m/m). The mean respiration flux of VNM could not be calculated due to experimental error. Based on colony counts of bacteria one week after soil samples were applied to agar plates (Table 3), treatment and water condition were found to have no effect on bacteria abundance in the soil 49 days after treatment (R^2=0.13, F(5,34)=1.01, p=0.429).

Treatment Solution Tests

Based on visual analysis, agar plates that were treated with VCT had higher bacteria abundances than those treated with autoclaved VCT or distilled water 40 hours after treatment (Fig. 3). The three treatments had similar pH measurements VCT had a slightly higher pH at 7.37, followed by deionized water at 7.18, followed lastly by autoclaved VCT at 7.15.

JURA

Journal of Undergraduate Research in Alberta • Volume 4 • 2014

Water condition	Plant Group	Growth rate			Height		
		Mean (cm/day)	95% confidence interval (±cm/day)	Letters indicating significant difference*	Least squared mean (cm)	95% confidence interval (±cm)	Letters indicating significant difference*
Ideal-water	VM	0.71	0.02	A	23.94	1.34	AB
	VNM	0.69	0.02	B	21.92	1.34	A
	WOC	0.75	0.02	B	25.22	1.34	B
Drought simulated	VM	0.23	0.02	C	15.10	1.35	C
	VNM	0.19	0.02	D	12.19	1.34	D
	WOC	0.18	0.02	D	13.05	1.3	CD

Table 1: *Mean growth rates, least squared mean heights, and variances of Helianthus annuus over 55-day period of measurement. Vermicompost tea (VCT), autoclaved VCT, and deionized water were applied to VCT with microbes (VM), VCT with no microbes (VNM) and water only control (WOC) plant groups, with 20 plant replicates per group, under drought simulated and ideal-water conditions. A repeated measures linear regression was conducted with individual plant and pot as random variables, treatment group and water condition nested in day of measurement, and (R^2=0.98, p<0.001) (n=20). Significant differences between treatment groups (shown by letters) were determined by comparing 95% confidence intervals..*

Dry Biomass Parameters	Overall Model				Treatment solution and water condition solution			Distance effects		
	R^2	DF	F	p	DF	F	p	DF	F	p
Aboveground	0.88	5,114	161.14	<0.001	2,114	24.2	<0.001	-	-	-
Belowground	0.59	9,50	7.84	<0.001	-	-	-	1,50	4.02	0.05
Belowground: Aboveground	0.47	5,54	9.63	<0.001	2,54	4.88	<0.001	-	-	-
Total Plant	0.93	9,50	70.13	<0.001	2,50	12.92	<0.001	1,50	4.94	0.03

Table 2: *Model summary statistics for variance in dry biomass parameters. The R^2, degrees of freedom (DF), F statistic (F) and p value for the overall model as well as the treatment and water interaction and the effect of distance are presented.*

Water Condition	Treatment group	Mean number of bacterial colonies	95% confidence interval (±cm)
Ideal-water	VM	22.00	41.70
	VNM	8.14	41.70
	WOC	33.57	41.70
Drought-Simulated	VM	2.00	41.70
	VNM	49.00	41.70
	WOC	4.14	41.70

Table 3: *Summary statistics for colony counts of soil bacteria one week after solutions containing diluted soil samples were applied to nutrient agar plates. Seven soil samples were taken each from the VCT with microbes (VM), VCT with no microbes (VNM) and water only control (WOC) plant groups, under both drought simulated and ideal-water conditions. There were no significant differences between the six treatment groups, as determined by comparing 95% confidence intervals.*

JURA
Journal of Undergraduate Research in Alberta • Volume 4 • 2014

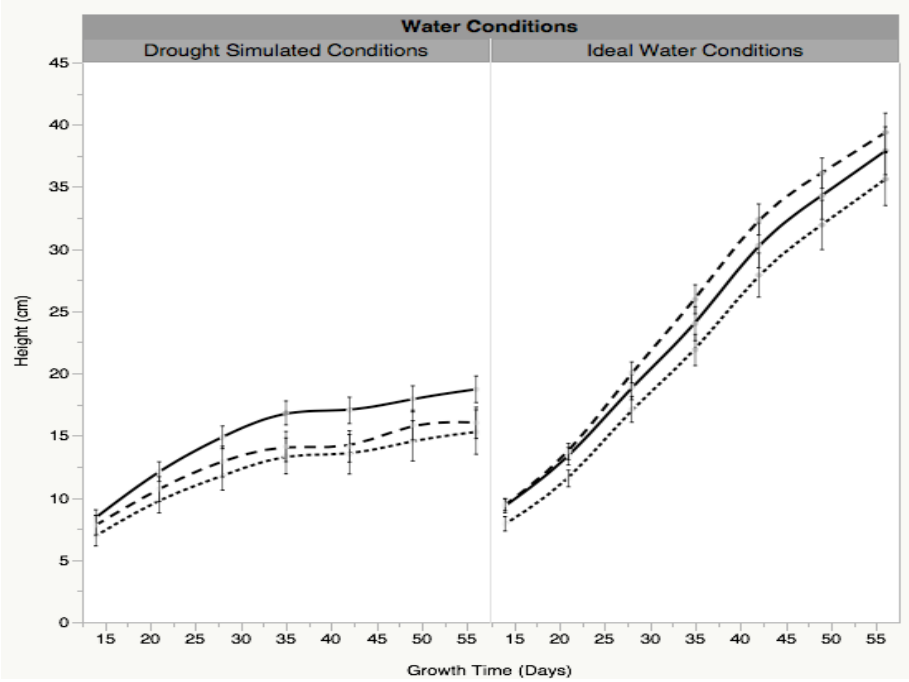

Figure 1:
Mean heights of Helianthus annuus over a period of 55 days (plants were grown in a greenhouse for 63 days in total). Vermicompost tea (VCT), autoclaved VCT, and deionized water were applied to VCT with microbes (VM ( )) VCT with no microbes (VNM (—)) and water only control (WOC ()) treatment groups, with 20 plant replicates per treatment group, under drought simulated and ideal-water conditions. Error bars indicate standard error (95% confidence intervals are not used here to increase clarity, as it is difficult to distinguish between them on the figure, n=20 for all treatment groups).

Discussion

Pattern 1: VM plants had higher growth than WOC and VNM plants in drought-simulated conditions

The first main pattern observed in this experiment was that plants with VCT applied (VM) had higher growth (shown most clearly in Table 1 by mean growth rate) than the control group of plants that only received water (WOC) and the group of plants that received autoclaved VCT (VNM) in drought-simulated conditions. Although the results for least squared mean (LSM) heights appear to follow this pattern, VM and WOC were not significantly different (Table 1). As noted in the methods, this lack of significance could be due to the fact that least square mean height is relatively insensitive to differences between treatment groups. There were also no significant differences between the aboveground biomasses of the treatment groups (Fig. 2). Mean biomass of VM plants were trending towards being the largest in both water regimes, however the results were not significant, possibly due to limitations of the weight scale that was used.

The higher growth of the VM under drought conditions may have been due to the presence of plant-growth promoting rhizobacteria (PGPR) in VCT. Previous research has shown that vermicompost has high amounts of PGPR [20] while the results of our soil treatment tests indicate that there were high amounts of microbes present in VCT and that at least initially, this increased soil respiration. PGPR can directly enhance the drought-tolerance of plants by supplying them with enzymes such as 1-aminocyclopropane-1-carboxylic acid (ACC) deanymase [10]. ACC deanymase reduces the level of ethylene in plants, which inhibits plant growth, especially in water-stressed conditions [21]. In addition to this, PGPR also play a role in solubilizing nutrients such as phosphorus and making them available for plant uptake within the rhizosphere [20].

JURA
Journal of Undergraduate Research in Alberta • Volume 4 • 2014

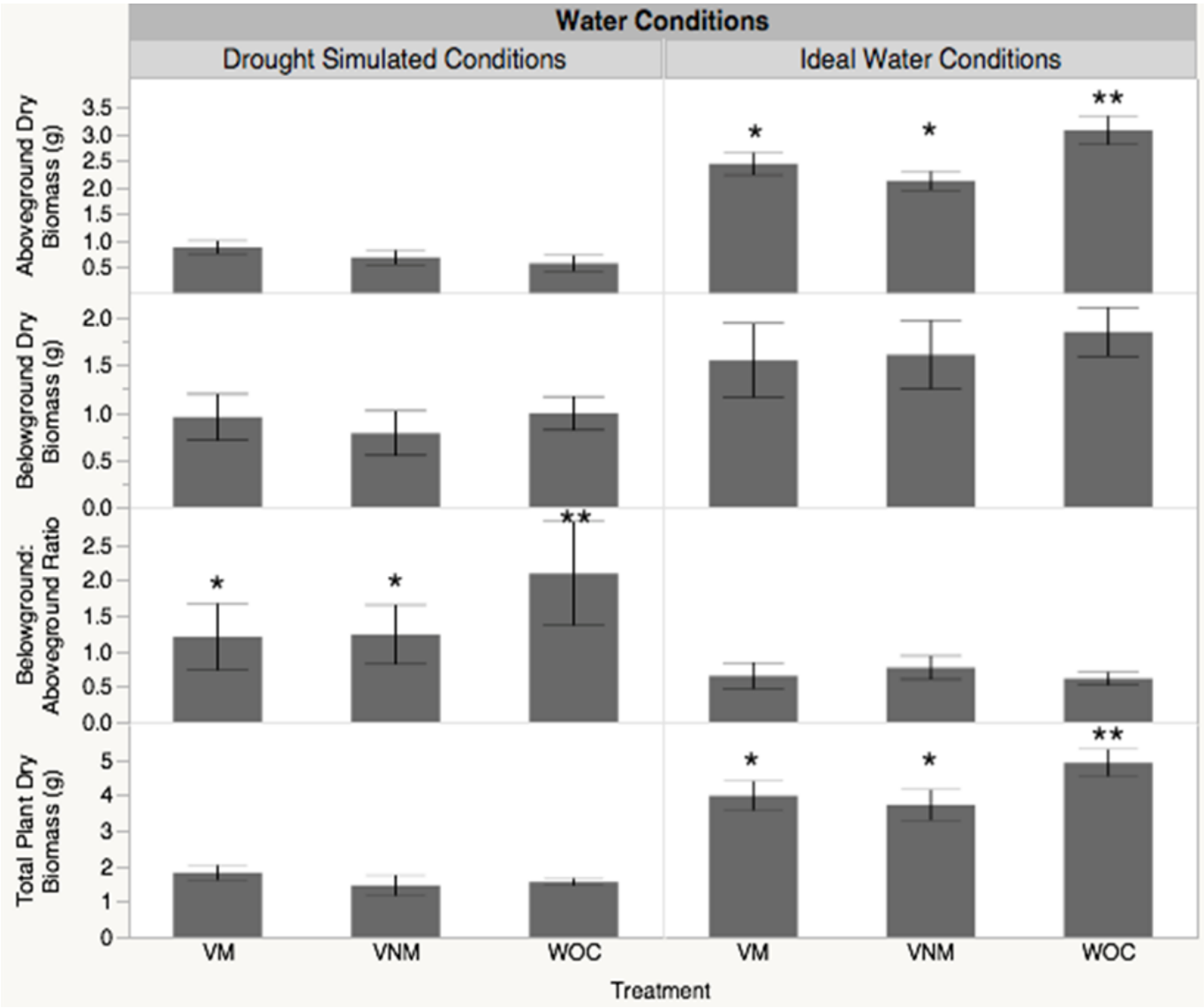

Figure 2:
Aboveground (upper), belowground (upper middle), belowground:aboveground ratio (lower middle) and total pot (lower) biomass of Helianthus annuus after 63 days. Vermicompost tea (VCT), autoclaved VCT, and deionized water were applied to VCT with microbes (VM) VCT with no microbes (VNM) and water only control (WOC) treatment groups, with 20 plant replicates per treatment group, under drought simulated and ideal-water conditions. Error bars indicate 95% confidence intervals. Multiple linear regressions were conducted Aboveground: R^2=0.88, F(5,114)=161.14, p<0.001. Belowground: R^2=0.59, F(9,50)=7.84, p<0.001. Belowground:Aboveground ratio: R^2=0.47, F(5,54)=9.63, p<0.001.$Totalpot$: R^2=0.93, F(9,50)=70.13, p<0.001. Significantly different groups within each water condition (determined by comparing 95% confidence intervals) are noted with asterisks. n=10 for treatment groups when belowground biomass and total plant biomass was measured; n=20 for treatment groups when aboveground biomass was measured.

JURA
Journal of Undergraduate Research in Alberta • Volume 4 • 2014

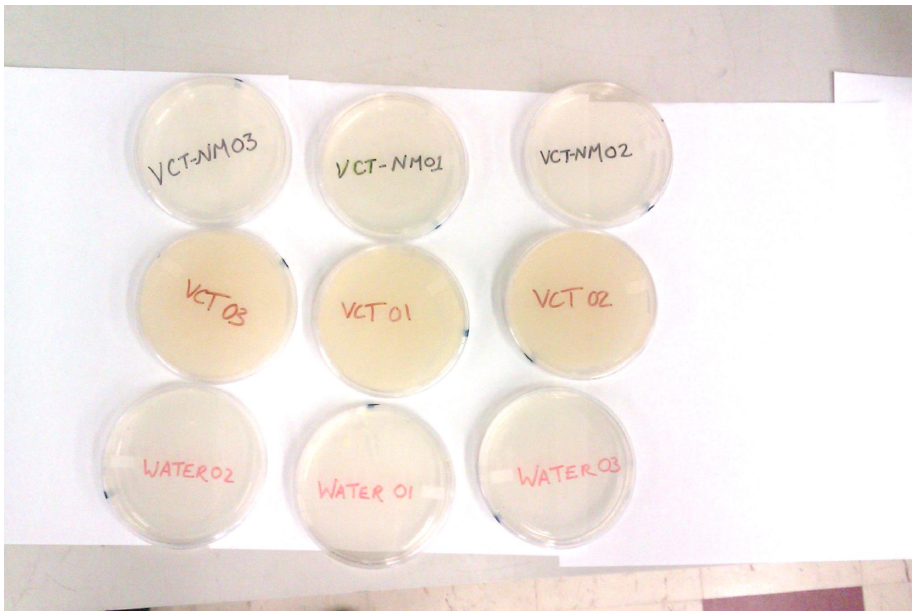

Figure 3:
Pictures of agar plates 40 hours after they were treated with one of three treatments. Plates in the top row were treated with vermicompost tea (VCT) that was autoclaved; plates in the middle row were treated with VCT; plates in the bottom row were treated with deionized water. Plates that are darker yellow in colour have more bacterial colonies.

The role of PGPR may be especially important in dry soils, where nutrients have a low mobility due to limited solubilization and transport from water. This can result in local nutrient deficiencies around the roots of plants in dry soil, even in relatively nutrient rich soils [22]. Indeed, the belowground:aboveground dry biomass ratio of WOC was higher than the other treatment groups, which could indicate that these plant had relatively low access to nutrients (Fig. 2) [23]. Overall, the ability of PGPR to supply enzymes that increase drought resistance, and as well solubilize and transport nutrients, may have increased their value in drought-simulated conditions, and explained why VM outperformed WOC and VNM.

Pattern 2: VNM plants had equal growth to WOC plants in drought-simulated conditions

Another observed pattern in drought-simulated conditions was that there were no differences between the heights (Table 1) and between the aboveground and total plant biomasses (Fig. 2) of the VNM and WOC treatment groups. This pattern can potentially be explained by the absence of PGPR in the autoclaved VCT solution, resulting in VNM plants being unable to uptake the nutrients present in autoclaved VCT. As explained above, because dry soil causes nutrients to have a low mobility and solubility, local nutrient deficiencies could form around the roots, even when the rest of the soil was nutrient rich [22]. PGPR can therefore be especially beneficial in dry soil because they solubilize nutrients and make them available for root uptake. The fact that VCT, which contains PGPR, appeared to benefit plants in drought-simulated conditions is further evidence for this explanation.

Pattern 3: VM and VNM plants had lower growth than WOC plants in ideal-water conditions

The third main pattern observed in this experiment was that VM and VNM plants had lower heights (especially growth rates, as shown in Table 1) and aboveground and total plant biomass (Fig. 2) than WOC plants in ideal-water conditions, in contrast to drought conditions. It is possible that there are different reasons for why VM and VNM plants follow this pattern.

VM plants may have had lower growth than that of WOC due to the formation of anaerobic conditions

around plant roots. Anaerobic soil conditions can form when excess water limits the amount of oxygen diffusion occurring between the atmosphere and soil pores. Oxygen is essential to soil respiration, and even temporary waterlogging has been shown to slow leaf and shoot growth, cause wilting and increase incidence of disease [24]. VM plants may have been especially susceptible to anaerobic conditions because of the high concentration of microbes and nutrients initially supplied by the VCT. This influx would have resulted in high levels of microbial respiration, potentially depleting oxygen in the soil. Potted plants may be especially at risk to anaerobic conditions due to compacted soils, high water content and the contained nature of the root system.

Anaerobic conditions could also have reduced plant growth by changing the composition of soil microbes. Certain microbes produce chemicals that are toxic to plants. In aerobic soils these chemicals are usually metabolized by other microorganisms and therefore do not accumulate. [24]. However, in oxygen-deficient conditions, anaerobic microbes can outcompete aerobic bacteria such as PGPR. This can result in microbes beginning to reduce Fe3+ and Mn3+, which act as alternative electron acceptors to oxygen. Where anaerobic bacteria are abundant, Fe2+ and Mn3+ can accumulate in the soil. These elements are toxic to plants at high concentrations. If pockets of anaerobic soils formed near the sunflower roots, this resulting toxicity could have contributed to the observed reduced growth in VM plants.

A possible explanation why VNM plants had lower growth than WOC is the soils of the VNM treatment group may have supported communities of toxigenic bacteria, which have been found to decrease both plant growth and seed weight [25]. Autoclaving may have disturbed the natural balance of the microbial community, removing PGPR and allowing for harmful bacteria to take over. Indeed, our results showed that after 49 days there were no differences between bacterial abundances of the three treatments (Table 3), suggesting that a recolonization may have occurred, however we are unable to determine which types of bacteria were dominant. Beneficial bacteria such as PGPR normally suppresses the growth of parasitic and toxigenic bacteria, its absence in the autoclaved VCT may have exasperated the proliferation of harmful bacteria colonies [25].

Conclusion

Vermicompost tea (VCT) increased plant growth in drought-simulated conditions and decreased sunflower growth in ideal-water conditions. Furthermore, the nutrients in VCT alone did not benefit sunflower growth, which may suggest that soil biology can significantly influence agricultural yield. It is proposed that plant-growth promoting rhizobacteria may play an important role in increasing plant growth and help to explain the observed results. The results of this study also suggest that soil microbial health is influenced by many factors including plant-microbe symbiotic relationships, nutrient availability and hydrological factors. With proper consideration of these factors, VCT has the potential to play an important role in increasing agricultural sustainability at a time when climate change, overpopulation and land degradation demand it.

Implications for future research

Based on this study and similar research that has been conducted, the influence that microbes have on plant health and productivity should continue to be investigated. Of particular importance is the observed beneficial effect that VCT had on sunflower growth under drought-simulated conditions. We recommended that future research be conducted on the influence and possible benefits of VCT on crop production in water stressed regions. This topic is especially pertinent to regions where climate change is expected to increase the incidence of drought. The effect of VCT on other agricultural crops, especially those that are of agricultural importance and grown without irrigation, should also continue to be investigated. It is believed that initial soil quality may influence the effect of VCT, so caution should be used when generalizing the results of this study. The commercial potting soil used in this study was relatively nutrient rich to begin with, and VCT may have different effects on crop production in soils that are nutrient poor. Additionally, previous studies have shown that adding PGPR into heavily used industrial agricultural soils has beneficial effects [26]. It is therefore important to further examine the effect that synthetic fertilizers and industrial agricultural practices have on soil microbial health because VCT application may be an option for restoring overworked

soils. Finally, a small but growing portion of the global food supply is produced in greenhouses under ideal-water conditions. Based on the results of this study, VCT application may actually be harmful to plants under these conditions. Further research is recommended to investigate whether this effect holds true for other plants that are grown under ideal-water conditions, both inside and outside the greenhouse.

References

1. J. H. C. Godfray, J. R. Beddington, I. R. Crute, L. Haddad, D. Lawrence et al., Science 327(5976), 2010.
2. N. Alexandratos, J. Bruinsma. World agriculture towards 2030/2050: the 2012 revision. ESA Working paper No. 12-03. Rome, FAO. 2012.
3. L.R. Oldeman, in Soil Resilience and Sustainable Land Use, D.J. Greenland and I. Szabolcs, Eds. CAB International, Wallingford, UK, 1994, p.p. 99 118.
4. T. Weis, J Agrar Change 10(3), 2010.
5. L. Brussaard, Ambio 26(8), 1997.
6. E. Barrios, Ecol. Econ. 64(2), 2007.
7. B. Lugtenberg, F. Kamilova, Annu. Rev. Microbiol. 63(1), 2009.
8. E.J. Gray, D.L Smith, Soil Biol. Biochem. 37(3), 2005.
9. D. Haas, G. Defago, Nat. Rev. Microbiol. 3(4), 2005.
10. B. R. Glick, Z. Cheng, J. Czarny, J. Duan, Eur. J. Plant Pathol. 119(1), 2007.
11. S. Mayaka, T. Tirosha, B. R. Glick, Plant Sci. 166(2), 2004.
12. J.I. Fritz, I.H. Franke-Whittle, S. Haindl, H. Insam, R. Braun, Can. J. Microbiol. 58(7), 2011.
13. A. Pant, T.J.K. Radovich, N.V. Hue, N.Q. Arancon. Compost Sci Util 19(4), 2011.
14. F.S. Mansour, G.A.M. El-Sayed, Egypt. J. Biol. Pest Control 21(1), 2011.
15. C. Pane, G. Celano, D. Villecco, M. Zaccardelli, Crop. Prot. 38(12), 2012.
16. B.A. Vick, J. Hu in Genetics, Genomics and Breeding of Sunflower, J. Hu, G. Seiler and C. Kole, Eds. Science Publishers, Enfield, NH, 2010, p.p. 313326.
17. M. Stevens, Plant Guide: Annual Sunflower Helianthus annuus. United States Department of Agriculture Natural Resources Conservation Service, University of California, Davis, CAL, 2007.
18. J. Pumpanen, P. Kolari, H. Ilvesniemi, K. Minkkinen, T. Vesala, et al., Agric. For. Meteorol. 123(3-4), 2004.
19. J. Pathma, N. Sakthivel, SpringerPlus 1(26), 2012.
20. M.C. Whitlock, D. Schluter, The Analysis of Biological Data, Roberts and Co. Publishers, Greenwood Village, COL.
21. S. Mayak, T. Tirosh, B. R. Glick, Plant Physiol. Biochem, 42(6), 2004..
22. P. Jupp, E. I. Newman, J. Appl. Ecol. 24(1), 1987.
23. P.B. Reich, D.W. Peterson, D.A. Wedin, K. Wrage, Ecol. 82(6), 2001.
24. M.C. Drew, J.M. Lynch, Annu. Rev. Phytopathol. 18(1), 1980.
25. T.V. Suslow, J.W. Klepper, M.N. Schroth, T.J. Burr. Calif Agr 33(11), 1979.
26. V. Chaudry, A. Rehman, A. Mishra, P.S. Chauhan, C.S. Nautiyal, Soil Microbiol. 65(2), 2012.

JURA
Journal of Undergraduate Research in Alberta • Volume 4 • 2014

A Pilot Study Of The Impact Of An Intergenerational Program For Socially Isolated Seniors: Examining LINKages

M. Shaw and C. Konnert
University of Calgary

An increasing number of elderly people are remaining at home long into their senior years. This is a highly vulnerable population, at risk of loneliness, isolation, depression and associated adverse health outcomes. Intergenerational social programs are intended to enable social contact, promote active participation and sharing, as well as provide a sense of meaning for seniors. The purpose of this pilot study was to examine social and health outcomes of long-term senior participants at the intergenerational organization, LINKages. Twenty-one participants completed the UCLA Loneliness Scale, Engagement in Meaningful Activities Scale, MOS Social Support Survey, the Short Form Health Survey and participated in a semi-structured interview. Results indicate that intergenerational programs do target lonely seniors, who have an average sense of engagement in meaningful activities compared with standardized norms. A stronger bond with a younger volunteer was associated an increased sense of social support. Finally, decreased loneliness, engagement in meaningful activities and sense of social support were all related to increased vitality. The study findings indicate that intergenerational programming is successful in targeting lonely older adults and that improvements in the social outcomes, such as loneliness, support and sense of meaning are associated with better health. **Keywords:** social isolation, intergenerational, volunteering, seniors programming, successful aging.

Introduction

Faced with an increasing older population, facilitating successful aging is increasingly important for promoting longevity, good health, activity, independent living and consequently minimizing healthcare costs that are associated with older age [1]. Most elderly people live at home as they age and more than 30% live alone [2]. This population is also the most vulnerable due to low income, high widowed status, loneliness, depression and isolation [3]. Isolation and loneliness are associated with a number of adverse health outcomes [4–6].

Epidemiology: It is estimated that approximately 17% of older adults in North America report self-perceived loneliness [5]. Gender and marital status appear to be related to loneliness and social isolation. Non-married males report the highest extent of loneliness, followed by non-married females. For married couples, females report higher incidence of loneliness than males. Finally, widowed individuals, report the highest extent of loneliness. While

some studies have reported a relationship between loneliness and socio-economic status, suggesting that loneliness is more prevalent among lower income groups, these findings have not been consistent [7].

Interventions: Numerous social programs have been designed and implemented in an attempt to minimize loneliness in the elderly [2, 8-9]. These programs include community empowerment interventions, self-help or educational interventions, direct services programs as well as volunteer linking interventions [10]. Data on the effectiveness of these interventions is widely varied [11–12]. A number of issues might contribute to the conflicting efficacy results of loneliness reduction interventions, including the variety of services offered, the length of time for which interventions are implemented, limitations with study design and the wide range of tools used to measure efficacy [11]. In addition, although the research interventions aim to reduce social isolation or loneliness, a minority of them specifically target people who are socially isolated. In most studies, social isolation is assumed in virtue of the specific client group, such as being a resident in a nursing home. Friendly visitor programs are a subtype of intervention that have the added benefit of being cost effective as they do not have to be run by a professional [14]. A meta-analysis of 15 studies of friendly visitor programs for socially isolated older adults found that these programs were associated with both a significant reduction in mortality and a significant reduction in admissions to long-term institutionalized care [14]. Friendly visitor programs specifically, target social activity and support, and some types of friendly visitor programs, such as intergenerational interventions, contain a participatory component. A review of interventions aimed at targeting loneliness found that programs containing these components, namely, participatory elements as well as social activity and support were most likely to be beneficial [12].

Intergenerational Programs and a Sense of Meaning: A particular type of friendly visitor intervention, that is not clearly represented in the literature on efficacy of social isolation interventions, are intergenerational programs. Intergenerational programs focus on pairing participants from different generations, with the aim of developing a reciprocal relationship where both participants are able to share with and learn from one another [14]. Intergenerational relationships provide the opportunity to explore common values and formulate shared agendas [15]. In contrast to interventions where seniors are visited by a nurse or a peer, intergenerational visitation does not make the senior feel like the sole recipient of visitation benefits but rather provides them with a participatory role and a sense of meaning, in accordance with Erik Eriksons theory of Generativity [16]. According to Erikson, generativity is the extension of care towards others. In this process, individuals derive meaning and purpose by passing on knowledge and wisdom to younger generations. The possible implication of this theory is that tapping into seniors desire for generativity could help to promote successful aging by enabling them to participate in meaningful activities through sharing with younger generations, while simultaneously minimizing feelings of loneliness and isolation through the building of social relationships [17–18]. Rowe and Kahn [19] define successful aging as a combination of three components: avoiding disease and disability; maintaining high mental and physical function; and sustained engagement with life which means participating in relationships with others and being productively involved in activities. Their studies on successful aging showed that older adults who scored high in mental and physical functioning were twice as likely to engage in volunteer activities as low-functioning senior adults. Some even remain productive despite limitations and chronic diseases, and this active engagement can lead to longer and healthier lives. Senior involvement in intergenerational programs has demonstrated improved feelings of self-worth, higher levels of social interaction and more prolonged ability to remain productive [2]. While the data gathered from these programs is promising, there is a need for more in-depth analysis into both qualitative and quantitative outcomes from intergenerational programs, in order to fully assess their benefit and role in reducing social isolation and loneliness among the elderly. The purpose of the current study is to help to identify the typical participant who elects to participate in intergenerational programing, to explore self-perceived effects of participation and to determine whether participation in intergenerational programs is related to loneliness and sense of purpose or meaning, as well as health functioning. The results from this pilot study will also be used to assess the feasibility of conducting a

long-term, randomized controlled trial in order to more accurately identify any benefits to seniors as a result of intergenerational programming. Based on prior research, it is hypothesized that seniors who are long-term participants (minimum of one year) in intergenerational programming are less lonely than the standardized population and have a higher sense of purpose and meaning in their daily activities. Higher level of involvement in intergenerational programming (as measured by self-reported commitment level, perceived bond strength with younger volunteer and perceived benefits from participation) is expected to be related to decreased feelings of loneliness, increased sense of social support and increased sense of engagement in meaningful activities. It is further expected that decreased loneliness, increased social support and higher engagement in meaningful activities will be associated with better health functioning.

Examining Intergenerational Programs: LINKages: LINKages Society of Alberta is a community-based registered charity that was originally founded as the Friends of Seniors Foundation in 1994. With an extensive amount of experience, LINKages is recognized for the successful implementation of programs that connect young people with seniors in a number of different living arrangements, such as seniors residences and independent-living (Appendix 7). LINKages provides the careful recruitment, screening and matching of both youth and seniors with ongoing training and support, structured activities and high expectations for regular and ongoing contact.

Methods

Participants: Participants were 21 seniors, aged 60 to 92. Participants included 8 males and 13 females. Participants were members of LINKages who have been active in the program for a minimum of one year.

Materials: Quantitative measures fell into two categories: 1) demographic and background data, including age, gender, ethnicity, education and marital status, and 2) primary outcome measures assessed both functioning related to physical and social health as well as loneliness. These consisted of: UCLA Loneliness Scale, the MOS Social Support Survey, the Engagement in Meaningful Activities Survey (EMAS) and the Short Form Health Survey (SF 36) [20–23]. Norms for the SF 36 are available for various age groups, including age 75 and over [24]. Measures were selected based on reliability, validity, sensitivity to change and brevity [20,25–27]. Measures are included in Appendices 1-6. Participants filled out a background questionnaire created by the main investigator (Appendix 1). They gave their date of birth (age) and selected from a number of categories to describe their gender, race/ethnicity, marital status, living situation (e.g., alone, with a spouse, with another adult or adults) and highest level of education. The purpose of the qualitative component of the study was to bring to light any issues or phenomena that might not have been detected by the quantitative methods, and to obtain deeper information from participants on a variety of questions, such as, their reasons for joining an intergenerational program, perceived benefits of participation, information on other volunteer activities they participate in, as well as feedback on their self-perceived loneliness and satisfaction with familial relationships (Appendix 6). Some questions in this section, such as perceived bond strength with ones younger volunteer, self-perceived loneliness, perceived program benefits and program commitment were scaled, so responses were used in the quantitative analysis.

Procedure: Participants were contacted by a LINKages employee via phone and e-mail and asked to participate in the study and be contacted by the researcher. Upon agreement, 26 participants were contacted via phone by the researcher and asked to set up a meeting time at their convenience. Twenty-one individuals agreed to participate in the study. Meeting times were set up with 21 individuals at their home. At the meeting, the consent form was reviewed and any questions were answered before participants began to complete other measures (Appendix 7). Participants were asked to sign the consent form and were informed that they could terminate participation at any time and this would not affect their membership at LINKages. First, demographic data was gathered from participants. The main outcome measures were then administered to participants. Finally, a semi-structured interview was administered. Participation in study took between one and two hours.

JURA
Journal of Undergraduate Research in Alberta • Volume 4 • 2014

Participant Demographics	Number	Percent
Widowed	14	66.7
Divorced/Separated	6	28.6
Never married	1	4.8
Living alone	17	81.0
Living alone with assistance	2	9.5
Living with another adult	2	9.5
Have children	19	90.1

Table 1: *Patient Demographic Data (N=21).*

Results

Analysis: Quantitative statistical analyses were conducted using SPSS statistical software Version 17.0.1. Frequencies for all study variables in the data set were examined for errors in data entry or scoring, and corrected if indicated. Items were recoded as needed to compute scale scores. Next, descriptive statistics were calculated for all variables. Correlations were run to assess the relation of demographic and other background variables to the main outcome measures.

Demographic Data: Twenty-one participants, consisting of 13 females and 8 males ranged in age from 60 to 92 (M = 76.7, SD = 5.67) . All participants were Caucasian. Demographics are presented in Table 1.

Descriptive Analysis: The means, standard deviations, ranges and reliability for the main-outcome measures are presented in Table 2. Scores on the UCLA Loneliness Scale for this sample (M = 36.8, SD = 7.7) were found to be significantly higher than standardized scores for the general senior population (M = 31.5, SD = 6.92), indicating that participants in this sample are, on average, more lonely, compared with the general senior population (t(20) = 3.15, p <.05 [19]. Results from the EMAS Engagement in Meaningful Activities Survey indicate an average score of 46.7 (SD = 4.2), which is not statistically different from standardized senior scores on the EMAS (M = 48.2, SD = 6.5), indicating that seniors in this sample do not differ significantly from the general senior population in the amount of meaningful activities in which they engage [26]. The large standard deviations for some scales, such as Physical Functioning, Pain, Vitality and Physical Limitations indicate a large variation in health status among participants.

Correlations Among Variables: Note that all correlations were one-tailed. Bond strength and self-reported loneliness were negatively correlated (r = -.39, p <.05) but there was no significant relationship found between bond strength and the UCLA Loneliness Scale. When participants were separated based on marital status, bond strength was significantly negatively associated with scores on the UCLA Loneliness scale for widowed individuals (r = -.45, p <.05) but not for married/divorced or never married individuals. In addition, a strong negative association was found between scores on the UCLA Loneliness Scale and the EMAS for widowed individuals (r = -.81, p <.01) but not for the other groups. A significant negative association was found between UCLA Loneliness Scale scores and the Physical Functioning portion of the SF-36 (r = -.46, p <.05), as well as UCLA Loneliness Scale scores and the Vitality portion of the SF-36 (r = -.47, p <.05). EMAS was positively associated with Vitality Scores (r = .46, p <.05). Scores on the MOS Social Support Survey were not associated with General Health Perception or Physical Role Limitations but were positively associated with Physical Functioning (r = .42, p <.05) and Vitality Scores (r = .37, p <.05).

Open-Ended Questionnaire Results: Results from analysis of the 17-item open-ended questionnaire indicate an overall positive experience at LINKages. In rating their commitment to the program on a 5-point scale from 1 or "Not Committed at all" to 5 or "Highly Committed", all participants responded that they were "Highly Committed". Similarly, all participants reported finding the program either "mostly" or "highly" beneficial. There was variability in participants assessment of bond strength with their LINKages volunteer. In response to Question 13, "What other benefit do you get from participating in

JURA
Journal of Undergraduate Research in Alberta • Volume 4 • 2014

Outcome Measure	N	Minimum	Maximum	Mean	Std Dev
UCLA Loneliness Scale	21	25	53	36.8	7.7
MOS Social Support Survey	21	14	26	18.9	3.1
EMAS*	21	39	55	46.7	4.2
SF-36 General Health Perception	21	30	80	60.3	13.8
SF-36 Physical Role Limitations	21	10	95	53.4	24.6
SF-36 Vitality	21	30	100	66.4	18.5
SF-36 Physical Functioning	21	25	100	61.9	23.6
SF-36 Emotional Role Limitations	21	68	92	87.1	7.9
SF-36 Pain	21	17	90	68.2	19.1
SF-36 Mental Health	21	60	100	82.4	8.6
SF-36 Social Functioning	21	60	85	76.4	11.1

Table 2: *Table 2 Descriptive Data on Primary Outcome Measures (N=21).*

the LINKages program?" a single theme emerged: social connectedness, including comments about meeting young people, learning about them and sharing about themselves as well as specific comments about the quality of interactions and the enjoyment of shared activities. In response to Question 8 "What did you dislike about the program or what weaknesses do you see in the program that may deter from your experience?", most respondents commented on the rarity with which they were able to see their volunteer and the brevity of time spent together, expressing an interest in more contact. Participants also mentioned a number of suggestions for improvement, including playing board games or engaging in educational activities, like cooking classes. Eight participants (38.1%) reported being lonely on the self-reported loneliness question. All widowed participants reported losing their spouse within the last five years and expressed experiencing an increased sense of loneliness and isolation after the death of their spouse. All widowed participants reported joining LINKages as part of an effort to curtail the loneliness and negative feelings associated with the loss of their spouse. Thirteen participants (61.9%) responded that they were satisfied with the amount of time they spent with their children and grandchildren, while 8 participants reported that they were not satisfied. Participants who were not satisfied did not differ significantly in either self-reported loneliness or UCLA Loneliness Scale scores from participants who were satisfied with their kin relationships. In addition, 12 participants (57.1%) reported volunteering for other organizations in addition to LINKages and 16 participants (76.2%) reported having volunteered for other organizations in the past. These seniors were not significantly less lonely, on either self-reported loneliness or the UCLA Loneliness Scale than seniors who reported not having volunteered elsewhere in the past. Finally, 19 participants (90.5%) reported feeling like they had a sense of being part of a community.

Discussion

The purpose of this study was to examine the impact of senior participation in intergenerational programming on a number of health-related and psychosocial outcomes. The hypotheses were, in some cases, supported by the results and in others not supported. It was expected that after long-term participation (minimum of 1 year) in the LINKages program, older adults would be less lonely than the general senior population. This hypothesis was not supported by results on the UCLA Loneliness Scale, as on average seniors in the program scored significantly higher than the general population. In support of these results, it was also found that subjective reports of loneliness were higher in the program than in the general population: 38% compared to 17% [5]. While, these findings indicate that despite participation in intergenerational programming, targeted seniors are still more lonely than average, the results provide reassurance that the program is attracting the participation of lonely seniors. The findings cannot be used to conclude that intergenerational programming is ineffective in reducing loneliness. Measures were taken at a single time point and it is unclear how these scores may have changed from

baseline measures. The second hypothesis was that participants would demonstrate an above-average sense of engagement in meaningful activities. This hypothesis was not supported by the results, which demonstrated almost equivalent scores between the studied group and the general senior population. Once again, it is unclear what the baseline participant scores were, so it is not possible to draw conclusions about whether or not participation in LINKages has led to an increase in sense of meaning. Level of involvement in intergenerational programming was measured by ratings on commitment level, perceived level of benefit from participation and bond strength. It was not possible to conduct correlational analysis with levels of commitment and perceived benefit because all participants rated these very highly and subsequently, there was insufficient variability between scores. The high positive ratings do however, indicate that participants are uniformly highly committed to participating in LINKages and also consistently feel that they benefit from participation. Bond strength was the only measure of program involvement that demonstrated variability and there was a positive association with sense of social support and bond strength. It remains unclear whether these relationships represent an effect of the program. Interestingly, in a post hoc analysis in which participants were separated based on marital status, a significant negative association was found between bond strength and UCLA loneliness scales for widowed individuals. Prior research suggests that widowed individuals are more lonely than their married or separated counterparts, and this finding may help to explain the current results [4]. Widowed individuals may be acutely faced with Social Breakdown Syndrome [27] and subsequently, resilient individuals may actively choose to seek out meaningful volunteer activities, such as intergenerational programs. Social Breakdown Syndrome refers to the shrinkage of social roles and reference groups that accompany older age, as well as the presence of negative behavioral expectations. For widowed individuals, Social Breakdown Syndrome is likely more pronounced than individuals who are married or separated earlier in life via some choice of their own. Finding a sudden shift in social roles and groups may explain the higher levels of loneliness that are typical of widowed individuals. However, it may be the case that widowed individuals who join intergenerational programs, such as LINKages, seek to overcome their increased loneliness because they are more resilient. Resilience is the capacity to maintain or regain high levels of well-being in the face of life challenges or transitions [28]. Thus, it may be the case that when widowed individuals are able to form a strong bond with new people (such as their volunteer), their loneliness decreases. Additional support for this theory comes from the finding of a negative association between loneliness and meaningful activities only for the widowed group. Finally, while decreased loneliness, sense of social support and engagement of meaningful activities were not consistently correlated with SF-36 health measures, they were associated specifically with increased vitality, which is an independently validated health measure [29].

Conclusion

The study findings indicate that intergenerational programming is successful in targeting lonely older adults and that improvements in the social outcomes, such as loneliness, support and sense of meaning are associated with better health. There are a number of limitations with this study. The correlational design prevents conclusions to be drawn about causality or directionality of the findings. The administration of measures to participants at a single point in time prevents the possibility of examining how scores may have changed over the course of individuals participation in LINKages, making it difficult to draw conclusions about the efficacy of the program based on quantitative data. In addition, this study examined only a single group and while comparisons with average seniors populations were made for some measures such as the UCLA Loneliness Scale and the EMAS, it was not possible to compare the sample scores with a control group for most measures. Finally, since participant numbers were not large, power may have been a problem for some correlations. Future research can seek to address the aforementioned limitations by following an incoming group of volunteers to LINKages over the course of one year, in order to track any changes in outcome measures. Baseline scores of an incoming group can be used for comparison with measures from the current group if both sets of participants are comparable on background and other

demographic measures. A randomized controlled trial can also be used to delineate the causal relationship between the intergenerational program and various health outcomes. Using research to determine the effect and feasibility of using social programs to promote successful aging is an important tool to best accommodate an aging population.

References

1. Elkan, R., Kendrick, D., Dewey, M., Hewitt, M., Robinson, J., Blair, M., Williams, D., and Brummell, K. British Medical Journal 323 (71924) 2001.
2. Bullock, J., and Osborne, S. Educational Gerontology (25) 1999.
3. Colin J G., and Lou F. The Journal of the Royal Society for the Promotion of Health (126) 2006.
4. Locher J. L., Ritchie C. S., Roth D. L., Baker P. S., Bodner E. V., and Allman R. Soc Sci Med, 60(4), 2005.
5. Walker, D., and Beauchene, R. E. Journal of American Dietary Association, 91(3), 1991.
6. Hawton, A. Green, C., Dickens, A. P., Richards, S. H., Taylor, R. S., Edwards, R., Greaves, C. J., and Campbell, J. L.Quality of Life Research 20(1) 2011.
7. Findlay, R. A. Ageing & Society, (23) 2003.
8. Masi, C., Chen, H., Hawkley, L., and Cacioppo, J. Personality and Social Psychology Review, 15(3), 2011.
9. Andersson, L. literature. Aging and Mental Health, 2(4), 2010.
10. Barron, J., Tan, E., Yu, Q., Song, M., McGill, S., and Fried, L. Journal of Urban Health, 86(4), 2009.
11. Cattan, M., White, M., Bond, J., and Learmouth, A. Ageing & Society, (25), 2005.
12. Dickens, A., Richards, S., Greaves, C., and Campbell, J. BMC Public Health (11), 2011.
13. Weintraub, A., and Killian, T. Journal of Applied Gerontology, 26(4), 370-384. 2007.
14. Flora, P. and Faulkner, G. . Journal of Intergenerational Relationships, 4(4), 63-74. 2006.
15. Erikson, E. Oxford, England: Josiah Macy, Jr. Foundation. In Milton J. E. (Eds), Symposium on the healthy personality 1959.
16. Debats, D. L. Journal of Humanistic Psychology, 29, 30-57. 1999.
17. Vanderven, K. Journal of Intergenerational Relationships, 11(3), 37-41. 2011.
18. Rowe, J., and Kahn, R. The Gerontologist, 38(2), 151-164. 1998.
19. Russell, D. . Journal of Personality Assessment, 66(1), 20-40. 1996.
20. Sherbourne, C., and Stewart, A. Soc. Sci. Med. 32(6), 605-714. 1991.
21. Goldberg B., Brintnell S., and Goldberg J. Occupational Therapy in Mental Health, 18(2),1744. 2002.
22. Ware, J., and Sherbourne, C. Medical Care, 30(6), 473-483. 1992.
23. Ware, J., Snow, K., Kosinski, M., and Gandek, B. Manual and Interpretation Guide. Boston, MA: New England Medical Center, The Health Institute. 1993.
24. Lyons, R., Perry, I., and Littlepage, B. British Geriatric Society, 23(3), 182-184. 1993.
25. Eakman, A., Carlson, M., and Clark, F. OTJR, 30(3), 111-121. 2010.
26. Stansfeld, S., Roberts, R., and Foot, S. Quality of Life Research, 6(3) 217-224. 1997.
27. Kuypers, J. and Bengston, V. Human Development, 16, 181-201. 1973.
28. Kling, K., Seltzer, M., and Ryff, C. Psychology & Aging, 12, 288-295. 1997.

Acknowledgements: This study was funded by a Markin USRP Undergraduate Studentship (2012) at the University of Calgary

Front Cover: This visualization was created by Melanie Burger and represents work done by students in the UofC nanoscience program. The 'black holes' are enabled and disabled by binding to DNA and are able to inhibit the luminescence of the nanoparticles.